Czech Technical University in Prague

Faculty of Electrical Engineering

Doctoral Thesis

May 2019

Ing. Jan Kudláček, DiS.

Czech Technical University in Prague

Faculty of Electrical Engineering
Department of Circuit Theory

Dynamics and Functional Organization of Neuronal Populations in Epileptic Brain

Doctoral Thesis

Ing. Jan Kudláček, DiS.

Prague, May 2019

Ph.D. Programme: Electrical Engineering and Information Technology

Branch of study: Electrical Engineering Theory

Supervisor: prof. MUDr. Přemysl Jiruška, Ph.D.

Abstract

Epilepsy is a neurological disorder affecting 0.5 to 1 % worldwide. The main manifestation of epilepsy is epileptic seizures. The seeming randomness and unpredictability of seizures constitutes a major debilitating factor for people with epilepsy. There is, however, increasing body of evidence that the seizures are not fully random, i.e. they are not a Poisson process. In this work we aimed at investigating the long-term dynamics of seizures in the tetanus toxin model of epilepsy in rats and proposing the mechanisms that could govern it.

Using statistical techniques, we have shown that the seizures in the tetanus toxin model of epilepsy in rats are not Poissonian. We have found that the seizures occur in clusters of approximately 2 days duration interleaved by approximately 2-day seizure-free periods. The main original finding of this work is the internal structure of the cluster. We have found that at the beginning of the cluster there are mostly focal seizures but with the cluster progression there is gradually increasing proportion of generalized seizures. The seizure rate gradually decreases with the cluster progression. We propose a theory that the focal seizures at the beginning of the cluster facilitate the generalization of later seizures possibly via kindling mechanism. Once the generalized seizures appear, they have rather inhibiting effect in that they gradually decrease the seizure rate. Accumulation of such inhibition may be then responsible for the termination of the seizure cluster.

We have also analyzed the long-term profiles of epileptic bursts, a less well known graphoelement observed in the tetanus toxin model of epilepsy. Bursts enabled us to investigate the dynamics of the epileptic brain during the inter-cluster periods where no seizures are present. We have found that during the inter-cluster period, the burst rate increases. The duration of the bursts initially decreases but with an approaching seizure cluster it increases again. The signal power of the bursts in the hippocampi increases. Cross-correlation function between the hippocampi as well as between the hippocampus and motor cortices increases. We interpret these changes as a manifestation of gradually increasing excitability of the brain and facilitation of the propagation of epileptic activity. This is an evidence of a hidden dynamic process which takes place during the inter-cluster period and which slowly leads to the next seizure cluster.

Our findings on long-term seizure dynamics have implications for understanding the principles of seizure generation, evaluation of epilepsy therapy, evaluation of seizure risk (seizure forecasting) and ultimately, they may help in introduction of patient-tailored treatment strategies, such as chronopharmacotherapy, which improve efficacy and reduce side effects of the drugs.

Keywords: Epilepsy, epileptic seizure, long-term seizure dynamics, seizure cluster, chronotherapy, tetanus toxin model of epilepsy, epileptic burst

Anotace

Epilepsie je chronické neurologické onemocnění postihující 0.5 až 1 % světové populace. Hlavním projevem epilepsie jsou epileptické záchvaty. Zdánlivá náhodnost a nepředvídatelnost záchvatů představuje jednu z nejvíce nepříjemných vlastností epilepsie. Nicméně objevuje se stále vice důkazů, že záchvaty nejsou zcela náhodné, tj. nereprezentují Poissonův proces. Cílem této práce bylo popsat dlouhodobou dynamiku záchvatů v tetanotoxinovém modelu epilepsie a navrhnout, jaké mechanizmy za ni mohou být zodpovědné.

Pomocí statistických technik jsme ukázali, že záchvaty v tetanotoxinovém modelu epilepsie nejsou poissonovské. Zjistili jsem, že záchvaty se vyskytují ve shlucích trvajících přibližně dva dny a jsou odděleny přibližně dvoudenními obdobími bez záchvatů. Hlavním původním výsledkem této práce je popis vnitřní struktury shluku. Zjistili jsme, že na začátku shluku se vyskytují především fokální záchvaty, avšak s postupem shluku se zvyšuje zastoupení záchvatů generalizovaných. Frekvence výskytu záchvatů se s postupem shluku postupně snižuje. Navrhujeme teorii, že fokální záchvaty na začátku shluku usnadňují generalizaci pozdějších záchvatů, pravděpodobně prostřednictvím mechanismu zvaného kindling. Když se pak objeví generalizované záchvaty, mají naopak inhibiční vliv ve formě zvyšování prahu pro vyvolání záchvatu, což vede ke snížení frekvence výskytu záchvatů. Kumulace tohoto inhibičního vlivu pak může vést k ukončení shluku záchvatů.

Analyzovali jsme také dlouhodobé profily epileptických sérií výbojů (angl. burst), což je méně známý grafoelement pozorovaný v tetanotoxinovém modelu epilepsie. Série výbojů nám umožnily zkoumat dynamiku epileptického mozku v období mezi shluky záchvatů, ve kterém se žádné záchvaty nevyskytují. Zjistili jsme, že v mezi-shlukovém období se zvyšuje frekvence výskytu sérií výbojů. Jejich délka z počátku klesá, ale s blížícím se následujícím shlukem záchvatů začne růst. Výkon signálu sérií výbojů v hipokampech se zvyšuje. Vzájemná korelační funkce mezi hipokampy, a taktéž mezi hipokampem a motorickou kůrou, roste. Tyto změny interpretujeme jako projev postupně se zvyšující excitability mozku a facilitace propagace epileptické aktivity. To je důkazem skrytého dynamického procesu, ke kterému dochází během mezishlukového období, a který vede k dalšímu shluku záchvatů.

Naše zjištění o dlouhodobé dynamice záchvatů mají význam pro porozumění mechanizmům vzniku záchvatu, při hodnocení úspěšnosti léčby epilepsie, při vývoji metod stanovování rizika záchvatu a v konečném důsledku mohou pomoci se zavedením individualizované péče o pacienty, jako je například chronofarmakoterapie, která zvyšuje účinnost a snižuje nežádoucí účinky léků.

Klíčová slova: epilepsie, epileptický záchvat, dlouhodobá dynamika záchvatů, shluk záchvatů, chronoterapie, tetanotoxinový model epilepsie, série výbojů

Declaration

I hereby declare that I did the work on this study entitled Dynamics and Functional Organization of Neuronal Populations in Epileptic Brain independently and used only the information from references listed in the thesis.

……

Jan Kudláček

Acknowledgement

I would like to thank Dr. Přemysl Jiruška for guidance, valuable advices and discussions and help with experiments. Likewise, I would like to thank other members of our research group, namely Dr. Jakub Otáhal, prof. Roman Čmejla, Ing, Jan Chvojka, Ing. Radek Janča, Ing. Pavel Vlk, Mgr. Ľubica Demeterová and Ing. et Ing. Antonín Pošusta for help with the experiments and valuable discussions about analyses. Thanks belong also to my family and my friends for supporting me.

Table of Contents

List of abbreviations

AED – anti-epileptic drug
AP – anterior-posterior
CEWT – conditional expected waiting time
D – depth
DHipp – dorsal hippocampus
dur – duration
EEG – electroencephalogram
fcn – function
FSCS – focal subclinical seizure
GABA - γ-aminobutyric acid
HFO – high-frequency oscillation
Hip – hippocampus
IBE – international Bureau for Epilepsy
IED – interictal epileptiform discharge
ILAE – international League Against Epilepsy
IQR – inter-quartile range
ISI – inter-seizure interval
L – lateral
LTP – long-term potentiation
MCx – motor cortex
mTLE – mesial temporal lobe epilepsy
NaN – not a number
NPY – neuropeptide Y
PTZ – pentylenetetrazol
pwr – power
SD – standard deviation
SE – status epilepticus
SEM – standard error of the mean
sz – seizure
UEWT – unconditional expected waiting time
VMR – variance to mean ratio

1 General introduction

1.1 Epilepsy

After a stroke, epilepsy is the second most common neurological disorder affecting between 0.5 and 1 % of the population worldwide (Mula & Cock 2015). According to International League Against Epilepsy (ILAE) and International Bureau for Epilepsy (IBE), epileptic seizure and epilepsy are defined as follows: "An epileptic seizure is a transient occurrence of signs and/or symptoms due to abnormal excessive or synchronous neuronal activity in the brain. Epilepsy is a disorder of the brain characterized by an enduring predisposition to generate epileptic seizures and by the neurobiological, cognitive, psychological, and social consequences of this condition." (Fisher et al 2005)

The symptoms of an epileptic seizure can be very diverse and include altered sensory functions (somatosensory, gustatory, olfactory, auditory, visual and internal sensations), altered motor function (i.e. convulsions or atonia), altered consciousness, altered emotional state, inability to speak or understand speech, amnesia, déjà vu and others (Fisher et al 2017, Fisher et al 2005). An important part of the definition of the epileptic seizure is the abnormal excessive or synchronous neuronal firing. There exist also other conditions producing seizures with clinical manifestations similar to epileptic seizures but not having as an underlying cause the excessive or synchronous neuronal firing (e.g. non-epileptic psychogenic seizures). While keeping in mind that epileptic seizures are a subset of all possible types of seizures, in the following text, by the term seizure, we will always mean an epileptic seizure. The abnormal excessive or synchronous neuronal activity is most easily detected by electroencephalography (EEG), i.e. the recording of electrical activity of the brain. A typical seizure EEG is depicted in Figure 1.

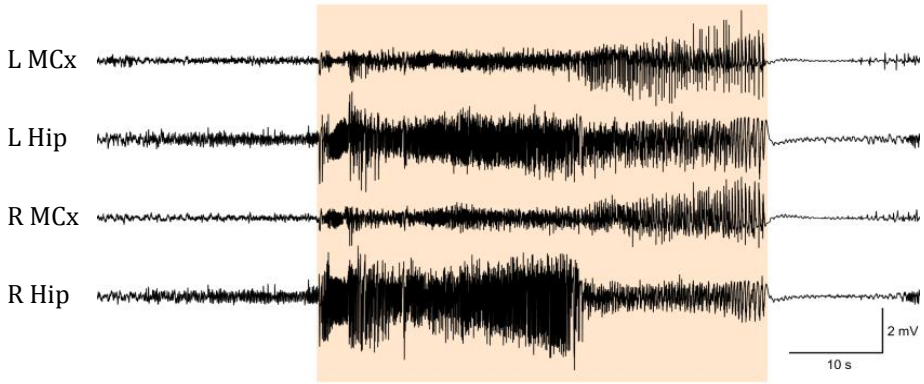

Figure 1: An example of EEG recording during seizure (orange shading) in a chronic model of temporal lobe epilepsy. Note the propagation of seizure activity to motor cortices 25 s after the seizure onset. Seizure is usually followed by post-ictal depression – flattening of EEG (amplitude attenuation) after the seizure termination. Hip – hippocampus, MCx – motor cortex.

EEG patterns similar to those seen during seizures but not having an observable clinical correlate are sometimes referred to as subclinical seizures (Fisher et al 2005). Apart from the seizures, EEG can also reveal various types of interictal (i.e. inter-seizure) epileptiform activity which can be used for diagnosis and monitoring of the disease (Blauwblomme et al 2014).

From the neuronal point of view, a seizure constitutes excessive and synchronous activity. There is a myriad of mechanisms involved in seizure generation. The most important one is a disbalance between excitation and inhibition. Indeed, agonists of excitatory postsynaptic

receptors are capable of inducing a seizure or a status epilepticus (a prolonged seizure lasting several hours). For example, kainic acid (or shortly kainate) is an agonist of glutamatergic receptors and is commonly used to induce an experimental status epilepticus in laboratory animals. Another typical example is pilocarpine, an agonist of cholinergic receptors, which is also used for the induction of status epilepticus. Antagonists of inhibitory postsynaptic receptors (usually GABAergic) are commonly used to induce experimental seizures (Scharfman 2007). Examples of such compounds are pentylenetetrazol (PTZ), picrotoxin and bicuculline. Conversely, several antiepileptic drugs (AEDs) such as diazepam or phenobarbital act through strengthening the GABAergic transmission.

The term epilepsy comprises a wide range of syndromes which have the common property of predisposing the brain to epileptic seizures. The ILAE and IBE definition of epilepsy requires a history of at least one seizure (which does not necessarily have to be unprovoked) and most importantly the enduring predisposition to future epileptic seizures. Comorbidities, such as cognitive, mood or behavioral problems and psychological and social disturbances (stigma) should be also considered as a part of the epileptic syndrome (Fisher et al 2005).

The etiology of epilepsy varies. Most common causes include genetic mutation (germinal or somatic), malformation of cortical development (often due to a somatic mutation), brain tumor, and an insult in the form of brain infection, hypoxia/ischemia (e.g. stroke), or traumatic brain injury (Scharfman 2007).

1.2 Mesial temporal lobe epilepsy (mTLE)

In this work, we used tetanus toxin model of epilepsy in rats. In this model, chronic epilepsy is induced by an injection of a minute dose of tetanus toxin into the hippocampus. Thus, it is a model of mesial temporal lobe epilepsy (mTLE). mTLE is the most common form of epilepsy in adults, and in the majority of cases, it is pharmacoresistant. i.e. patients do not achieve adequate seizure control with drug therapy (Sloviter 2005). Some of these patients can benefit from surgical resection of the epileptogenic brain tissue; most commonly anterior temporal lobe is resected (Thom et al 2010). Several studies reported seizure freedom after the surgery in 60 – 80 % of patients (Javidan 2012).

In the mTLE, seizures originate in the limbic system, most commonly in the hippocampus or in the amygdala, but other limbic structures (e.g. piriform and perirhinal cortices) can be involved as well. This is why sometimes it is referred to as limbic epilepsy. However, there is also some evidence that structures outside the limbic system (thalamus, substantia nigra) may play an important role in the pathophysiology of the limbic seizures (Bertram 2009, Toyoda et al 2013).

1.3 Animal models of mTLE

Most frequently used models of mTLE involve status epilepticus (i.e. prolonged seizure, usually lasting few hours) which initiates the conversion of a healthy brain to an epileptic brain (a process called epileptogenesis). The status epilepticus can be induced either chemically (kainite of pilocarpine models) or by electrical stimulation of the brain using implanted intracerebral electrodes. Typically, after few days the animal develops spontaneous seizures, which then last for its lifetime (Dudek & Staley 2011a, Dudek & Staley 2011b). There are, however, doubts regarding to what extent these models mirror the human condition (Sloviter 2005). Moreover, the status epilepticus usually causes severe, widespread, bilateral brain damage, which makes these models inappropriate for the study of causal relationships between the structures involved in seizures as well as in epileptogenesis (Sloviter 2005).

In this project, we utilize tetanus toxin model of mTLE in rats. The epilepsy is induced by unilateral injection of a small dose of tetanus toxin into the hippocampus (Jefferys et al 2015,

Mellanby et al 1977). The only structure directly affected by the tetanus toxin action is the injected one; the tetanus toxin doesn't propagate to other brain regions (Ferecsko et al 2014). Tetanus toxin model is characterized by mild neuronal loss and absence of initial status epilepticus (Jefferys et al 1992, Jiruska et al 2013). For these reasons, tetanus toxin model is considered a model of non-lesional focal epilepsy.

1.4 Transition to a seizure

To gain insight into the mechanisms of seizure generation it is necessary to study the dynamics of epileptic brain at various time scales which are depicted in Figure 2. From the bottom to the top, the time scale is shorter and the likelihood of a seizure in near future is higher.

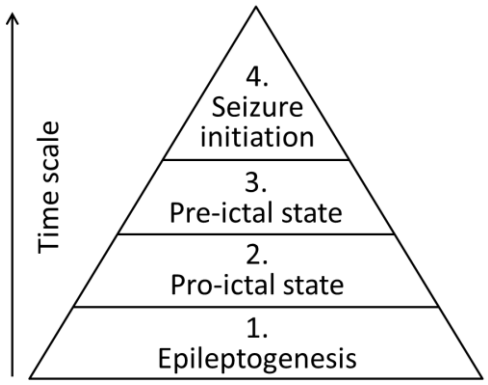

Figure 2: Time scales of transition to seizure

The first time scale is labeled Epileptogenesis. Epileptogenesis is a process by which a healthy brain is reconfigured to an epileptic brain after an initial insult (Scharfman 2007). The insult may be e.g. an injury, infection, ischemia or a genetic defect. Epileptogenesis can involve myriad of changes at cellular, synaptic and molecular levels such as loss of neurons, changes in expression of ion channels, metabolic changes, immunological processes and gliosis (Blauwblomme et al 2014). The time from the initial insult to the first clinical seizure can vary from days to years (Williams et al 2009). It was shown that epileptogenesis continues beyond the first spontaneous seizure (Bertram & Cornett 1994, Williams et al 2007, Williams et al 2009). In this work we will touch the epileptogenesis only briefly.

At the second time scale, labeled Pro-ictal state, we deal with long-term fluctuation of seizure probability. We will see that there are periods of time with little or no seizures and periods with high seizure rate. Thus, the brain can be in an anti-ictal state or a pro-ictal state, respectively. In experimental animals, this time scale is measured in days or weeks (Goffin et al 2007) whereas in patients it can vary from days to weeks (Karoly et al 2016), months (Balish et al 1991, Binnie et al 1984) or even years (Bauer & Burr 2001, Griffiths & Fox 1938). We will investigate the patterns of seizure occurrence and propose some candidate mechanisms which can govern these patterns. Chapters 3 and 4 will be devoted to the long-term seizure dynamics and thus mainly to the alternation of pro-ictal and anti-ictal states.

At the third time scale, labeled Pre-ictal state, we describe transition to an individual seizure. This time scale is in the range of minutes to days.

At the fourth time scale, labeled Seizure initiation, we talk about seconds or less around the seizure beginning.

1.5 Long-term seizure dynamics

Considerable portion of this thesis will be devoted to the long-term dynamics of seizures and fluctuations of seizure probability. Thus, in this section we will deal with the second stage of the pyramid in Figure 2.

1.5.1 Importance of the long-term seizure dynamics

From the patient's perspective, seizures are usually unpredictable and occur suddenly with no apparent relationship to previous seizures, i.e. they seem to represent a so-called Poisson process. The unpredictability of seizures constitutes a significant debilitating factor for people with epilepsy (Cook et al 2013, Fisher et al 2000). However, numerous studies have demonstrated temporal relationships between seizures or at least fluctuations of seizure probability over time. Catamenial epilepsy in women, where seizures are related to menstrual cycle, is a common example of such fluctuations (Backstrom 1976, Bandler et al 1957, Griffiths & Fox 1938, Herzog et al 2004, Herzog et al 1997, Tauboll et al 1991). Nevertheless, fluctuations of seizure probability are well documented also in male patients suggesting that there exist also other factors governing temporal distribution of seizures than the menstrual cycle (Griffiths & Fox 1938, Tauboll et al 1991). The knowledge about long-term seizure dynamics and factors driving it is crucial for understanding epilepsy and for treatment. It can significantly contribute to our understanding of the mechanisms behind seizure generation. The knowledge of the spontaneous long-term seizure dynamics is crucial in testing of antiepileptic drugs (or other treatment strategies) where the natural fluctuation in seizure susceptibility can distort the results if it is not taken into account. Long-term fluctuation increases the variance of seizure frequency compared to a Poisson process which is commonly, but rather incorrectly, taken as a model of seizure distribution (Balish et al 1991). From a clinical perspective, understanding the seizure dynamics can facilitate introduction of chronotherapy into the treatment of epilepsy which take into account the existence of periods with and low risk to seizures. It can help to improve algorithms for seizure prediction (Karoly et al 2016, Sunderam et al 2007, Tauboll et al 1991) or at least forecasting seizure probability (Baud et al 2018).

1.5.2 Are seizures Poissonian?

In mathematics, a process generating events completely randomly with no temporal relationships is called a Poisson process. The absence of temporal relationships between events implies that the Poisson process is memoryless (Binnie et al 1984). The memorylessness means that the waiting time until the next event does not depend on how much time has elapsed since the last one (Sornette & Knopoff 1997). This property dictates that the inter-event intervals x in the Poisson process are independent and identically distributed according to the equation

$$f(x) = \lambda \mathrm{e}^{-\lambda x}, \quad (x \geq 0, \lambda > 0) \qquad \textbf{(1)}$$

where λ is the probability rate of occurrence, the only parameter of the Poisson process (Cox & Lewis 1966). The number of events N_i in an interval of a given length t can be shown to have a Poisson distribution

$$\mathrm{prob}(N_i = r) = \frac{(\lambda t)^r \mathrm{e}^{-\lambda t}}{r!}, \quad (r = 0, 1, \dots) \qquad \textbf{(2)}$$

If there are n events during an observation period t_0, it can be shown that an unbiased estimate of the probability rate of occurrence is

$$\hat{\lambda} = \frac{n}{t_0} \quad \textbf{(3)}$$

If certain process is not Poissonian then there are time dependencies between the events and memory exists in the process; it has to remember at least when the last event happened in order to properly schedule the next event (Cox & Lewis 1966).

Several studies have investigated whether long-term seizure profiles as recorded in patients' seizure diaries are Poissonian (Balish et al 1991, Bauer & Burr 2001, Binnie et al 1984, Milton et al 1987, Tauboll et al 1991). In these studies, the first step was to confirm, that the seizures of a given patient are stationary, i.e. their probability rate of occurrence does not change over the course of the study. A common but not the only sources of non-stationarity were a change in medication or surgical treatment. Binnie et al (1984), Milton et al (1987) and Tauboll et al (1991) either removed the non-stationary diaries from subsequent analysis or split them into several stationary diaries. Balish et al (1991) and Bauer & Burr (2001) used a method of analysis where possible trends can be revealed and do not confound the analysis of Poissonian character or clustering. Whether seizures were Poissonian was examined by testing the following hypotheses:

1. Inter-seizure intervals (ISIs) have an exponential distribution
2. The number of seizures per day follow a Poisson distribution
3. The successive ISIs or seizure counts on consecutive days are uncorrelated (Balish et al 1991 and Bauer & Burr 2001)
4. The variance-to-mean ratio (VMR) of daily seizure counts equals 1 (which is a characteristic of the Poisson distribution; (Balish et al 1991 and Bauer & Burr 2001)

If any of these hypotheses was rejected for a given seizure diary, it was deemed non-Poissonian. The results of the five mentioned studies are fairly consistent and they are summarized in Table 1. The percentage of diaries which were proved to be non-Poissonian was between 42 and 92% in these studies.

Table 1: Results of studies investigating whether patient seizures represent Poisson process

Study	Total number of diaries	Number of stationary diaries	Number of non-Poissonian
Balish et al (1991)	13	7	12
Bauer & Burr (2001)	63	26	52
Binnie et al (1984)	40	31	18
Milton et al (1987)	24	22	10
Tauboll et al (1991)	21	17	11

(Sunderam et al 2007) analyzed seizures of 26 epilepsy surgery candidates undergoing pre-surgical invasive exploration. They have shown that inter-seizure intervals (ISIs) and seizure intensities are inter-correlated with up to three previous seizures in 12/26 and 13/26 patients, respectively. This observation represents a proof that seizures in these patients are non-Poissonian. Cook et al (2014) revealed much longer inter-dependencies in the long-term (up to two years) intracranial records which they acquired during their clinical trial of a seizure prediction device (Cook et al 2013). Baud et al (2018) evaluated the rate of interictal epileptiform discharges (IED) and seizures detected from intracranial EEG recorded by a chronically implanted device (Morrell 2011). The authors reported phase locking of seizures to

cycles of IED rate. The seizures preferred the rising edges of the IED rate. Thus, seizure occurrence was likely influenced either by the IEDs per se or by the same mechanism that governs the IED rate. This observation renders the existence of patterns in seizure occurrence highly probable and thus argues against Poissonian nature of the seizures.

1.5.3 Do seizures follow power law?

Power-law behavior was reported in a wide range of natural as well as man-made systems such as earthquakes, forest fires, word frequency, scientific paper citations, visits to web pages and many others (Bak 1996, Newman 2005, Osorio et al 2009).

Power-law distribution of a variable *x* can be defined as

$$p(x) = Cx^{-\alpha}, \quad \alpha > 1, x > 0 \qquad \textbf{(4)}$$

where parameter α is called the exponent of the distribution and C is a normalizing constant ensuring that the integral of the distribution is equal to one. In the real world the power law holds only for limited range of x. Thus, it is practical to define the minimum possible value x_{min} such that $x \geq x_{min}$. Then,

$$C = (\alpha - 1)x_{min}^{\alpha-1}, \ \ \alpha > 1 \qquad \textbf{(5)}$$

(Newman 2005).

Since the brain is a complex system composed of interconnected non-linear oscillators (neurons), the power law can also be suspected in its dynamics. Indeed, Parish et al (2004) have shown that fluctuations of EEG energy in human hippocampus follows a power law. Sizes of neuronal avalanches in cortical organotypic cultures as well as in acute cortical slices were found to follow power-law distribution with α = 1.5 (Beggs & Plenz 2003). The same results were found also in the cortex of urethane-anesthetized rats and in awake macaque monkeys (Klaus et al 2011, Petermann et al 2009). It was argued that the the power-law behavior suggests that the cortical networks are in a critical state near the transition between order and disorder (Petermann et al 2009). Such state optimizes the information transmition (Beggs & Plenz 2003). In another studies (Osorio et al 2009, Osorio et al 2010), sizes of seizures (defined as a product of maximum power during the seizure and the duration of the seizure) as well as inter-seizure intervals (ISIs) followed power-law distribution. The exponent α of the distribution of event sizes was 1.67. For the ISI distribution, both Osorio et al (2009) and Cook et al (2014) came to the same estimate of the power-law distribution exponent α = 1.5.

1.5.4 Expected waiting time to the next event

The task of seizure prediction or forecasting can be also formulated as how long are we going to wait until the next seizure occurs. If seizures were a Poisson process, the knowledge of the time of the last event would not improve our estimate of the waiting time until the next one. However, there is ample evidence that seizures in the majority of patients are non-Poissonian (see paragraph 1.5.2), and, therefore, measuring the time from the last event is likely to be helpful.

In the research of timings of earthquakes, Davis et al (1989) examined a hypothesis: “The longer it has been since the last earthquake, the longer the expected time till the next”. Sornette & Knopoff (1997) have shown analytically that whether this hypothesis is true depends on the probability distribution of the inter-event times. It is true for fat-tailed distributions such as the power-law distribution. Osorio et al (2010) examined this hypothesis in both earthquakes and seizures respectively. In both cases, the hypothesis was true, indicating fat tails of inter-event interval distributions of both systems. Interestingly, they found many more similarities between statistical properties of seizures and earthquakes suggesting that these two phenomena may share the common dynamical principles, possibly the self-organized criticality (Bak 1996).

1.5.5 Circadian fluctuations of seizure probability

The circadian rhythms are responsible for one of the most common types of seizure probability fluctuation. The association between the occurrence of seizures and sleep/wake cycle has been well documented in the past (Frederick L. Patry 1931, Griffiths & Fox 1938, Quigg et al 2000). Hence, dozens of studies addressed circadian rhythmicity in epileptic seizure occurrence. Hofstra et al (2009) found statistically significantly non-uniform seizure distribution in patients undergoing intra-cranial EEG monitoring. It is now increasingly recognized that the timing of circadian seizure clustering is highly individual and depends on the specific type of epileptic disorder. Mirzoev et al (2012) performed a meta-analysis of multiple studies focused on circadian seizure probability. They concluded that the peak in circadian incidence of seizures is determined by the location of the seizure focus. In mesial temporal lobe epilepsy (mTLE), two peaks in seizure incidence were found in the majority of the reviewed studies. The first peak occurred in the morning and the second one in the afternoon. In a recent study, Karoly et al (2016) analyzed long-term intracranial EEG records of chronically implanted pharmacoresistant patients. In their data, circadian patterns of seizure occurrence were observed in 13/15 patients. Goldenholz et al (2018) analyzed 633 thousands of seizures of 9 698 patients who entered their seizures in to Seizure Tracker database. Seizure clusters (defined as certain number of seizures within a certain time period, e.g. 3 seizures within one day) occur during daytime with higher odds ratio than isolated seizure events.

Regarding animal studies, Bertram & Cornett (1994) examined seizures in mTLE model in which spontaneous recurrent seizures develop following electrically induced status epilepticus (SE) in rats. They observed the majority of seizures during the light period of the 12/12 hour light/dark regime. Importantly, in the same model, Quigg et al (2000) have shown that these fluctuations in seizure propensity persist even in constant dark environment suggesting that they are truly of circadian nature and not just a simple reaction to light or darkness.

In another post-SE model of mTLE, in which the SE was induced by intra-peritoneal administration of pilocarpine , Arida et al (1999) reported higher seizure incidence during the day which is in agreement with circadian distribution of the first spontaneous seizures of rats in the study of Cavalheiro et al (1991). Pitsch et al (2017) explored the pilocarpine model in mice and they found that the seizures tended to cluster between 4 p.m. and 7 p.m. which represents the end of inactive period in mice (mice, as well as rats, are nocturnal animals). This finding possibly corresponds to the morning incidence of seizures in two patients reported by Karoly et al (2016) and to the morning peak of seizure probability in patients with mTLE (Mirzoev et al 2012). On the other hand, Bajorat et al (2011), reported the absence of any circadian fluctuation in the pilocarpine model of mTLE in rats which seems to be in contradiction with Arida's results. Bajorat et al. speculated that difference in the age of SE (1 month vs. 2 months in Arida's vs. Bajorat's study) could be responsible for the contradictory results of these two studies.

In a post-SE model of mTLE induced by intraperitoneal kainic acid (shortly kainate model), Hellier & Dudek (1999) observed significantly more seizures during an inactive state of the rats compared to active states such as walking, grooming or eating. They also observed more seizures during light period compared to dark period although the difference was not statistically significant. Raedt et al (2009) observed higher seizure incidence during light period in the intrahippocampal kainic acid model in rats.

Stewart et al (2008) analyzed circadian variation in seizure occurrence of Aldh5a1 null mice, model of succinic semialdehyde dehydrogenase (SSADH) deficiency. It models an autosomal recessive disorder of GABA metabolism associated with motor impairment and epileptic seizures. They found a peak in seizure incidence at the beginning of the dark period (beginning of the active part of the day of the mice).

Another type of studies investigated acute seizures induced by various means. For instance, acute seizures induced by intraperitoneally administered pilocarpine were more severe and occurred with shorter latency during the dark phase compared to seizures induced during the light phase (Stewart et al 2001).

Fenoglio-Simeone et al (2009) have shown in Kcna1-null mice that also the opposite effect is true: not only circadian rhythms influence the seizure propensity, but also seizures have capacity to disrupt physiological circadian rhythms. Interestingly, feeding animals with ketogenic diet not only decreased the seizure frequency but also abolished circadian seizure periodicity and restored physiological circadian rhythms.

From our perspective, an important study is a work of Sedigh-Sarvestani et al (2014) in which they examined the circadian nature of seizure occurrence in the tetanus toxin model. They reported that during the light period the seizure rate was 1.3±0.32 seizures per hour and during the dark period it was 0.84±0.34 (mean±SD).

High clinical importance of the study of the circadian (and potentially other) fluctuations in seizure propensity is illustrated by studies reporting better seizure control or better drug tolerance in chronotherapeutic (i.e. adjusted to patient-specific circadian variation of the seizure propensity) dosing of anti-seizure drugs in patients (Guilhoto et al 2011, Yegnanarayan et al 2006).

1.6 Seizure clustering

The most common form of long-term seizure dynamics is seizure clustering. Seizure clustering was seen in most of the studies reviewed in the previous chapter. In this section, we will review these and other studies from the clustering point of view.

1.6.1 Definition of seizure clustering

Various definitions of seizure clusters can be found in literature. Basically, they can be divided into two types. The first type defines the cluster as a specified number of seizures within a certain time interval, e.g. at least 3 seizures in one day (Haut et al 2005b). These clusters are sometimes referred to as acute repetitive seizures (Fisher et al 2015). The second type defines a seizure cluster statistically (e.g. as a 3-fold increase of seizure frequency with respect to baseline; Fisher et al 2015). The advantage of the first type is its simplicity which makes it suitable for clinical application. However, substantial shortcoming of this type of definitions is its dependence on absolute seizure frequency. For example patients with high seizure frequency would experience clusters every day which is not congruent with general notion of the term clustering. Thus, many authors define clustering statistically.

1.6.2 Seizure clustering in patients

Seizure clustering was reported in a number of patient studies. The main results are summarized in Table 2.

Table 2: Studies reporting seizure clustering in patients.

Study	Proportion of patients with seizure clusters	Definition of seizure cluster
Balish et al (1991)	10/13 (78 %)	Number of seizures on a given day correlated with the number of seizures on the previous day
Bauer & Burr (2001)	36/63 (57 %)	Significant increase of seizure frequency compared to Poisson process
Cook et al (2014)	5/8 (63 %)	Hurst exponent $0.5 > H > 1$ was interpreted as clustering of seizures
Fisher et al (2015)	36.5 %	≥ 2 seizures within one calendar day
Griffiths & Fox (1938)	Not quantified	A marked increase in seizure frequency
Haut et al (2005a)	37/87 (43 %)	≥ 3 seizures in 24 hours (clinical definition)
Haut et al (2005a)	19/87 (22 %)	More days containing ≥ 2 seizures than would correspond to Poisson distribution (statistical definition)
Milton et al (1987)	3/24 (13 %)	More days containing a high number of seizures than would correspond to Poisson distribution
Osorio et al (2009)	Only population data presented	Seizure probability 30 min before and after a seizure, the power-law behavior of ISI
Sillanpaa & Schmidt (2008)	26/120 (22 %)	≥ 3 seizures in 24 hours
Tauboll et al (1991)	8/15 (53 %)	1) More days containing a high number of seizures than would correspond to Poisson distribution 2) Comparing the number of series of days with seizures to the number of series seizure-free days 3) Autoregressive feature in autocorrelogram of daily seizure counts

Fisher et al (2015) noted that the patients with such defined clusters had higher average seizure frequency than those who never experienced clusters which is of no surprise with the clinical definition of a seizure cluster. Interestingly, Haut et al (2005a) came to the same result regarding the seizure frequencies of clusterers and non-clusterers also with the statistical definition of clustering (non-Poissonian distribution of daily seizure counts). Periods of high seizure incidence were present in 7/15 patients analyzed by Karoly et al (2016) although they did not evaluate clustering quantitatively and, therefore, we did not include this study in the Table 2. Clustering (defined as ≥ 3 seizures in 24 hours) during AED treatment (but not clustering prior to beginning of treatment) is also associated with poorer prognosis in terms of remission and mortality as was shown in 120 children with epilepsy (Sillanpaa & Schmidt 2008).

1.6.3 Seizure clustering in animal models

Studies reporting seizure clustering in animal models are less frequent. These studies prove the existence of seizure clustering in various animal models.

Pitsch et al (2017) reported seizure clustering in mice with chronic epilepsy caused by pilocarpine-induced status epilepticus (SE) although they did not clearly state whether the clustering was of circadian nature or had a longer period. Cavalheiro et al (1991) reported clusters of 4 – 7 seizures in one day in 4/7 pilocarpine-treated rats with mean seizure frequency 2 – 4 seizures/week. A strong clustering pattern was described in the same model of epilepsy by Bajorat et al (2011). In 5/11 rats, they observed clusters with duration of 4 – 6 days interleaved by 4 – 22 days of seizure freedom. Their results replicated those of Arida et al (1999) and loosely also the results of Goffin et al (2007) who described cyclic seizure clustering pattern with a period of 5 – 8 days. Seizure clustering with inter-cluster periods of 1 – 14 days was also observed in mouse pilocarpine model (Mazzuferi et al 2012).

In the kainate model of epilepsy, Grabenstatter et al (2005) described occasional clusters of 6 – 18 seizures per 6 hour epoch. Intra-cluster ISIs were between 9 and 44 minutes. Williams et al (2009) also described clustering of seizures in this model of epilepsy. They reported typical inter-seizure interval less than 250 min (n>160 ISI) but also found a second peak in the ISI histogram at 3 – 4 days which corresponded to inter-cluster intervals.

Kadam et al (2010) studied epilepsy in rats which experienced hypoxic-ischemic injury at postnatal day 7. They observed up to two-day long clusters of 2 to 22 seizures separated by seizure-free periods of few days to several weeks.

Clusters of 3 to 7 seizures with ISI of 4 – 9 hours, separated by roughly 35-day inter-cluster periods were also observed in dogs with naturally occurring epilepsy (Howbert et al 2014).

An extremely important study from the perspective of our work is the one by Hawkins & Mellanby (1987). They used tetanus toxin model of mesial temporal lobe epilepsy in rats. They reported cyclic variation of the seizure frequency at the period of 4 – 6 days. In the later stages of the syndrome, the fluctuations were less pronounced in some rats.

Overall, the reviewed body of literature shows that in most patients as well as animal models seizure clustering is a common phenomenon. However, none of these studies addressed internal structure of the clusters. Thus, the main novelty of our work consists in the description of the intra-cluster seizure dynamics and proposition of a theory on the mechanisms behind this seizure dynamics.

1.7 Interictal epileptiform graphoelements

In the EEG recorded from an epileptic brain, not only seizures can be seen. There are several other electrographic abnormities commonly observed in the EEG, such as an interictal epileptiform discharges (IEDs; de Curtis et al 2012), high-frequency oscillations (HFOs) or disrupted rhythmogenesis such as focal slowing or frontal intermittent rhythmic delta activity (FIRDA; Javidan 2012).

1.7.1 Interictal epileptiform discharges (IEDs)

IEDs are the most common interictal electrographic phenomenon used in clinical practice to determine the presence of the epileptic brain tissue (Figure 3).

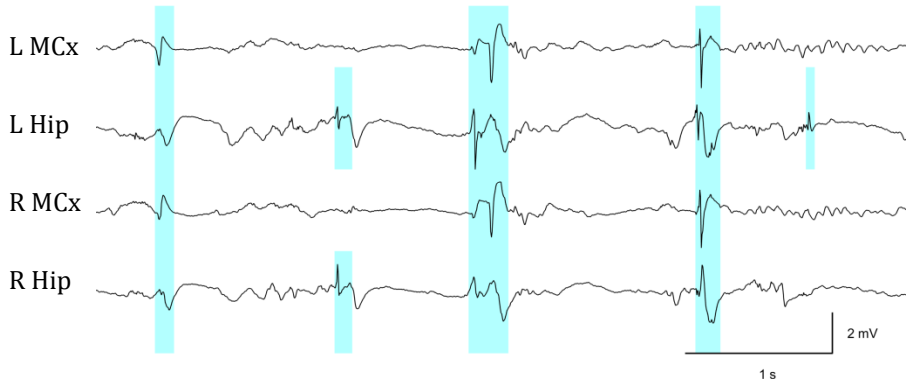

Figure 3: Examples of interictal epileptiform discharges (IEDs) recorded from rat R16. Note that some IEDs propagate from the hippocampi also to the cortices and some do not. One IED is unilateral in the left hippocampus. All IEDs except for the first and the last one are followed by a slow wave. Hip – hippocampus, MCx – motor cortex.

IEDs are routinely used for the diagnosis of epilepsy, diagnosis of specific epileptic syndromes, estimation of the risk of seizure recurrence after medication withdrawal and identification of surgically remediable epilepsies (Javidan 2012). IEDs are recorded in approximately 92% of patients with epilepsy and are very specific. Only 0.5% of adults without epilepsy have IEDs in their EEG (Javidan 2012). In mTLE, IEDs are usually more frequent during the non-REM sleep.

Mechanistically, the IED is a manifestation of a sudden synchronized activity of a neuronal population. It has been shown that both excitatory (glutamatergic) and inhibitory (GABAergic) neuronal networks are capable of IED generation. In the EEG, they present as a sharp spike (usually of 50 to 100 ms duration) often followed by a slow wave (usually of 200 to 500 ms duration) which constitutes a period of inhibition. Less sharp IEDs of duration 100 to 300 ms are called sharp waves. IEDs can occur in bursts or other patterns and often contain a superimposed high frequency oscillations (HFOs; Jiruska & Bragin 2011, Kudlacek et al 2017). During invasive intra-cranial EEG monitoring, IEDs are recorded from the seizure onset zone (SOZ) and from the surrounding tissue, so called the irritative zone. Some evidence suggests that IEDs recorded from the irritative zone may involve different mechanisms than those generated within the SOZ. In surgical treatment of epilepsy, the invasively recorded IEDs along with clinical and imaging data are routinely used for the delineation of the resection margin (Janca et al 2018, Javidan 2012).

1.7.2 Epileptic bursts

Bursts represent another type of interictal activity which was described experimentally in chronic model of temporal lobe epilepsy. It is a focal short high-amplitude oscillation at a frequency of 8 – 15 Hz and duration of 1 – 8 s. This type of activity was previously noted by Hawkins & Mellanby (1987). We will see that bursts have some interesting spatial as well as temporal properties. Chapter 5 will be devoted to the analysis of long-term changes in average burst properties.

1.8 Aim of this work

To investigate the long-term dynamics of seizures in the tetanus toxin model of epilepsy from a statistical perspective.

Hypotheses:

1. Seizures are not fully random, i.e. they are not a Poisson process

2. Seizures follow power law
3. Seizures cluster in time
4. Seizure profiles are governed by the character of seizures themselves
5. Inter-ictal activity is indicative of the impending seizure cluster

2 General methods

2.1 Animals

Two groups of animals were used. The first group consisted of 11 adult male Sprague-Dawley rats weighing approximately 250 g and it was part of the study which examined neurogenesis in tetanus toxin model of temporal lobe epilepsy and animals were implanted with wire-less telemetry (Jiruska et al 2013). The second group consisted of 9 Wistar rats weighing between 350 and 540 g. The animals were housed under standard conditions in a room with controlled temperature (22±1°C) and 12/12 hours light/dark cycle. The animals had ad libitum access to food and water. All animal experiments were performed under the Animal Care and Animal Protection Law of the Czech Republic fully compatible with the guidelines of the European Union directive 2010/63/EU or with the Animal Scientific Procedures Act (1986) of the United Kingdom and Institutional Ethical Review.

2.2 Surgery, electrode implantation and recording

In the first group, tetanus toxin injection and electrode implantation were performed under generalized ketamine/methibromide or isoflurane anesthesia. Small trephine openings were drilled symmetrically over both hippocampi at coordinates 4.1 mm caudal to bregma and 3.9 mm either side of the midline using the atlas of Paxinos & Watson (1998). Using a Hamilton microsyringe and infusion pump (KD Scientific Inc., USA) 1 µl of tetanus toxin (Sigma-Aldrich, UK) solution was injected into the stratum radiatum of the right dorsal hippocampal CA3 area. Tetanus toxin solution contained 25 ng of tetanus toxin in 1 µl of 0.05 M phosphate buffered saline (PBS; Sigma-Aldrich, UK) and 2% bovine serum albumin (Sigma-Aldrich, UK). Tetanus toxin solution was injected at speed of 200 nl/min. The microsyringe was left in place for five minutes after the injection ended to avoid backflow up the injection track. Following the injection, silver ball electrodes were inserted into both openings epidurally over both cortices and fixed to the skull using dental acrylic. Electrodes were connected to single channel bipolar telemetric transmitters (Data Sciences International, s'Hertogenbosch, Netherlands) which were implanted subcutaneously over the dorsal aspect of the thorax and secured with sutures. Following surgery, animals were housed in single cages and continuous electrocorticography monitoring started on the 4th day and continued until the 17th day. Electrocorticographic signals were recorded using Dataquest A.R.T. 4.3 acquisition system (Data Sciences International, s'Hertogenbosch, Netherlands) and sampled at 100 Hz. On day 17, animals were humanely overdosed with ketamine and then perfused using 0.9% saline followed by 4% paraformaldehyde. Brains were extracted and postfixed in 4% paraformaldehyde.

In the second group, surgery was performed under generalized isoflurane anesthesia. Using Hamilton 7001 syringe with blunt needle and electronic infusion pump (KD Scientific Inc., USA) 1 µl of tetanus toxin solution (Quadratech, UK) was injected into the stratum radiatum of the right dorsal hippocampal CA3 area, at coordinates AP: -4.1, L: 3.9, D: -3.8, using atlas of Paxinos & Watson (1998). Tetanus toxin solution contained 10 ng of tetanus toxin in 1 µl of 0.05 M phosphate buffered saline (PBS; Sigma-Aldrich, UK) and 2% bovine serum albumin (Sigma-Aldrich, UK). Tetanus neurotoxin solution was injected at speed of 200 nl/min and the microsyringe was left in place for five minutes after the injection ended to avoid backflow up the injection track. Afterwards, the animals were implanted bipolar twisted electrodes bilaterally in the dorsal hippocampus and motor cortex. The electrodes were made from silver wire with bare diameter of 120 µm insulated by 30 µm layer of PFA (A-M Systems, Inc., Carlsborg, Washington, USA). The two contacts of each electrode were 0.5 mm apart. The coordinates of hippocampal and cortical electrodes with respect to bregma were [AP: -4.6, L: 2.6, D: 3.3] and [AP: 1.5, L: 3.0, D: 1.5] respectively, according to atlas of Paxinos & Watson (1998). Ground/reference stainless steel jeweler's screws were placed over cerebellum. Following 5-day recovery period, the

animals were subjected to video-EEG monitoring for at least three weeks. Two different recording setups were used. The Neuralynx setup, consisted of a headstage unit gain amplifier HS-27 (Neuralynx, Bozeman, Montana, USA) and Lynx-8 amplifier (Neuralynx, Bozeman, Montana, USA) set to gain of 196, high-pass filter at 0.1 Hz and low-pass filter at 3 kHz. The signal was then digitized using Power 1401 AD converter (Cambridge Electronic Design, Cambridge, UK) at the sampling frequency of 10 kHz and 16 bit resolution and recorded to a computer using Spike2 software (Cambridge Electronic Design, Cambridge, UK). The synchronized video was recorded by Spike2 using a USB webcam. Signals recorded using Intan setup, were amplified, analog-filtered and digitized by RHD2132 headstage board (Intan Technologies, Los Angeles, California, USA). The digitized signals were transferred via swivel using SPI bus to RHD2000 evaluation board, which was connected to a computer via USB. The analog high-pass filter was set to 0.1 Hz and the low-pass filter to 1.7 kHz. Sampling frequency was 5 kHz and resolution was 16 bit. Custom-made software was used for recording. Video was recorded by a USB camera using also custom-made software.

2.3 Data analysis

Recorded signals were exported, reviewed and analyzed using Spike2 (Cambridge Electronic Design, Cambridge, UK) and custom made programs written in Matlab (Mathworks Inc., USA). The EEG recordings from the second group of rats were analyzed in the unipolar. Seizures were identified visually or we used a simple automatic detector based on thresholding of integral envelope of power in the frequency band 15 to 45 Hz. The threshold was set empirically for each rat to gain 100% sensitivity. Seizure labels were then manually reviewed and false detections removed. If the presence of artifacts complicated identification of seizures, visual analysis was combined with spectral analysis. Using fast Fourier transform, time-frequency maps were constructed and seizures were determined according to their characteristic spectral profiles (Figure 4C; Cook et al 2014, Schiff et al 2000). Only ictal discharges lasting more than 15 seconds were selected for subsequent statistical analysis and seizures less than 3 minutes apart were joined into 1 event. For each animal we obtained a series of seizure's onsets and durations.

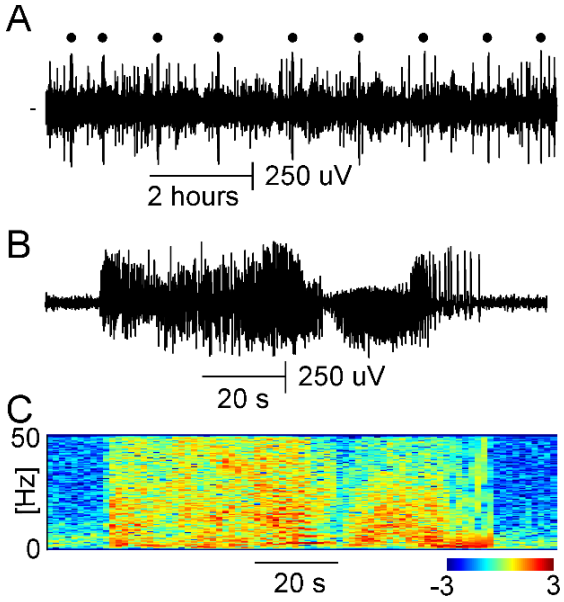

Figure 4: Telemetric electrocorticographic recording in a rat from the first group with temporal lobe epilepsy induced by injection of tetanus toxin to right dorsal hippocampus. A: Approximately 10 hours of spontaneous electrocorticogram. Seizures are marked by a black dot. B: Example of ictal recording and corresponding time-frequency plot (spectrogram; C).

3 Long-term temporal distribution of seizures

3.1 Introduction

In the first task, we aimed to explore whether seizures in the tetanus toxin model form the Poisson process. If Poissonian character is rejected then searching for inter-dependencies or patterns within the events is justified. The non-Poissonian character of seizure distribution suggests the existence of a specific principle governing the seizure dynamics. In multiple patient studies, the seizure profiles were found non-Poissonian. However, the results may be influenced by antiepileptic drug (AED) treatment or other therapeutic interventions. Animal studies have the advantage of providing long-term intra-cranial EEG data from subjects with untreated epilepsy.

If the seizure series is non-Poissonian, the next task is to find the nature of the seizure distribution and mechanisms behind the existence of possible inter-dependencies between seizures. The application of statistical approaches from the theory of complex systems suggested that seizures could behave according to the power law. Two groups have revealed power-law distributions of inter-seizure intervals (ISIs) in patients (Cook et al 2014, Osorio et al 2010).

Another approach to explore long-term seizure dynamics, ISI distribution and the existence of inter-dependencies is based on the conditional expected waiting time to the next event conditioned on the time elapsed since the last event. Osorio et al (2010) have shown that the conditional expected waiting time (CEWT) is an increasing function of the time since the last event which can be formulated that the longer it has been since the last seizure, the longer the expected time till the next.

A commonly accepted type of fluctuation of seizure probability is the circadian one. Sleep/wake cycle has been shown to influence seizure susceptibility in both patients and animal models. Hence, we will also analyze the circadian distribution of seizures in our animals.

3.2 Methods

3.2.1 Artificial data generation

In our analysis, we search for mathematical model which best describes the data. Hence, it is useful to generate artificial data according to those models to compare them to the original (recorded) data. We generated artificial quasiperiodic data (for simplicity labeled Periodic), a Poisson process and power-law data. Each artificial dataset contained the number of events equal to the average number of seizures in rats and the seizure frequency was also set to the rats' average seizure frequency.

3.2.1.1 Quasiperiodic data

In some analyses, it is illustrative to compare the results from seizure data to periodic data, i.e. data in which inter-event interval is constant. Because strictly periodic data are unlikely to occur in nature, we generated quasiperiodic data with inter-event intervals not precisely constant but normally distributed with mean equal to the mean ISI observed in animals and standard deviation equal to 0.25 times mean.

3.2.1.2 Artificial Poisson process

Poisson process was generated as a sorted vector of uniformly distributed numbers ranging from the average time of the first seizure to the average time of the last seizure counted from the

tetanus toxin injection in rats. Since the numbers were independent and uniformly distributed, they represent a Poisson process by the definition (Cox & Lewis 1966).

3.2.1.3 Artificial power-law series

Power-law series was generated using the following procedure. First, we assumed that the actual seizure profiles have power-law distributed inter-seizure intervals (ISIs) and estimated its exponent α. The exponent of power-law distribution can be estimated from the graphs with logarithmic scales on both axes using equations (20) or (22) (see section 3.2.2.4). However, this estimate is known to be biased (Newman 2005). Therefore, we estimated exponents of our data using maximum likelihood estimate according to the equation (Newman 2005)

$$\hat{\alpha} = 1 + \mathrm{n}\left[\sum_{i=1}^{n} \ln \frac{x_i}{x_{min}}\right] \quad \textbf{(6)}$$

where x_i are the actual ISIs, x_{min} is minimum inter-event time for which the power law holds and ln denotes natural logarithm. x_{min} was set to one hour since this was the value at which ISI log-log plot starts to be at least roughly linear (Figure 11). Using this formula we obtained $\alpha = 2.40$. We generated a series of power-law distributed ISIs and using cumulative sum, we transformed it into time series. Afterwards, the data were stretched by multiplying all the event times by a factor ensuring that the time between the first and last event was equal to the average range of the original seizure data. This transformation is possible because power-law distribution is scale invariant, i.e. if we scale x by a constant c the distribution remains the same except for the multiplicative constant $c^{-\alpha}$ (Newman 2005)

$$p(cx) = (\alpha - 1)x_{min}^{\alpha-1}(cx)^{-\alpha} \quad \textbf{(7)}$$

$$p(cx) = c^{-\alpha}\left[(\alpha - 1)x_{min}^{\alpha-1}(x)^{-\alpha}\right] \quad \textbf{(8)}$$

$$p(cx) = c^{-\alpha}p(x) \quad \textbf{(9)}$$

Finally, we added the average first seizure time (counted from tetanus toxin injections) to the event times.

3.2.2 Statistical analysis of seizure profiles

Animals in which signal dropouts or artifacts obscured significant number of seizures were excluded from the study. In the examination of seizure occurrence, animals from both groups were pooled. To examine possible patterns in seizure occurrence we performed the following analyses:

1. Visual inspection of seizure profiles
2. Tests whether the seizure profiles of individual animals are Poissonian
3. Tests whether the seizure profiles of individual animals follow power law
4. Calculation of expected waiting time till the next seizure
5. Calculation of expected inter-seizure interval
6. Analysis of possible circadian fluctuations in seizure incidence

3.2.2.1 Visual inspection of seizure profiles

Seizure profiles of each rat were plotted in two forms: events in time and a daily seizure count. For visual comparison, quasiperiodic, Poisson and power-law artificial data generated and plotted (Figure 5).

3.2.2.2 Graphical tests whether the seizure profiles are Poissonian

We used two graphical methods and three computational methods of assessing whether seizure profiles of our rats differ from Poisson process. The first graphical method is the one used by Cook et al (2014), Osorio et al (2009) and Osorio et al (2010). It is based on plotting the histogram of ISIs with logarithmic scale on the ordinate. The histogram is expected to be exponential according to equation (1) scaled by a constant C. If we take the logarithm of the histogram we obtain a linear function

$$\log(f(x)) = \log(\mathrm{C}\lambda \mathrm{e}^{-\lambda x}) \tag{10}$$

$$\log(f(x)) = \log(\mathrm{C}\lambda) + \frac{\ln(\mathrm{e}^{-\lambda x})}{\ln(10)} \tag{11}$$

$$\log(f(x)) = \mathrm{const} - \frac{\lambda}{\ln(10)} x \tag{12}$$

where log represents decadic logarithm although logarithm with any base could be used. Thus, logarithmic histogram of inter-event intervals in Poisson process is a straight line with the slope equal to the negative probability rate of occurrence divided by ln(10), i.e. approximately –0.43λ. Non-linearity of the logarithmic histogram of ISIs indicates their non-exponential distribution which is an evidence of non-Poissonian character of the data. The histogram method is not optimal when only small samples are available. In such case, to obtain reasonable ISI counts in each histogram bin, the bins need to be relatively wide and only few. Since we expected fewer points in higher values, we performed logarithmic binning. We used 8 logarithmic bins ranging from 0.1 to 100 hours. The counts in the bins were normalized by the bin size in hours. Despite the logarithmic binning, some bins still contained no data point.

In order to overcome problems arising from small data samples, we implemented a method recommended by Cox & Lewis (1966) which consists in plotting logarithmic empirical survivor function using ranking of the ISIs instead of grouping into bins. Empirical survivor function $R(x)$ is defined as the proportion of inter-event intervals longer than x plotted against x.

$$R(x) = 1 - \frac{i(x)}{n} \tag{13}$$

where i is the rank (order statistic) of an ISI of value x (in other words how many inter-event times in the data set are shorter or equal to x) and n is the total number of ISIs in the sample. Logarithmic empirical survivor function can then be defined as

$$\log\big(R(x)\big) = \log\left(1 - \frac{i(x)}{n+1}\right) \tag{14}$$

where in the denominator, $n + 1$ is used instead of just n to avoid problems arising at the highest x when $i(x) = n$ and thus the argument to the log would be zero (Cox & Lewis 1966). Theoretical survivor function $r(x)$ for exponentially distributed inter-event intervals x is

$$r(x) = P(X > x) = \int_{x}^{\infty} f(X)\mathrm{d}X = \int_{x}^{\infty} \lambda \mathrm{e}^{-\lambda X}\mathrm{d}X = \mathrm{e}^{-\lambda x} \quad \textbf{(15)}$$

where $f(X)$ is the probability distribution function (PDF) of ISI. Logarithmic theoretical survivor function is then

$$\log\big(r(x)\big) = \log\big(\mathrm{e}^{-\lambda x}\big) = -\frac{\lambda}{\ln(10)}x \quad \textbf{(16)}$$

Thus, logarithmic survivor function of data generated by Poisson process should, like the logarithmic histogram, follow a straight line with slope approximately –0.43λ. Non-linearity of logarithmic empirical survivor function again indicates non-Poissonian character of the data (Cox & Lewis 1966).

3.2.2.3 Numerical test whether seizure profiles are Poissonian

We adopted two methods proposed by Tauboll et al (1991). In the first method, we compute event counts in successive intervals of constant duration and compare the distribution of counts to a fitted Poisson distribution using the χ^2 goodness-of-fit test. The duration of the intervals was chosen one hour. In the second method, we compare the empirical distribution of inter-event times to a fitted exponential distribution, again using the χ^2 goodness-of-fit test. For the test, we used eight logarithmic bins ranging from to shortest to the longest inter-event interval observed in the analyzed series.

Next, we computed the Spearman correlation coefficient of successive ISI and corresponding p-values for the test of the null hypothesis that there is no correlation. Presence of the correlation suggests the absence of the Poisson process.

3.2.2.4 Graphical tests whether the seizure profiles follow power law

In analogy to the analysis of the Poisson process, the easiest way of assessing whether the series follows power law is based on a loglog plot of ISI histogram. In this case, both axes are in logarithmic scales. This type of plot is often called a loglog plot. The power-law probability density function (PDF) has the following form

$$p(x) = Cx^{-\alpha} \quad \textbf{(17)}$$

If we take logarithm of $p(x)$, we get

$$\log(p(x)) = \log(Cx^{-\alpha}) \quad \textbf{(18)}$$

$$\log(p(x)) = \log(C) + \log(x^{-\alpha}) \quad \textbf{(19)}$$

$$\log(p(x)) = \log(C) - \alpha\log(x) \quad \textbf{(20)}$$

Hence, in a loglog plot, the histogram of a power-law distributed quantity forms a straight line with slope equal to the exponent α of the distribution. Since the power-law distributed data have very few points at higher values, it is practical to construct histograms with logarithmic

binning. Since the abscissa is logarithmic, the bins appear linearly spaced on it. We used eight logarithmic bins spanning from 0.1 to 100 hours.

Due to limited number of ISI samples, we constructed the logarithmic empirical survivor function according to the equation (14). Theoretical survivor function of the power-law distributed inter-event intervals x is

$$r(x) = P(X > x) = \int_x^\infty f(X)\mathrm{d}X = \int_x^\infty CX^{-\alpha}\mathrm{d}X = \frac{C}{\alpha - 1}x^{-(\alpha-1)} = C_r x^{-(\alpha-1)} \quad \textbf{(21)}$$

The survivor function also follows power law but with exponent of $\alpha - 1$. Now we take the logarithm of the survivor function

$$\log\big(r(x)\big) = \log(C_r) - (\alpha - 1)\log(x) \quad \textbf{(22)}$$

The survivor function of a power-law distributed series should appear as a straight line with slope $\alpha - 1$ in a loglog plot. Deviation from linearity of the plot suggests that the series does not follow the power law.

3.2.2.5 Expected waiting time till the next seizure

Let's first consider unconditional expected waiting time to the next event. Imagine we appear at random time point and have no knowledge about any of the past or future events but we know the probability distribution $p(x)$ of inter-event intervals. Then, the probability density of being in an inter-event interval of length x is the fraction of total time occupied by inter-event intervals of that length

$$P(x) = \frac{xp(x)}{\int_0^\infty Xp(X)\mathrm{d}X} \quad \textbf{(23)}$$

where x is the inter-event interval and X is a dummy variable for integration of inter-event interval PDF p (Sornette & Knopoff 1997). Now, assume we appear at any random point (with uniform probability distribution) within the inter-event interval of length x so the expected waiting time within that inter-event interval is $x/2$. Then, the unconditional expected waiting time (UEWT) till the next event is

$$UEWT = \int_0^\infty \frac{x}{2}\frac{xp(x)}{\int_0^\infty Xp(X)\mathrm{d}X}\mathrm{d}x \quad \textbf{(24)}$$

In the case of empirical data, we estimate the unconditional expected waiting time according to the formula

$$\widehat{UEWT} = \sum_i^N \frac{x_i^2}{2\sum_k^N x_k} \quad \textbf{(25)}$$

where x is an inter-event interval, N is the total number of inter-event intervals in the data set and i and k are indices of the inter-event interval used for summation.

Let's now consider the situation when we know that certain time t has elapsed since the last event and we ask what the expected time τ that we will wait till the next event is. Thus we are seeking for the conditional expected waiting time

$$CEWT(t) = \mathrm{E}(\tau|t) \tag{26}$$

(Osorio et al 2010, Sornette & Knopoff 1997). This is equal to the mean of the portion of the $p(x)$ after t normalized by the probability that no event has occurred since the last event (in other words that the event is going to occur from now on)

$$CEWT(t) = \frac{\int_0^\infty \tau\, p(t+\tau)\mathrm{d}\tau}{\int_t^\infty p(x)\mathrm{d}x} \tag{27}$$

(Sornette & Knopoff 1997). By a simple change of variable ($x = t + \tau$) we get

$$CEWT(t) = \frac{\int_t^\infty (x-t)\, p(x)\mathrm{d}x}{\int_t^\infty p(x)\mathrm{d}x} \tag{28}$$

which is than easily transformed into the form suitable for algorithmization and computation with empirical data

$$\widehat{CEWT}(t) = \frac{\sum((x-t)|x>t)}{n_{x>t}} \tag{29}$$

where in the numerator all inter-event intervals x longer than t are lowered by t (thus transformed to τ) and summed. The denominator is simply the number of inter-event intervals longer than t. Since there is no relationship of successive inter-event intervals involved, this formula can be used with no modification also for an aggregate of inter-seizure intervals (ISIs) from multiple subjects.

3.2.2.6 Circadian fluctuations of seizure probability

To explore the circadian changes in seizure occurrence, we adopted and modified the method used by Quigg et al (2000). We divided the time of the day into eight three-hour bins. Certain studies (e.g. Raedt et al 2009, Hellier & Dudek 1999, Bajorat et al 2011) used only two bins for statistical evaluation (light and dark phase of the day). This approach may be less suitable in cases with two or more circadian peaks in seizure occurrence (e.g. with mesial temporal lobe epilepsy) or in cases when a single peak occurring at the transition between light and dark periods (Pitsch et al 2017). The selection of a low number of bins is insufficient to explore circadian dynamics in greater detail and could lead to false negative observations. Hence, we used the eight bins not only for visualization but also for the statistical computations.

For each rat, we constructed histograms of seizure incidence in the eight bins (Figure 14). The histograms were normalized by the total duration of recording available for given time-of-day bin to account for the border effects resulting from the fact that the animals were not connected and disconnected from the monitoring at the same time of the day (e.g. if the rat was connected to the monitoring in the morning and after the recording period disconnected in the evening, more recording was available for the day time than for the night time). The histograms were visually reviewed. Next, we performed χ^2 goodness-of-fit test to determine whether the numbers of seizures in the bins differed significantly from uniform distribution which was

expected under the null hypothesis of no circadian fluctuation. The same analysis was done with the aggregate of all seizures from all rats. The result can be, however, confounded by large inter-individual variation in total number of seizures.

For the population statistics we also adopted the approach used by Stewart et al (2001) who used analysis of variance (ANOVA) to evaluate whether the seizure probability in the time bins differs from the uniform distribution. The input to the ANOVA test was seizure probabilities of each rat in each time bin. This ensured that all rats had the same weight regardless of their total number of seizures.

3.3 Results

3.3.1 Qualitative visual inspection of seizure profiles

Seizure profiles as well as artificial quasi-periodic, Poissonian and power-law data are plotted in Figure 5. In 15/17 rats, we observed long-term fluctuation and clustering of seizures. Moreover, gradual increase of ISI during the course of individual clusters can be observed in multiple animals.

Clustering, visually somewhat similar to the one observed in seizure profiles, can be observed also in the artificial data with power-law distributed ISIs whereas in quasi-periodic and Poissonian artificial series the events are more evenly distributed. We will analyze the seizure clusters more thoroughly in Chapter 4.

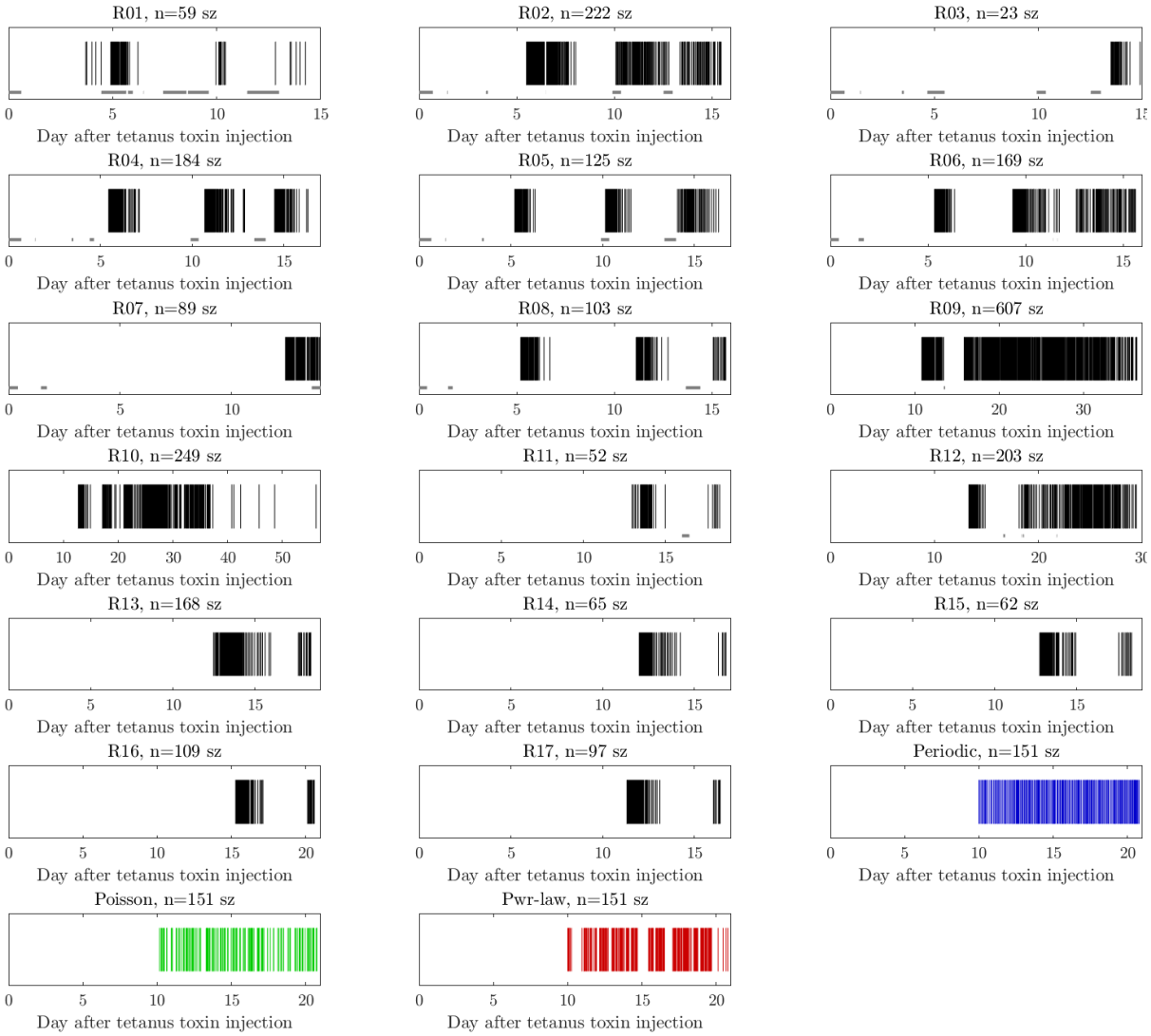

Figure 5: Seizure profiles of individual rats and artificial quasi-periodic, Poissonian and power-law data. Exponent of the power-law series is $\alpha = 2.40$. Grey line marks signal dropouts. In 15/17 we observed clustering of seizures. In R03 and R07, clustering could not be assessed due to brevity of the recording. Rats R09 and R12 experienced one typical cluster followed by a long period where no clustering was apparent. R10 had two clusters followed by the long non-clustering period. Note that the clustering seizure profiles are qualitatively most similar to the power-law artificial data.

Looking at Figure 6, we can again see clear clustering tendencies in seizure profiles which manifest as deep fluctuations in the daily seizure count. Similar pattern of clusters of events is observed in the power-law data. In the Poissonian data, some fluctuations of the daily seizure count are visible as well but are less prominent than in the power-law or seizure data. In the quasi-periodic data the daily event count is, expectedly, almost constant.

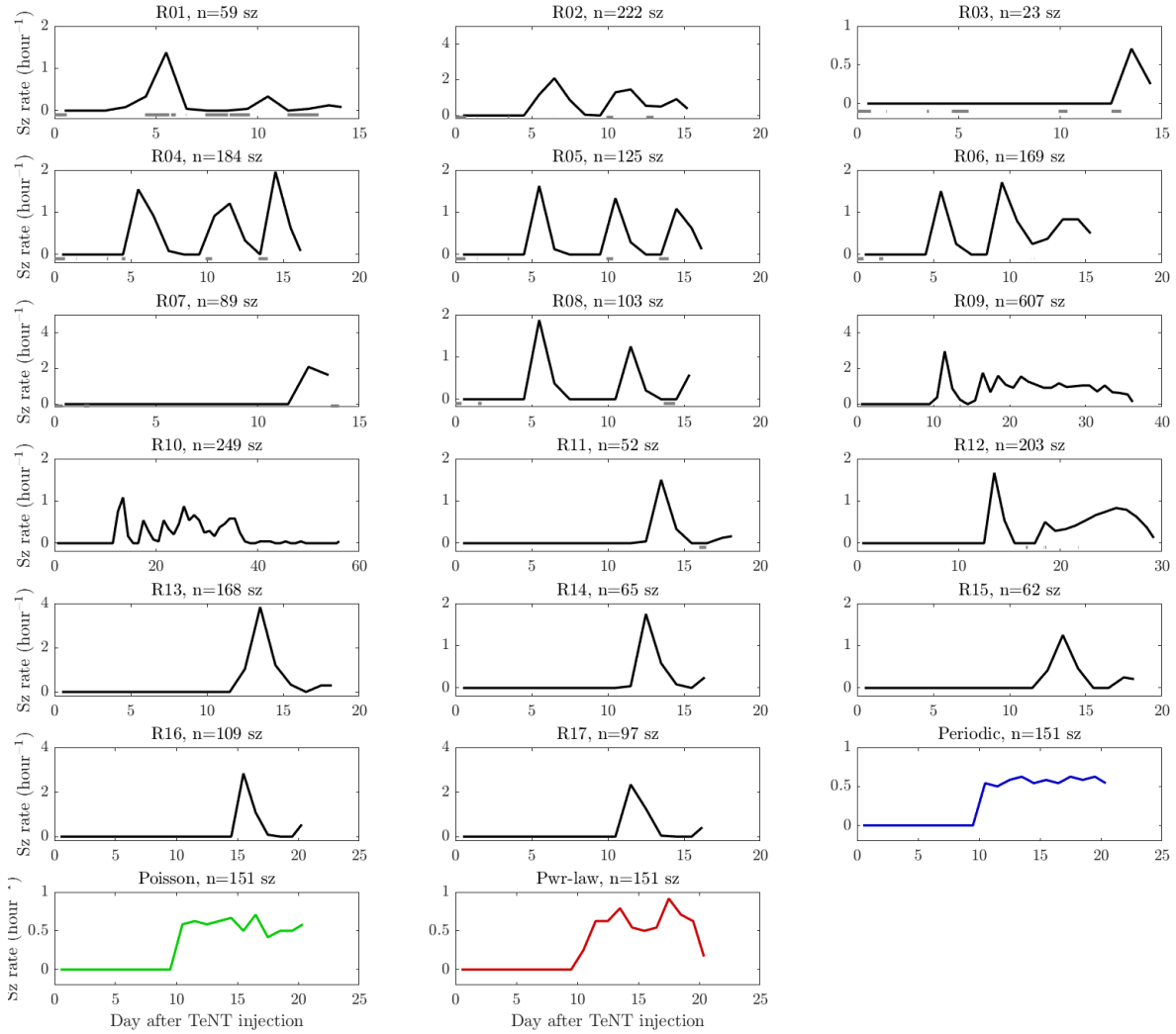

Figure 6: Seizure rate in the original seizure profiles and artificial data series evaluated in 24-hour bins. The seizure fluctuations of seizure series are qualitatively most similar to the fluctuation of event frequency of the power-law artificial data.

3.3.2 Basic statistics

Data will be given as mean±std (median). We analyzed on average 152±33 (109) seizures from each of the 17 animals. First seizure occurred on day 12±1 (14), where the day of tetanus toxin injection was day 0. Average seizure duration was 81±2 (52) s. Mean inter-seizure interval (ISI) was 103±9 (40) min. In total, we identified 26 clusters and 9 intercluster periods. Mean cluster duration was 46±3 (42) hours and mean intercluster period was 61±10 (56) hours.

3.3.3 Are the seizure profiles Poissonian?

We used graphical as well as numerical methods of assessing whether the seizures form a Poisson process.

3.3.3.1 Graphical methods

To assess whether the seizure profiles represent a Poisson process, we first plotted logarithmic histogram of ISIs (Figure 7). Logarithmic histogram of the inter-event times of the artificial Poisson process is a straight line with a slope of approximately –0.22. The mean event frequency λ of the artificial Poisson process is 0.58 events/hour which implies that the predicted slope of the logarithmic histogram should be $-0.43 \cdot 0.58 = -0.25$. The discrepancy between the

predicted and actual value of slope is probably due to the brevity of the data and lack of sufficient number of the longer intervals. In 16/17 rats there is a non-negligible proportion of extremely long ISI which can be regarded as a so called fat tail of the ISI distribution indicative of clustering tendency of the seizures.

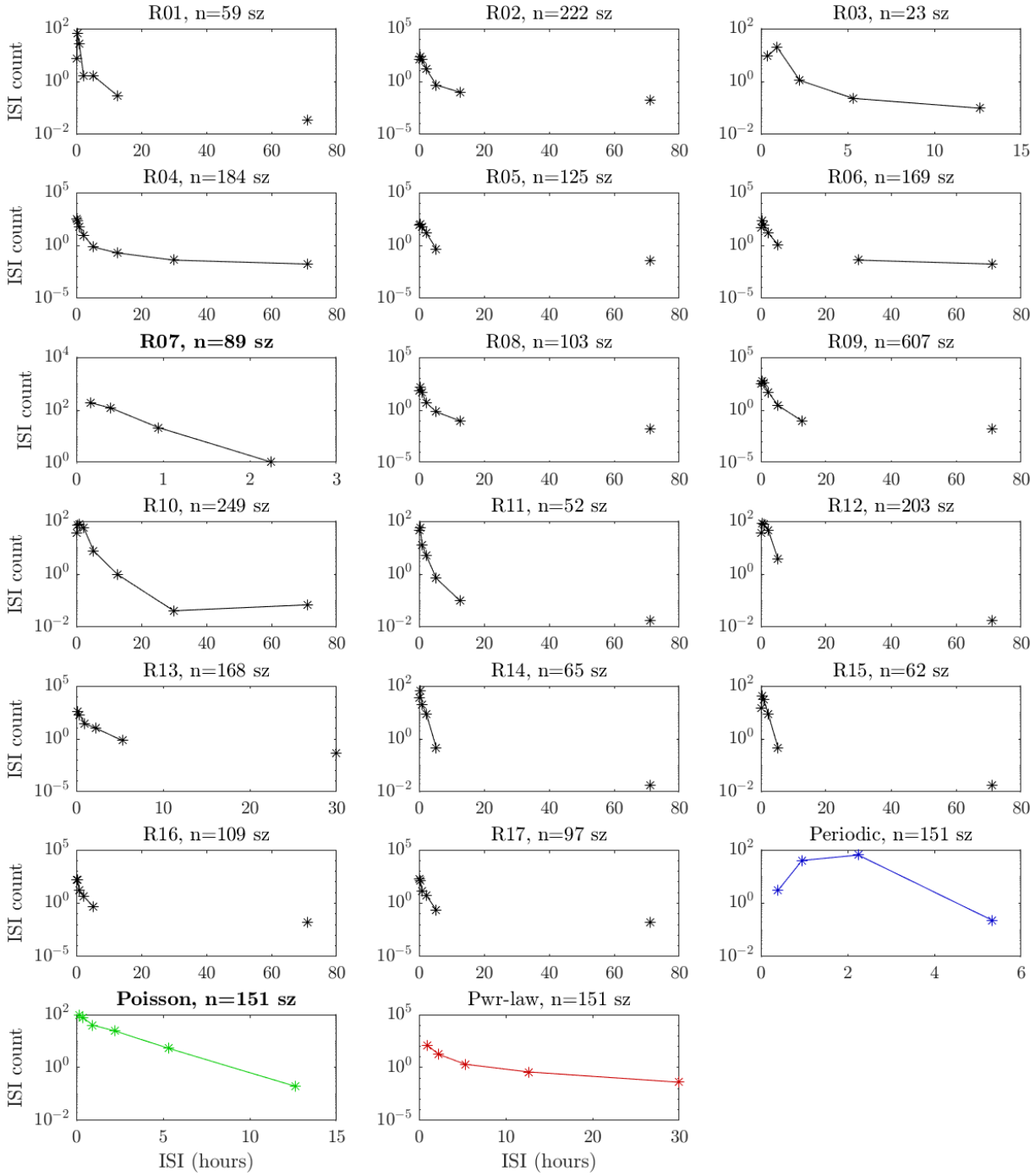

Figure 7: Logarithmic histograms of ISIs and inter-event intervals of artificial series. In most subjects, some bins were empty which lead to the break of the line, often the last bin was preceded by several empty bins resulting in a single marker at the tail of the distribution. Straight line is consistent with the Poisson process (title in bold font). Note that all rats except for R07 contain non-negligible proportion of extremely long ISIs. Compare the seizure data to the artificial Poisson and power-law series and note the tendency for a fat tail of most rats' ISI distribution.

In most rats, the logarithmic histograms suffer from low number of bins due to low numbers of seizures. In Figure 8, we plotted logarithmic survivor functions for each rat and corresponding artificial Poisson process. The survivor functions of all rats except for rat R07 were non-linear which suggests non-Poissonian character of their seizure profile. The survivor function of the Poisson process is linear, again with the slope of –0.22, which is approximately equal to the negative of hourly event rate λ divided by ln(10), i.e. $-0.43 \cdot 0.58 = -0.25$.

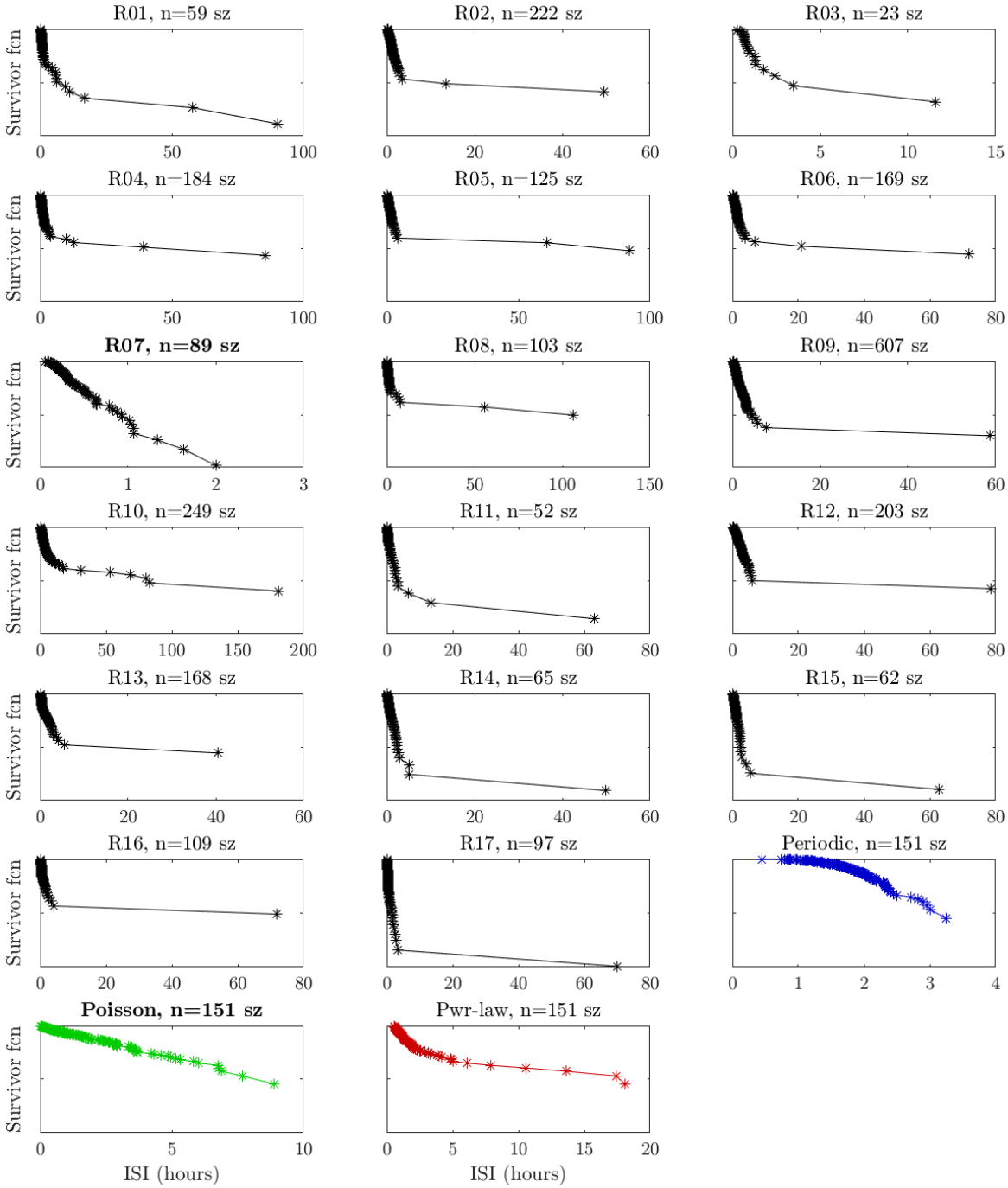

Figure 8: Logarithmic survivor function of ISI and inter-event intervals of artificial series. Straight line is consistent with the Poisson process (title in bold font). Note that all rats except for R07 contain non-negligible proportion of extremely long ISIs. Compare the seizure data to the artificial Poisson and power-law series and note the tendency for a fat tail of most rats' ISI distribution.

3.3.3.2 Numerical tests

At first, we compared empirical distributions of hourly counts of seizures or artificial events to a fitted Poisson distribution using χ^2 goodness-of-fit test. The resulting p-values are in the first column of Table 3. In 12/17 rats the seizure counts did not have a Poisson distribution.

Then we compared the ISI or inter-event interval distribution to a fitted exponential distribution again using χ^2 goodness-of-fit test (second column of Table 3). In 16/17 rats, the ISI distribution was different from exponential.

An important property of the Poisson process is the uncorrelated inter-event intervals. Thus, we tested Spearman's rank correlation of successive ISI or inter-event intervals. Third row of Table 3 shows the Spearman correlation coefficients (not p-values like the previous two columns). Green shading indicates statistical significance of the correlation at $p<0.05$. In all rats the successive ISI were significantly correlated whereas in the artificial data, there is no significant correlation. Quasi-periodic and power-law data are significantly different from the Poisson process in both tests whereas Poissonian data are not, as expected. All artificial series have uncorrelated successive inter-event intervals whereas in all rat seizure series the correlation of successive ISI is statistically significant (3rd column of Table 3). Thus, none of the seizure profiles is Poissonian. Counts of seizures and ISI distribution bring additional evidence for non-Poissonian character of the seizures in most animals (1st and 2nd column of Table 3).

Table 3: First column: p-values of χ^2 goodness-of-fit test whether hourly seizure or event count follows Poisson distribution. Green shading indicates $p<0.05$. Second column: p-values of χ^2 goodness-of-fit test whether inter-event interval distribution follows exponential distribution. Green shading indicates $p<0.05$. Third column: Spearman correlation coefficient of successive inter-event intervals. Green shading indicates that the correlation coefficient is statistically significantly different from zero with $p<0.05$. In R03 the ISI distribution could not be tested for difference from exponential due to the brevity of the data (NaN - Not a Number).

	Counts Poisson	ISI Exponential	ISI Correlation
R01	0.00	0.00	0.66
R02	0.96	0.00	0.46
R03	0.38	NaN	0.66
R04	0.00	0.00	0.56
R05	0.00	0.00	0.58
R06	0.03	0.00	0.68
R07	0.46	0.00	0.62
R08	0.00	0.00	0.57
R09	0.01	0.00	0.33
R10	0.19	0.00	0.70
R11	0.00	0.00	0.48
R12	0.00	0.00	0.63
R13	0.00	0.00	0.45
R14	0.00	0.00	0.56
R15	0.48	0.00	0.48
R16	0.00	0.00	0.42
R17	0.00	0.00	0.59
Periodic	0.00	0.00	-0.01
Poisson	0.29	0.27	-0.02
Pwr-law	0.00	0.00	0.02

3.3.4 Do the seizures follow power law?

We plotted ISI histograms and survivor functions for each rat. This time the plot has logarithmic scaling on both axes (loglog plot) because, according to equation (22), in this type of

plot, power-law distributed data appear as a straight line. The slope of the line is equal to the exponent $-\alpha$ of the distribution in histograms and $-(\alpha - 1)$ in the survivor functions.

Although the histograms of most rats are not linear, all rats except R07 exhibit some form of fat tail. The fat tail is caused predominantly by inter-cluster intervals. The artificial power-law series which was generated with the exponent $\alpha = 2.40$ (see paragraph 3.2.1.3 for the details) has the slope –2.32 which is roughly in agreement with the equation (20).

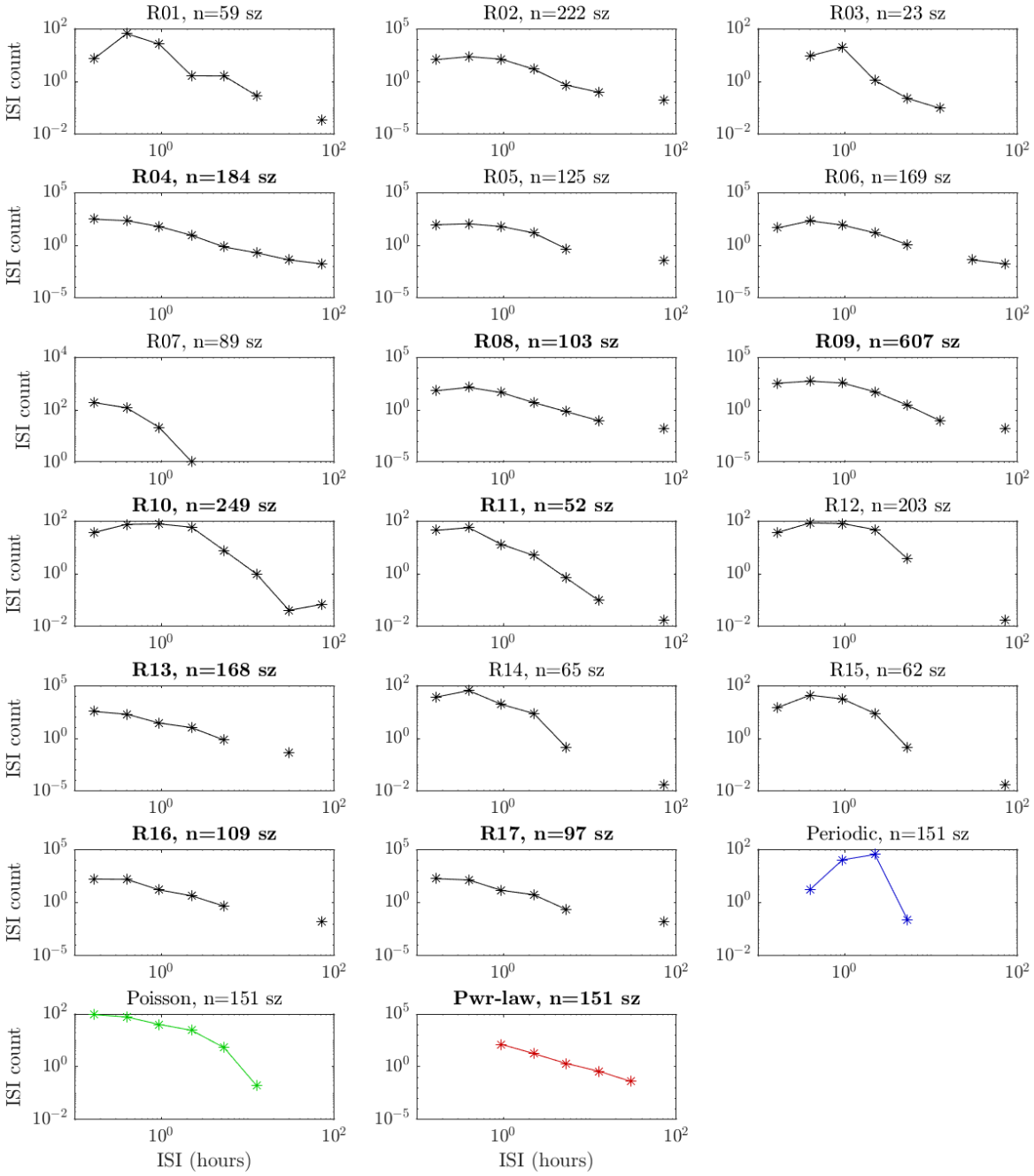

Figure 9: ISI histograms with logarithmic scaling on both axes. Data points on a straight line indicate power-law distribution of ISI. Profiles in which at least part of the ISI range displays power-law behavior are marked by the bold font of the title. In several subjects, some bins were empty which lead to the break of the line. All rats excepts for R07 tend to fat-tailed distribution of ISIs. Compare the seizure data to the artificial Poisson and power-law series and note the tendency for a fat tail of most rats' ISI distribution.

Survivor functions are more informative since they display more data points. In 8/17 rats, power-law behavior was observed in limited ranges of ISI. The artificial power-law data are on a straight line with the slope of –1.36 which corresponds quite well, due to equations (21) and (22), to the exponent α = 2.40 with which the series was created (see paragraph 3.2.1.3).

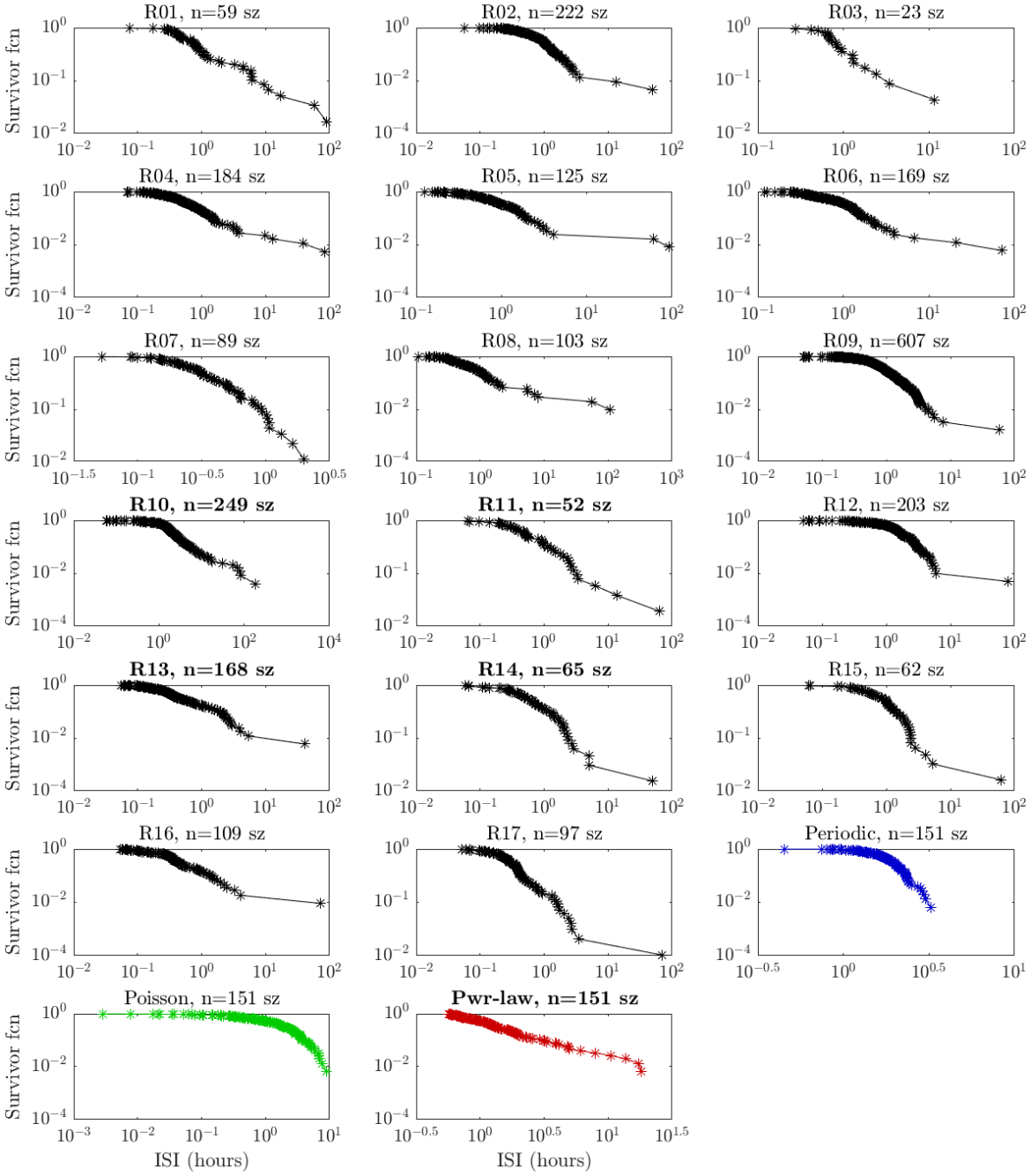

Figure 10: Logarithmic survivor functions with logarithmic scaling also on abscissa. Points lying on a straight line indicate power-law distribution of the ISIs. Profiles in which at least part of the ISI range (most often 0.5 to 5 hours) displays power-law behavior are marked by the bold font of the title. Compare the seizure data to the artificial Poisson and power-law series and note the tendency for a fat tail of most rats' ISI distribution.

3.3.5 Population graphs

We plotted ISI histograms and survivor functions for aggregate of ISIs of all analyzed rats since by the aggregation we get more data and thus more power to detect deviation from

Poissonian and power-law behavior (Figure 11). Before the aggregation, for the logarithmic plots, the time series of individual rats were transformed to a mean rate of 1 event/hour. This normalization ensured that if all individual seizure series were Poissonian their ISI histograms and logarithmic survivor functions would form straight lines with the same slope. Then, the aggregate logarithmic ISI histogram and logarithmic survivor function would be also linear. In case of the power-law data this normalization would have no effect due to the scale-free property.

The graphs in Figure 11A and Figure 11B have logarithmic scaling on ordinate and thus their linearity would indicate Poissonian behavior of the series. However, the histogram as well as the survivor function display strong non-linearity marked by fat tails.

The graphs Figure 11C and Figure 11D contain loglog plots and their linearity would indicate power-law behavior. They seem linear in a very limited range of less than a decade (1 to 5 hours) but this is insufficient to consider the data power-law distributed. The non-linearity could be theoretically caused by differences in the exponents of individual series that were aggregated. However, the loglog plots of individual series do not seem linear either except for some limited ranges (see section 3.3.4, Figure 9 and Figure 10). Moreover, Figure 11C reveals so called characteristic scales, i.e. typical sizes of ISI, which is in contradiction with the power law. The characteristic scales are 15 hours and 70 hours. The latter one is more pronounced and probably reflects the inter-cluster intervals.

To conclude, the data exhibit neither Poissonian nor power-law behavior.

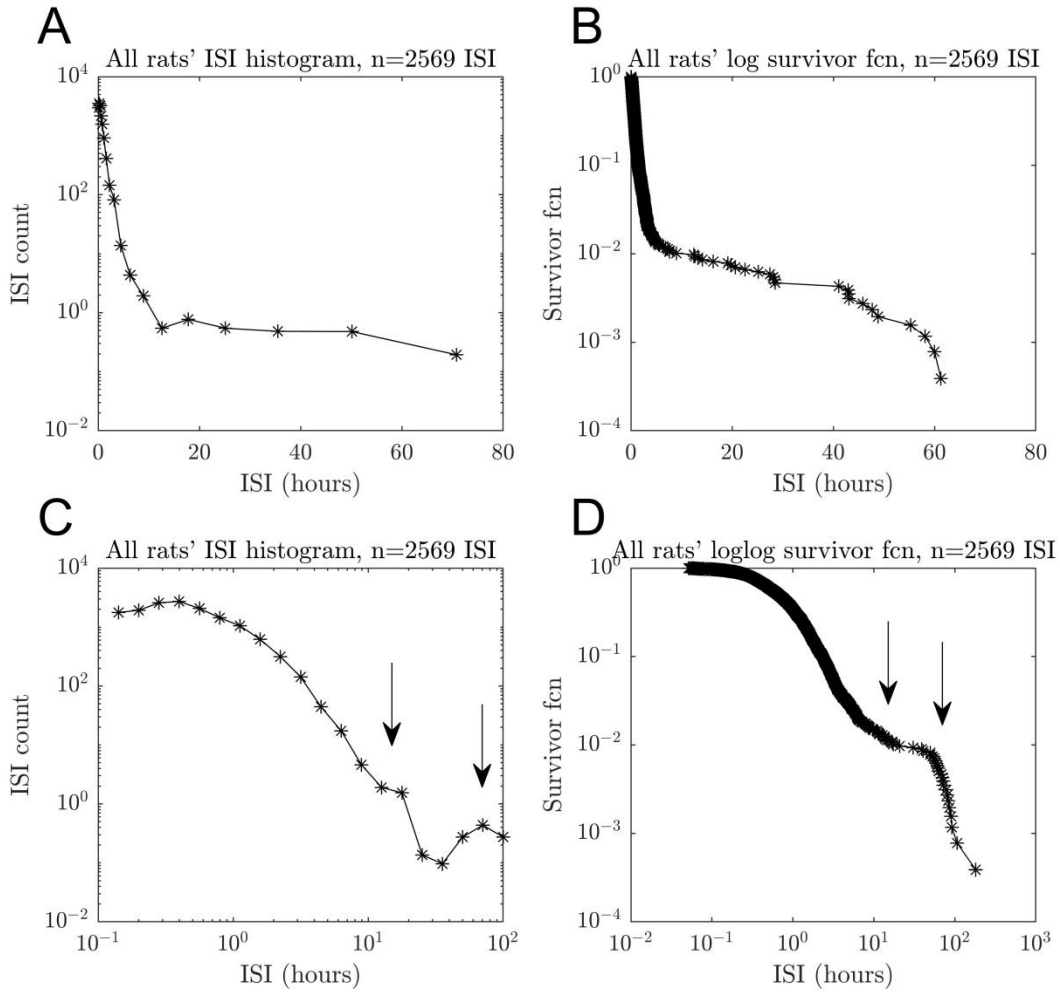

Figure 11: ISI histograms and survivor functions for aggregated ISIs of the whole population of 17 rats. Linearity of the logarithmic histogram (A) and logarithmic survivor function (B) would indicate Poissonian behavior. However, the graphs are clearly non-linear with pronounced fat tail. Linearity of the loglog histogram and loglog survivor function (C, D) would suggest power-law behavior. These graphs are linear in a very limited range of 1 to 5 hours. Note the characteristic scales at 15 and 70 hours (arrows). In the survivor function, the characteristic scales manifest as a steeper decrease. The 70 hour scale may correspond to the inter-cluster intervals.

3.3.6 Expected waiting time to the next seizure

In Figure 12 we plotted conditional expected waiting time (CEWT) to the next event conditioned on the time elapsed since the last one calculated according to equation (29). For comparison we also plotted unconditional expected waiting time (UEWT, dashed line) which does not take into account any knowledge of the past event, only the ISI distribution. In all subjects except for R07, CEWT is clearly increasing function which was confirmed by the statistically significantly positive Pearson correlation coefficient *r*. For the *r* calculation, both CEWT and time since the last event was transformed by decadic logarithm so that the *r* was calculated on the same data that is visible in the plots. Note that for artificial Poisson process the CEWT is constant and equal to the UEWT which means that the knowledge of past event does not improve our estimate of when the next event will happen. This is actually one of possible definitions of the Poisson process. In case of quasiperiodic series, CEWT is decreasing.

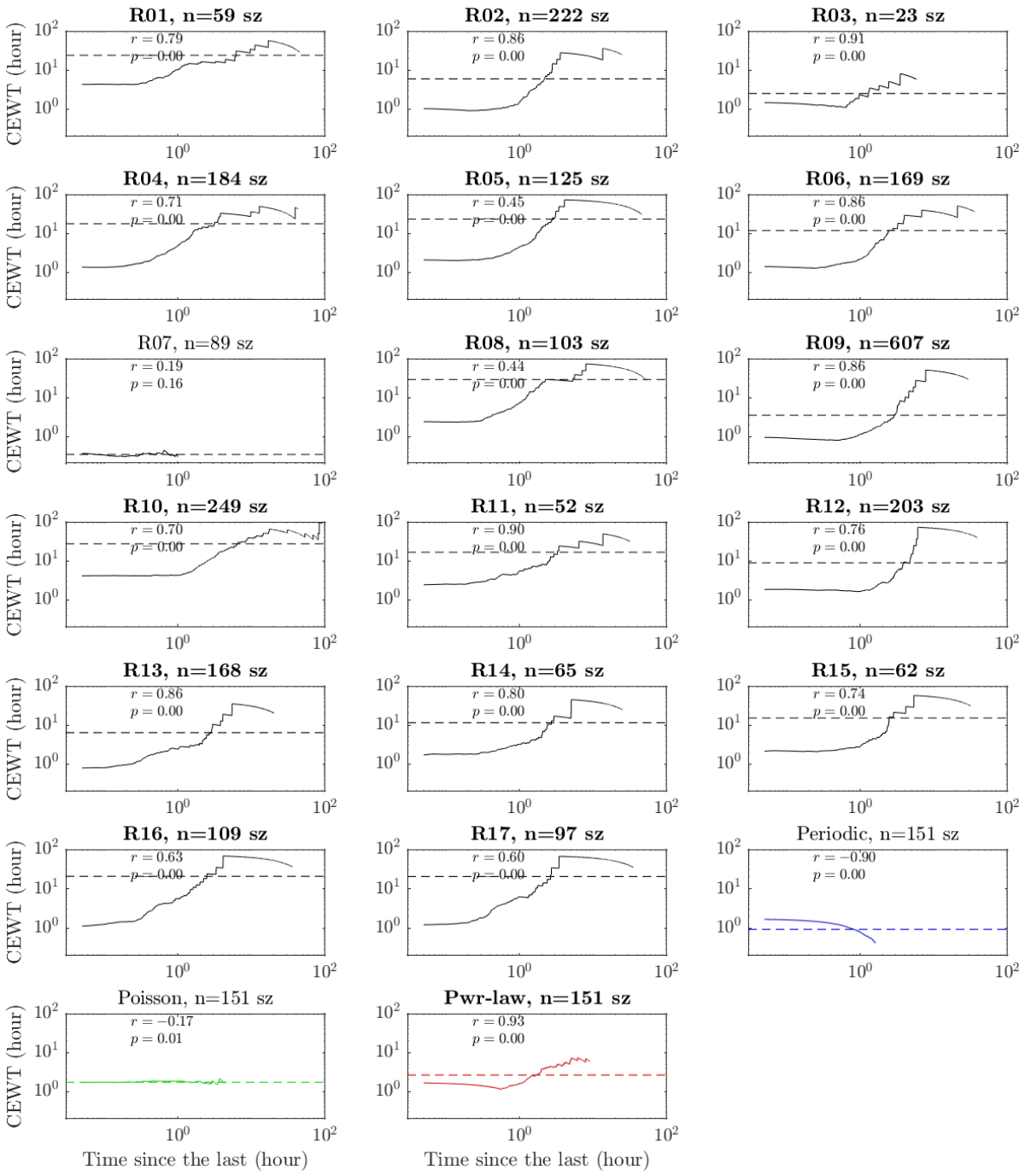

Figure 12: Conditional expected waiting time (CEWT, solid line) to the next event calculated from inter-seizure intervals as a function of the time since the last event. Dashed line indicates the unconditional expected waiting time (UEWT). CEWT is an increasing function for all series except for R07, the quasiperiodic series (denoted as Periodic for simplicity) and the Poisson series. For the artificial Poisson process, the CEWT is equal to the UEWT. In case of quasiperiodic series the CEWT is decreasing. *r* – Pearson correlation coefficient, *p* – *p*-value of the *r*

Analysis of CEWT from the aggregate of all ISIs from all 17 animals of is in Figure 13. The increasing trend is prominent although at longer times since last event the curve decreases and increases again. This is likely an effect of the extremely long inter-cluster intervals. The Pearson's *r* was computed the same way as in the case of individual seizure profiles.

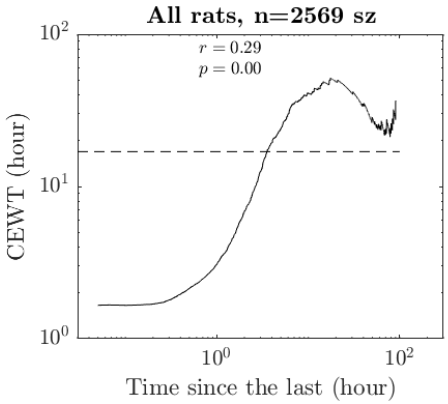

Figure 13: Conditional expected waiting time (CEWT) analysis of the aggregate of all ISIs from all 17 animals. CEWT is clearly increasing with a local decrease at the higher times since the last event. *r* – Pearson correlation coefficient, *p* – *p*-value of the *r*

3.3.7 Circadian fluctuations of seizure probability

First, we plotted histograms of seizure incidence according to time of the day for each rat and artificial series (Figure 14). Next, we analyzed whether these histograms differ from uniform distribution using χ^2 goodness-of-fit test. In 8/17 the fluctuation was significant with slight prevalence of seizures during the light period although the patterns of individual rats did not look similar.

When all seizures of all rats were aggregated into one data set (Figure 15), the difference of the circadian distribution of seizure incidence from the uniform was significant with $p<0.0001$. To assess whether the observed circadian fluctuations were consistent across subjects we performed one-way ANOVA on the set of individual rats' profiles. The trend was not significant ($p = 0.19$) which can be visually confirmed by the boxplot in Figure 16.

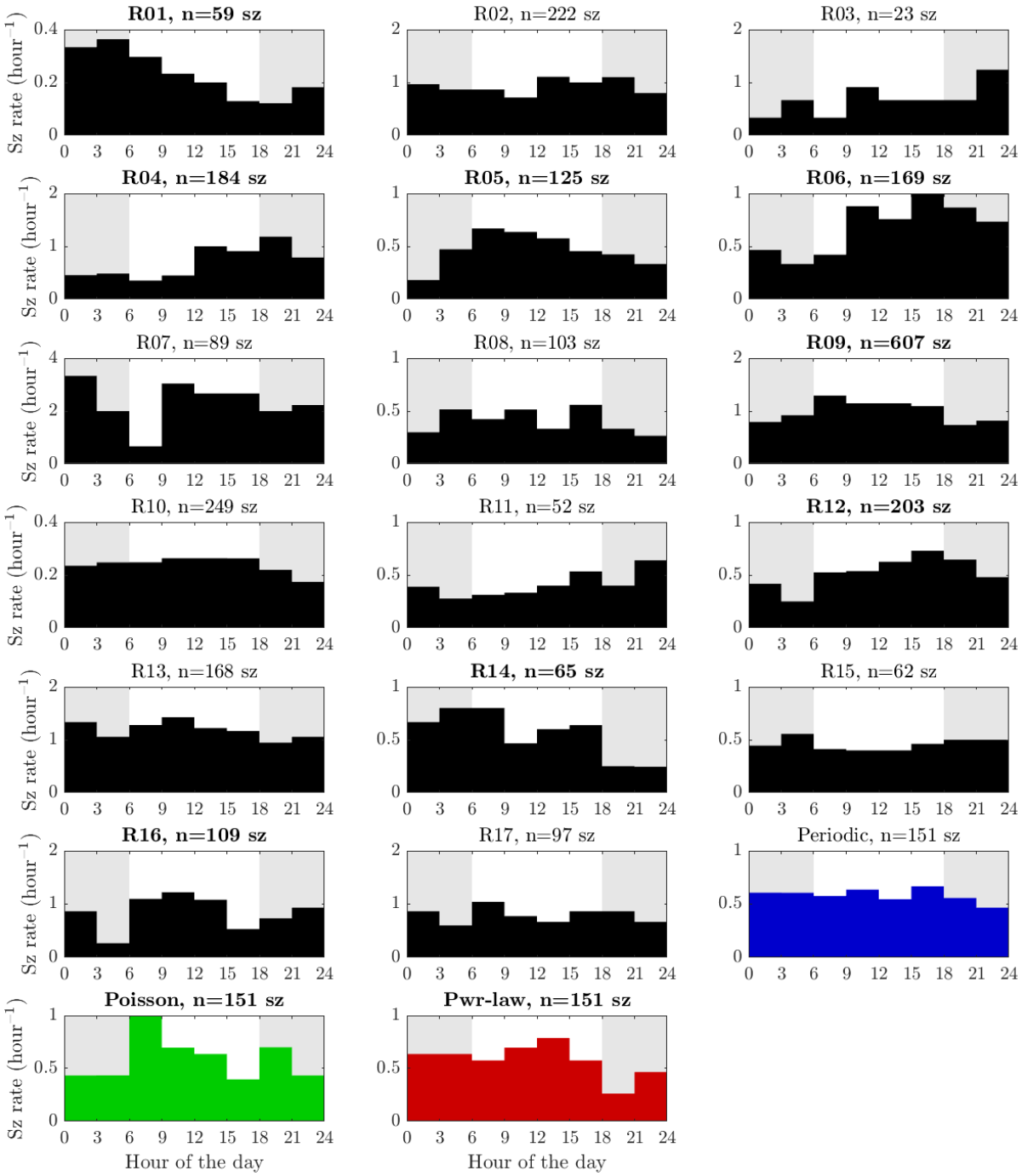

Figure 14: Histograms of seizure incidence with respect to time of the day. Light bars - non-significant, dark bars - significant fluctuation of seizure probability ($\chi 2$ goodness-of-fit test, $p<0.05$). Light grey shading indicates dark periods. Poisson and power-law artificial data also showed non-uniform circadian distribution.

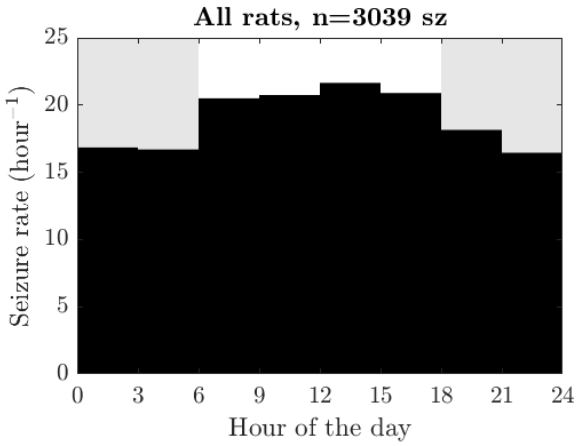

Figure 15: Histogram of seizure incidence according to time of the day for the aggregate of all seizures of all rats. The $\chi 2$ goodness-of-fit test is significant with p <0.0001. Light grey shading indicates dark periods.

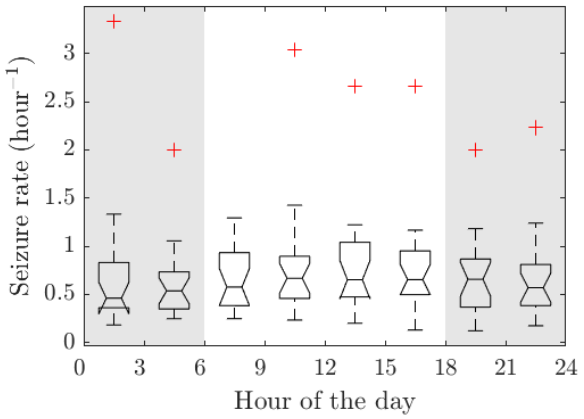

Figure 16: Boxplot of the aggregate data. Horizontal lines at the center of each box represent medians. Bottom and top edges of the boxes represent 1st and 3rd quartiles, respectively. Whiskers extend to most distant data points not considered as outliers. Outliers are specified as the data points deviating more than 1.5 times inter-quartile range from the quartile. Notch indicates 95% confidence interval. Note that all confidence intervals overlap with each other indicating that the trend in daily fluctuation is not significant which was confirmed by ANOVA resulting in p=0.94. Light grey shading indicates dark periods.

3.4 Discussion

In this chapter we have shown that:

1. Seizures tend to occur in visually identifiable clusters although non-clustering patterns were observed as well, especially in the later part of the recordings of several animals.
2. Seizure profiles are by no means a Poisson process.
3. Seizure profiles in 47% of rats exhibit power-law behavior in a limited range of less than one decade (order of magnitude).
4. The conditional expected waiting time (CEWT) till the next event is an increasing function of the conditioning time since the last event.
5. In terms of circadian distribution, there is a weak but significant trend for higher seizure incidence during the light phase of the day. However, the circadian patterns are not consistent across animals.

Clustering is a commonly observed type of seizure susceptibility fluctuation in patients as well as in animal models. Although clustering could be considered as evidence of non-Poissonian character of seizures we decided to disprove the possibility of Poissonian distribution of seizures by more rigorous mathematical methods. We had two reasons for this

1. Poisson process plays a pivotal role in the analysis of series of events because it is the only memoryless process (Cox & Lewis 1966). Presence of memory in seizure profiles is good news because it raises the possibility of forecasting the seizure probability or even prediction of individual seizures. If seizure distribution would follow the Poissonian process the predictability or forecasting of seizure would be difficult or virtually impossible since the memorylessness property indicates the absence of any underlying mechanism (Varsavsky et al 2011).
2. Poisson process is commonly (and probably wrongly) considered a model of seizure occurrence (Balish et al 1991, Hopkins et al 1985). We provide additional evidence that this assumption can't be applied to all seizures and epilepsies.

In all the reviewed human studies, a considerable proportion (42 to 96%) of patients was proved non-Poissonian. Animal studies of this kind are lacking but in most animal models of epilepsy, the seizures tend to cluster which suggests their non-Poissonian nature.

In contrast to the Poisson process, the power-law behavior is compatible with seizure clustering (Sornette & Knopoff 1997). Two studies have reported power-law distribution of ISI (Cook et al 2014, Osorio et al 2009). Although Osorio et al (2009) included in their study also extremely short ISI (in the order of seconds), the power-law behavior was apparent also in the higher ISI ranges of up to 1 day. Cook et al (2014) found power-law behavior of ISI at the time-scales of 1 to 50,000 hours. Although the Cook's data are less convincing since the data points do not form an absolutely straight line, an important fact is that both studies came to the same value of the exponent α = 1.5. Combining these two pivotal studies, we can conclude that the power-law behavior is present in human ISI in an extraordinarily wide time scale range of eight decades, i.e. ranging from few seconds to several years. In our data we did not confirm any strong power-law behavior. It is plausible that seizures in the tetanus toxin model display different dynamics compared to seizures in humans with pharmacoresistant epilepsy. Another possible limitation of our study is the brevity of the recordings in most rats, especially compared to the recordings obtained in patients with chronically implanted devices (Cook et al 2014). Interestingly, our ISI histograms often have even fatter tails than power-law distribution, probably due to the presence of the inter-cluster intervals.

In this study, we have confirmed that the CEWT is an increasing function of the time since the last event. This observation can be interpreted as the positive answer to question "The longer it has been since the last seizure the longer the expected time till the next?" (Sornette & Knopoff 1997). This is probably connected with the clustering. Intuitively, if we are within a seizure cluster we are not waiting any long since the last seizure and the next seizure is likely to happen early. A long time since the last seizure can happen only outside the clusters and if we are outside of the clusters we are quite likely to wait long till the next seizure. This has also mathematical connection to the fat tail of the ISI distribution (Sornette & Knopoff 1997).

As opposed to most human and animal studies we found no circadian pattern of seizure occurrence that would be consistent across animals similarly to Bajorat et al (2011) who experimented with pilocarpine treated rats. However, when the seizures from all subjects were aggregated, the increase of seizure incidence during the light period was significant which corresponds to the results of Hellier & Dudek (1999) obtained in pilocarpine treated rats and to the results of Stewart et al (2008) obtained in Aldh5a1 null mice. Pitsch et al (2017) proved non-uniform circadian seizure distribution in pilocarpine treated mice by ANOVA applied to profiles of individual animals, i.e. not in aggregate data and thus, suggesting a consistent pattern across the animals which we did not find. Similar results were found also in rats after an electrically

induced status epilepticus (Quigg et al 2000) and in kainate treated rats (Raedt et al 2009) where seizures occurred preferentially during the light period.

To conclude, the overall pattern of seizure incidence in our rats was non-Poissonian and largely non-power-law. The ISI distributions had fat tails due to the presence of large inter-cluster intervals. Circadian patterns were inconsistent across animals but in aggregate data slight preference of the light period was found.

4 Seizure clusters

4.1 Introduction

Definition of seizure clustering is rather inconsistent across different studies. In clinical setting, seizure clusters are usually defined as a certain number of seizures per day which is an easily applicable criterion. We will use a statistical definition of clustering because it is independent of the absolute seizure frequency (Fisher et al 2015). Seizure clustering is a very common phenomenon observed in 13 – 78 % of human patients. It was also reported in dogs with naturally occurring epilepsy and, importantly, in experimental rodent models of epilepsy.

4.2 Methods

Based on visual observation of seizure profiles from our rats, we defined a cluster of seizures as a group of at least 10 seizures separated by inter-seizure interval (ISI) of no more than 12 hours and lasting no more than 96 hours. Some of the analyses which were performed for the whole seizure profiles were performed also for the clusters. We also generated artificial series that match cluster properties using the same procedure as for the series matching whole seizure profiles (see section 3.2.1). The exponent of the power-law series was estimated to α=2.8 which was more than the exponent of the whole profiles.

4.2.1 Correlations of seizure parameters with intra-cluster time

Correlations of various parameters (e.g. intra-cluster time and seizure duration) were in individual clusters assessed using Spearman's non-parametric correlation coefficient ρ as implemented in Matlab R2017b function `corr`. The p-values for the null hypothesis that the ρ is zero were obtained from the same Matlab function as its second output argument.

In the case of population analyses, we used slightly different approach. First, we divided the cluster into equal time bins and calculated the mean (or median) of the parameter measured on all seizures within the bin. For the purpose of visualization, we calculated bin means over clusters and standard errors of the means (SEM). For statistical evaluation, we fitted the bin means from each cluster by a straight line using the Matlab function `polyfit`, extracted the linear term coefficient (slope of the line) and then determined whether the slopes of the lines are significantly different from zero using Wilcoxon signed rank test (Matlab function `signrank`).

4.2.2 Propagation of seizure activity and behavioral manifestations

Since we use the model of mesial temporal lobe epilepsy (mTLE), the seizures originate in mesial temporal structures, most often in the hippocampus and occasionally in another component of the limbic system. Some seizures propagate also to other brain regions. If the whole brain is finally involved in the seizure we call this process of seizure spreading a secondary generalization. Secondary generalization was assessed using the behavioral correlates and power in the motor cortices. To quantify the behavioral correlates of seizures, we used the Racine scale as proposed by Racine (1972), (Table 4).

Table 4: Racine scale of behavioral correlates of seizures.

Racine class 1	Mouth and facial movements	Non-motor
Racine class 2	Head nodding	Non-motor
Racine class 3	Forelimb clonus	Motor
Racine class 4	Rearing	Motor
Racine class 5	Rearing and falling	Motor

We marked seizures using video recording as motor seizures if their behavior corresponded to Racine class 3 or more. Racine class 1 or 2 seizures were classified as non-motor seizures.

The power of EEG signal is increased during seizures. Thus, power of EEG signal in motor cortex can be used to evaluate if and how much the seizure spread to the motor cortex. Since the seizures always start within the limbic system and usually spread to the cortex after tens of seconds, we decided to take into account only the last 10 seconds of the seizure. We computed the mean signal power during the last ten seconds of the seizure in all four motor cortex (MCx) electrodes (two contacts in each hemisphere) and averaged it over the channels.

4.2.3 Interictal epileptiform discharges (IEDs)

IEDs were detected using a detector designed by Janca et al (2015). We detected IEDs in each channel separately. Subsequently, we combined the detections from all four motor cortex channels into one series and detections from all four hippocampal channels into another series. During the aggregation we treated events in different channels closer than 0.2 s as one event (they were considered as a single propagating IED). We analyzed long-term profile of IED rates separately in hippocampi and motor cortices.

4.3 Results

4.3.1 Visual inspection of seizure profiles

Seizure profiles of individual clusters and artificial series are plotted in Figure 17. Majority of clusters (23/26) display gradual increase of ISI towards the end of the cluster. This trend is clearly visible in daily seizure counts in Figure 18.

Figure 17: Seizure profiles of individual clusters and artificial series. Seizure profiles which display decrease of seizure rate towards the end of the cluster are marked by the bold font of the title.

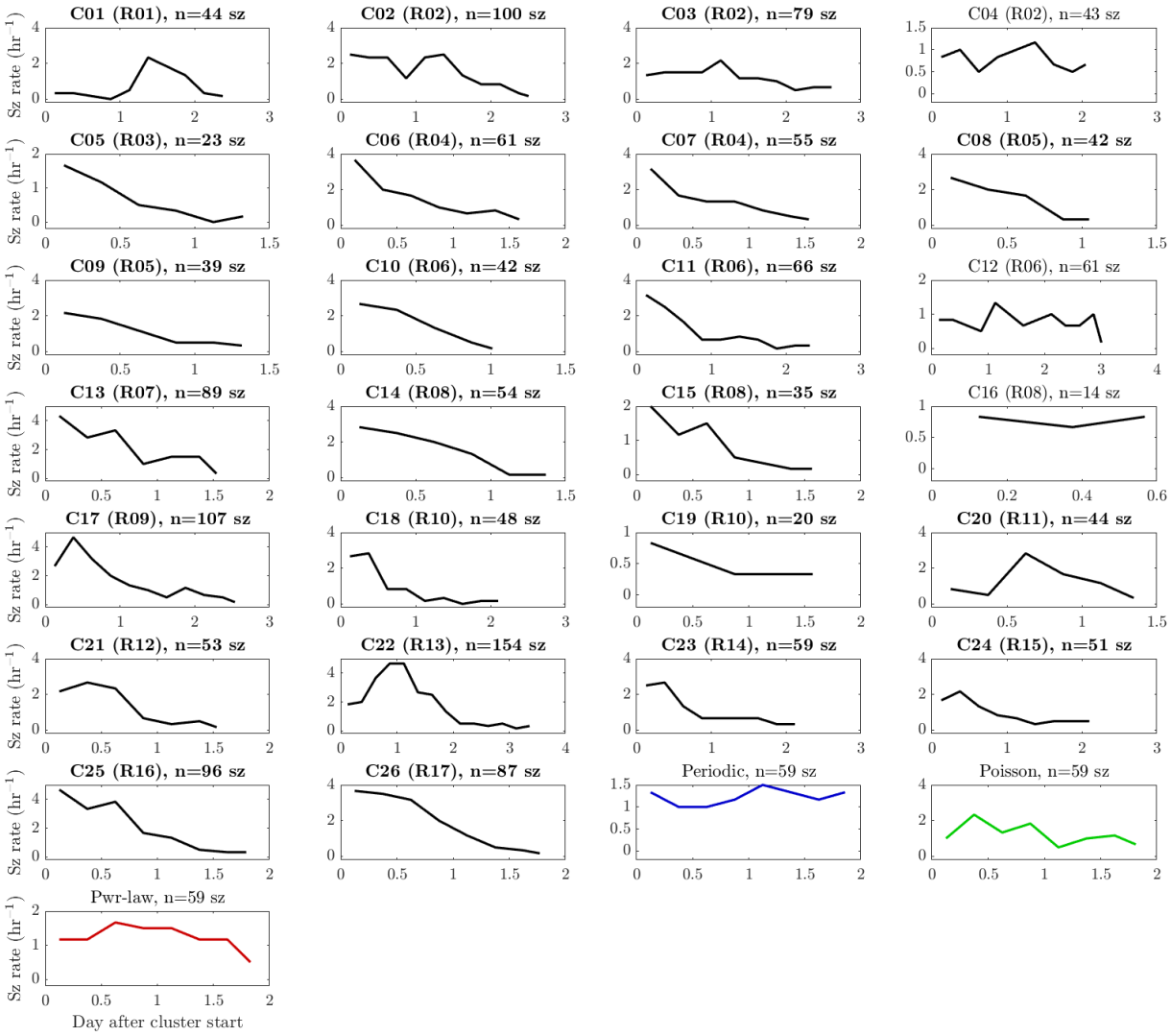

Figure 18: Seizure rate evaluated in 6-hour bins. Seizure profiles which display decrease of seizure rate towards the end of the cluster are marked by the bold font of the title.

4.3.2 Basic statistics

Data are given as mean±std (median). Mean number of seizures in a cluster was 60±6 (54). Intra-cluster inter-seizure interval (ISI) was 46±2 (28) min. Cluster duration was 46±3 (42) hours.

4.3.3 Are the clusters Poissonian?

First, we tested whether the intra-cluster seizure distribution is Poissonian. We used both graphical and numerical methods.

4.3.3.1 Graphical methods

Logarithmic histograms of intra-cluster ISIs are depicted in Figure 19. Due to brevity of the data, they have low number of bins and low number of values in each bin. Thus, we plotted also logarithmic survivor function which is in Figure 20. Using these graphical methods, in none of the clusters Poisson process can be clearly rejected. Thus, we applied numerical methods.

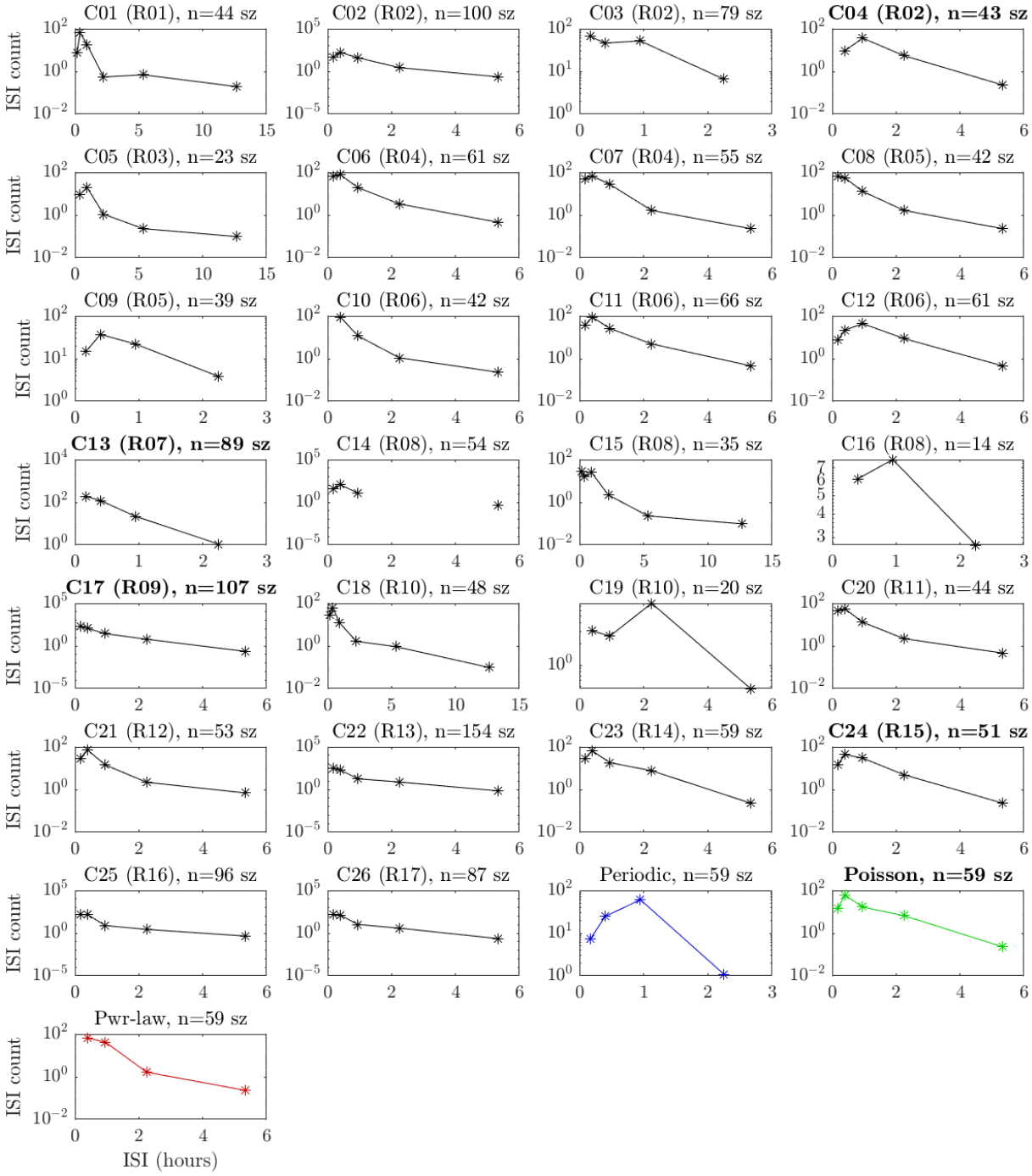

Figure 19: Logarithmic histograms of intra-cluster ISIs. Straight line is consistent with the Poissonian behavior of the seizures (marked by the bold font of the title).

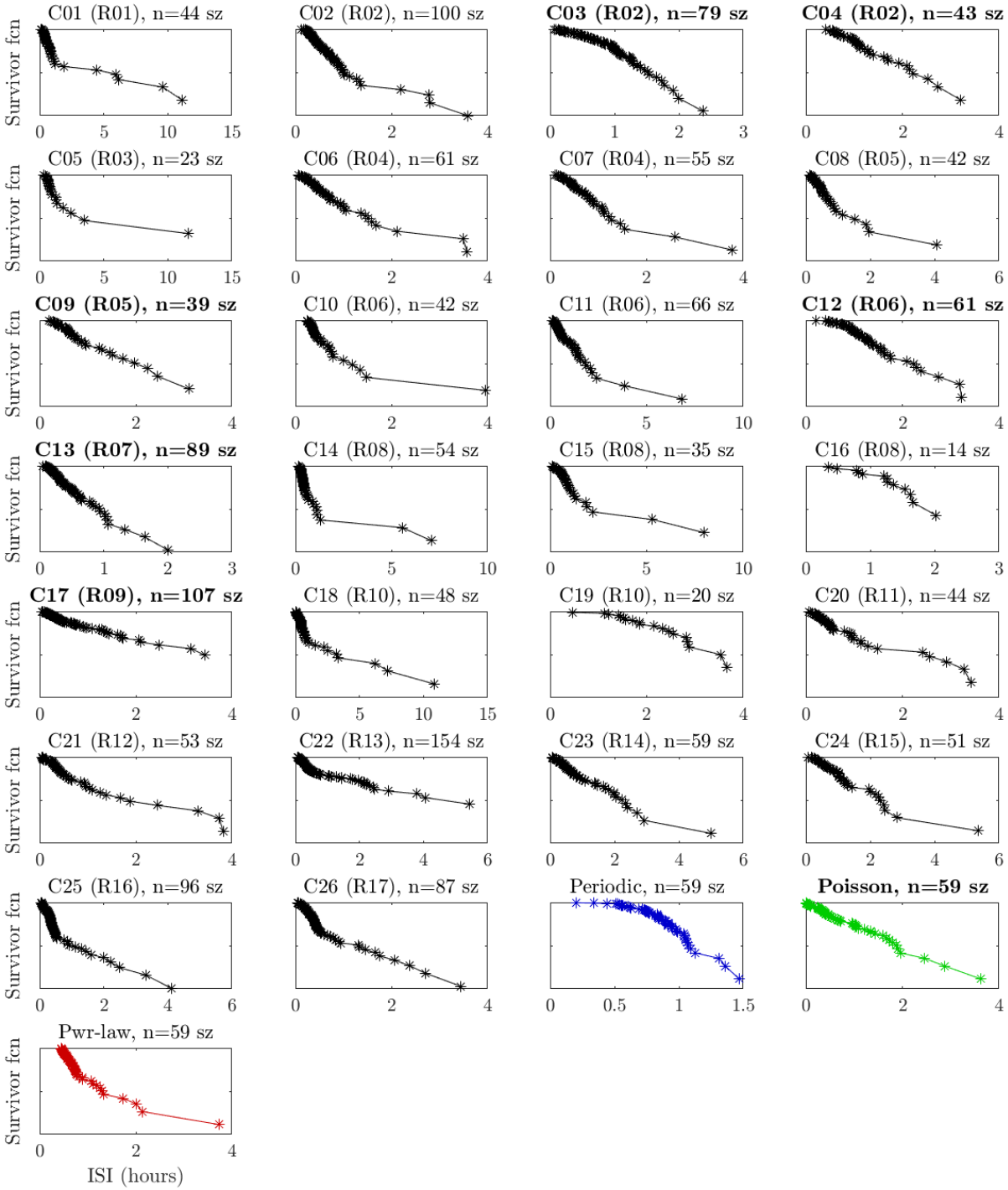

Figure 20: Logarithmic survivor functions for intra-cluster ISIs. Straight line is consistent with the Poissonian behavior of the seizures (marked by the bold font of the title).

4.3.3.2 Numerical tests

To numerically determine whether the intra-cluster profiles form Poisson process, we used the same methods as with the whole seizure profiles (see paragraphs 1.5.2, 3.2.2.3 and 3.3.3.2). The results are in Table 5. All clusters, except for C20, were proved non-Poissonian by least one of the three tests. However, the non-Poissonian character of C20 was demonstrated by other analyses, e.g. CEWT analysis presented in section 4.3.6.

Table 5: First column: *p*-value of χ^2 goodness-of-fit test whether hourly event count follows Poisson distribution. Green shading indicates $p<0.05$. Second column: *p*-values of χ^2 goodness-of-fit test whether inter-event interval distribution follows exponential distribution. Green shading indicates $p<0.05$. Third column: Spearman's correlation coefficient of successive inter-event intervals. Green shading indicates that the correlation coefficient is statistically significantly different from zero with $p<0.05$. NaN stands for Not a Number which arises when the test could not be performed due to brevity of the data.

	Counts Poisson	ISI Exponential	ISI Correlation
C01 (R01)	0.26	0.00	0.50
C02 (R02)	0.23	0.00	0.50
C03 (R02)	0.01	0.00	0.21
C04 (R02)	0.00	NaN	-0.02
C05 (R03)	0.38	NaN	0.66
C06 (R04)	0.52	0.03	0.51
C07 (R04)	0.09	0.00	0.53
C08 (R05)	0.74	0.01	-0.01
C09 (R05)	0.17	NaN	0.60
C10 (R06)	0.32	NaN	0.46
C11 (R06)	0.53	0.02	0.73
C12 (R06)	0.00	0.00	0.17
C13 (R07)	0.46	0.00	0.62
C14 (R08)	0.02	0.00	0.18
C15 (R08)	0.63	0.00	0.46
C16 (R08)	NaN	NaN	0.61
C17 (R09)	0.07	0.00	0.41
C18 (R10)	0.03	0.00	0.42
C19 (R10)	NaN	NaN	0.50
C20 (R11)	0.16	0.67	0.25
C21 (R12)	0.02	0.00	0.15
C22 (R13)	0.00	0.00	0.33
C23 (R14)	0.86	0.15	0.50
C24 (R15)	0.03	0.10	0.54
C25 (R16)	0.00	0.00	0.31
C26 (R17)	0.13	0.00	0.54
Periodic	0.00	0.00	-0.01
Poisson	0.62	0.11	0.11
Pwr-law	0.05	0.00	-0.16

4.3.4 Do clusters follow power law?

To the clusters, we applied the same methods as in the analysis of the whole seizure profiles (see paragraphs 1.5.3, 3.2.2.4). Loglog survivor functions (Figure 22) are more informative than loglog histograms (Figure 21).

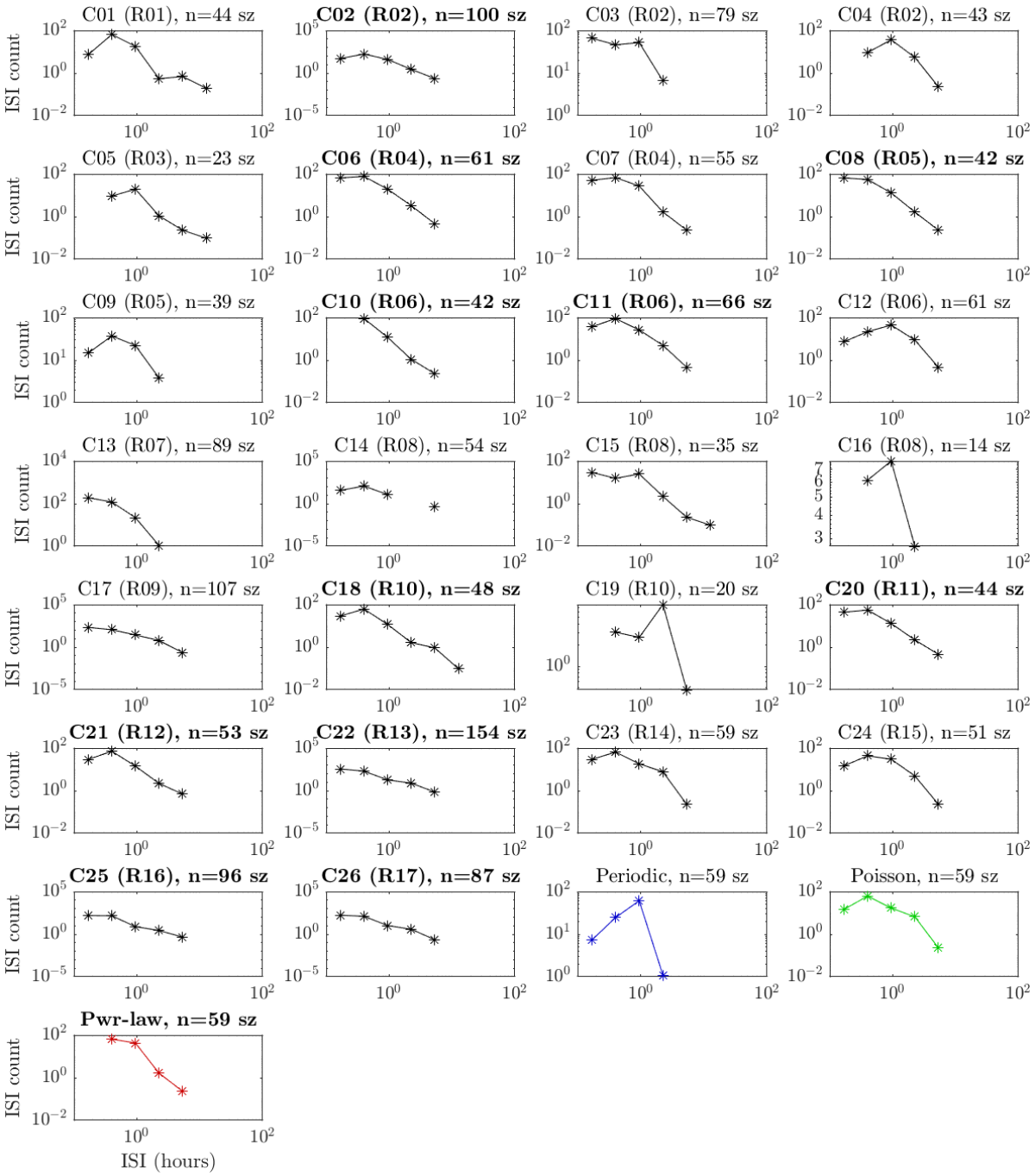

Figure 21: Loglog plot of ISI histograms of individual clusters and artificial data. Power-law distributed data create a straight line. In the clusters marked by the bold font of the title the straight line was observed in at least some range of the data.

From the survivor function in Figure 22, one can guess approximate power-law behavior in some range of values in 11/26 clusters. However, the range is always limited to approximately one decade which makes this evidence of power-law behavior very weak.

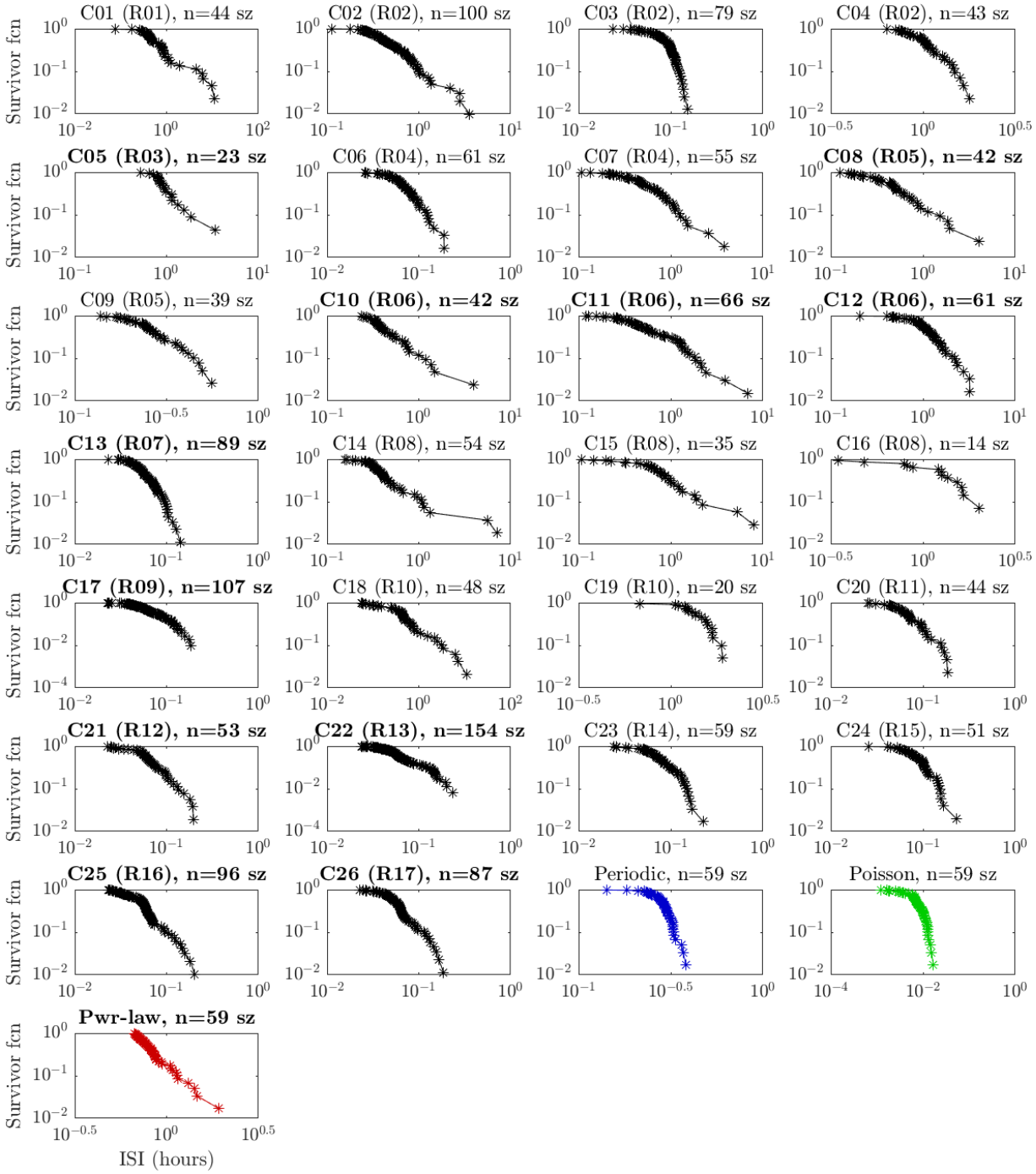

Figure 22: Loglog survivor functions of individual clusters and artificial data. Power-law series appears as straight line. In the clusters marked by the bold font of the title the straight line was observed in at least some range of the data.

4.3.5 Population graphs

By aggregating ISIs from all clusters, we obtain a data set similar to the one presented in section 3.3.5 but with no inter-cluster intervals and without ISI belonging to seizures out of clusters. Logarithmic and loglog histograms and survivor functions are in Figure 23. The histogram of ISIs in the section 3.3.5 contained a peak (characteristic scale) at approximately 70 hours and we speculated that it could have reflected the inter-cluster intervals. Such a peak is not present in histograms of intra-cluster ISIs (Figure 23) suggesting that our previous speculation was correct, i.e. the peak at 70 hours in Figure 11 is indeed caused by the inter-cluster periods.

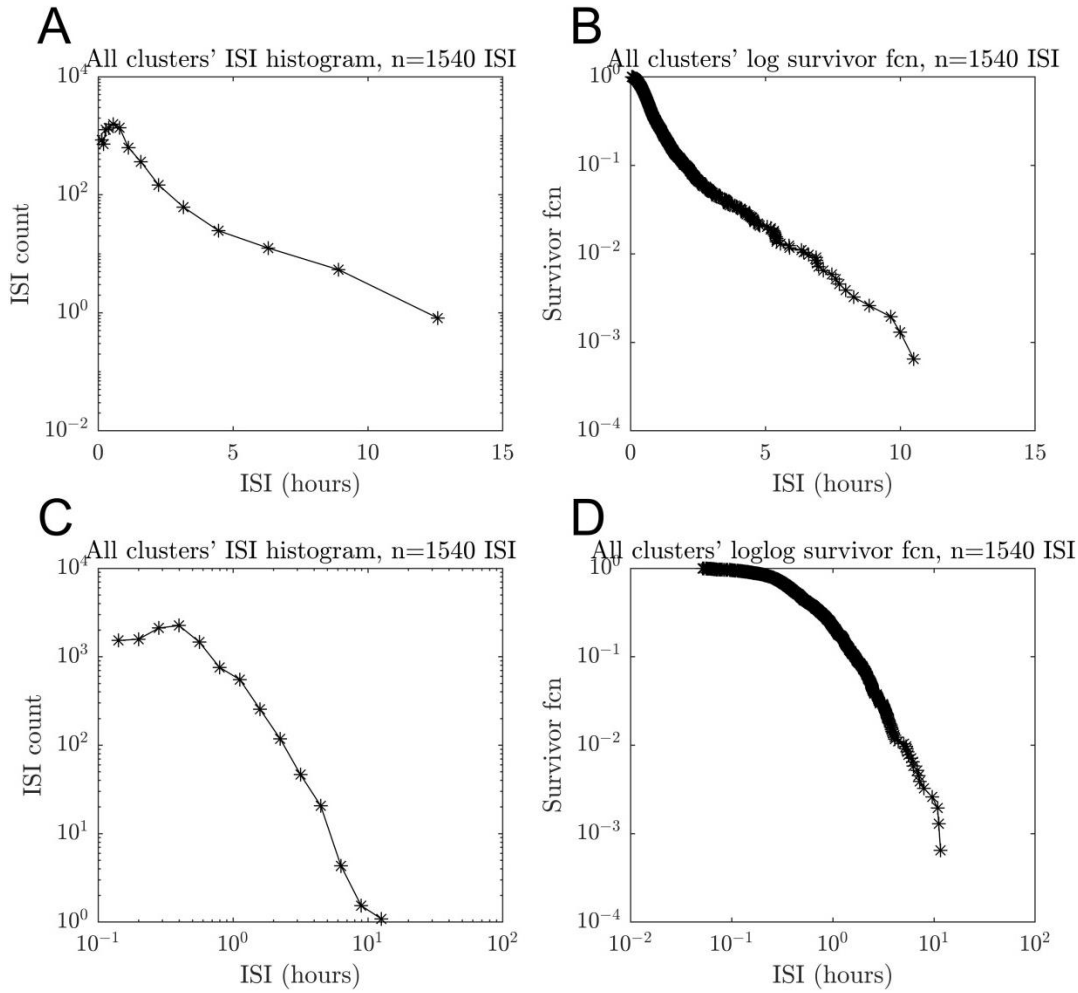

Figure 23: ISI histograms and survivor functions for aggregated ISIs of the whole population of 26 clusters. Linearity of the logarithmic histogram (A) and logarithmic survivor function (B) would indicate Poissonian behavior. However, the graphs are clearly non-linear and display a fat tail. Linearity of the loglog histogram and loglog survivor function (C, D) would suggest power-law behavior. These graphs are roughly linear in a very limited range of 1 to 5 hours.

4.3.6 Expected waiting time to the next seizure within clusters

Increasing CEWT per se is an evidence of seizure clustering in the sense that there are periods of higher and lower incidence of the events. Conversely, decreasing CEWT implies rather periodic occurrence of the events. Flat CEWT is a hallmark of Poisson process. To see whether seizures within clusters tend to periodic, Poissonian or clustered occurrence, we analyzed CEWT for intra-cluster seizures. The results are depicted in Figure 24. For 17/26 clusters, the CEWT was increasing, for 5/26 clusters, it was decreasing and for 4/26 clusters, the CEWT profile is flat. Interestingly, in the first cluster of 14/17 rats, CEWT is increasing and in the remaining 3/17 rats (R07, R14 and R15) it is flat. Decreasing CEWT is only found in second or third cluster of given rat, although in some rats even the second cluster has an increasing CEWT. These observations suggest that early clusters display intra-cluster dynamics with alternating periods of higher and lower seizure incidence whereas later clusters have a tendency to periodic seizure occurrence.

Figure 24: Conditional expected waiting time (CEWT, solid line) to the next event calculated from inter-seizure intervals as a function of the time since the last event. Dashed line indicates the unconditional expected waiting time (UEWT). CEWT is an increasing function for 17/26 clusters and for the power-law artificial data. For the artificial Poisson process, the CEWT is equal to the UEWT. In case of quasiperiodic series the CEWT is decreasing.

The analysis of CEWT from the aggregate of all ISIs from all 26 clusters in Figure 25 reveals a strong increasing trend. This shows that the dynamics of seizures within the cluster has the character of alternating periods of high and low seizure incidence and not periodic seizure occurrence.

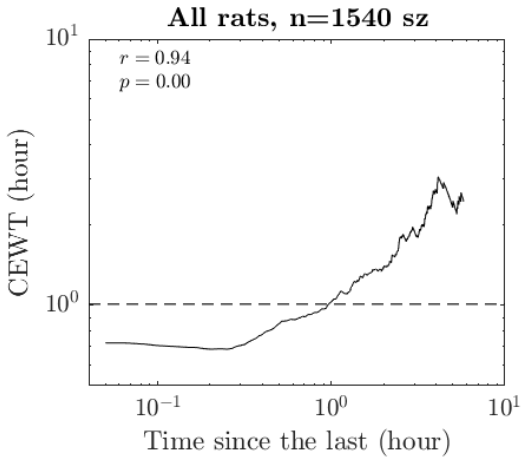

Figure 25: Conditional expected waiting time (CEWT) analysis for the aggregate of ISIs from all 26 clusters. *r* – Pearson correlation coefficient, *p* – *p*-value for the *r*

4.3.7 Correlation of seizure properties with intra-cluster time

We have already noticed that with the intra-cluster time, the ISIs tend to increase in most clusters. To investigate the plausible mechanisms responsible for inter-cluster and intra-cluster dynamics, we examined correlation of intra-cluster time with the following parameters of seizures: duration, behavioral severity and energy in regions of secondary propagation, namely the motor cortices.

4.3.7.1 Prolongation of inter-seizure interval with intra-cluster time

The dependence of ISI on the time from the beginning of the cluster can be observed in Figure 29. In 21/26 clusters, ISI is significantly positively correlated with intra-cluster time (Spearman's ρ, $p<0.05$). Clusters C01 and C20 contain few long ISI at the beginning but after them the trend of gradual ISI prolongation is obvious. Clusters C04, C12 and C16 did not show any trend in ISI. Interestingly, all clusters that are the first or the second ones in a given subject do exhibit ISI prolongation. C12 and C16 are both third clusters of given animals.

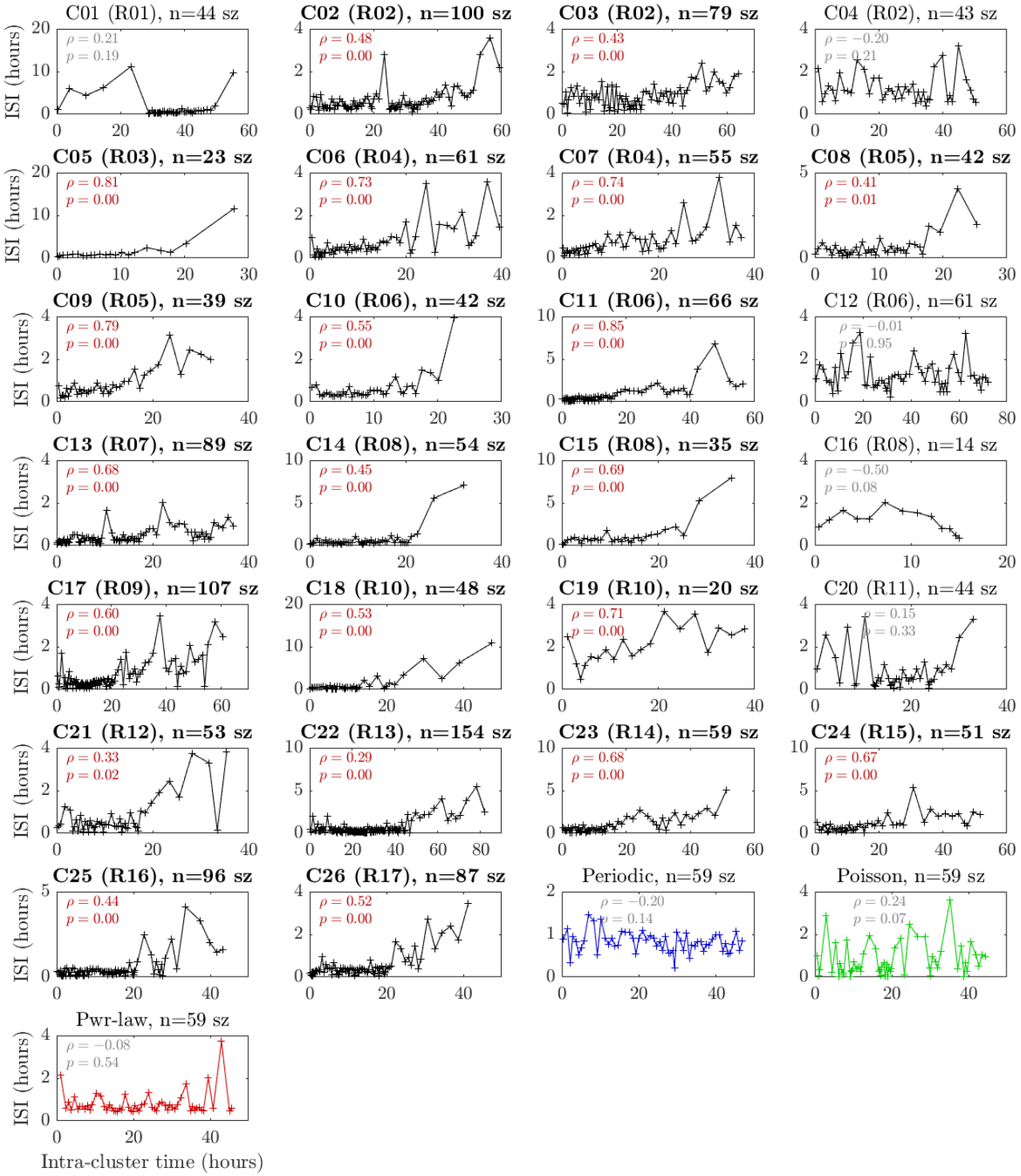

Figure 26: Dependence of ISI on intra-cluster time. In 21/26 clusters ISI is significantly positively correlated with intra-cluster time (Spearman's ρ, $p<0.05$). Cluster C01 contains few long ISI at the beginning. Spearman's ρ and its p-value are provided in each plot. Red color of the text and bold title indicate positive statistically significant correlation whereas grey color and normal title denote no significant correlation.

For the population analysis, each cluster was divided into 10 equal time segments in which the mean ISI was calculated. Then the bin means of each cluster were fitted by a straight line. The median of the slopes of the lines was statistically significantly positive (Wilcoxon signed rank test, $p<0.0001$) although for clusters C01, C04, C12 and C16 the slopes were negative.

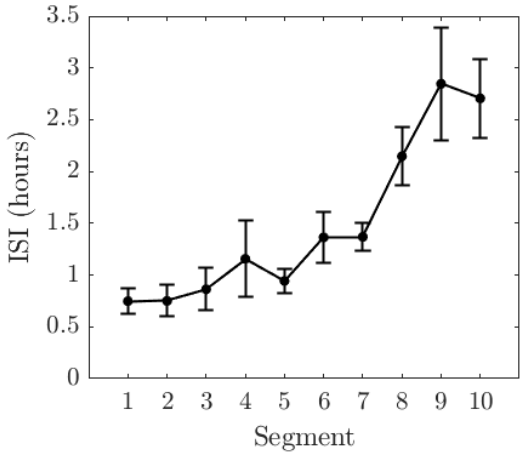

Figure 27: Population data of ISI prolongation. ISI increases more than 3-fold towards the end of the cluster. Data are shown as mean±SEM.

The existence of mutual relationship between successive ISIs and the prolongation of ISI with time from the cluster onset (intra-cluster time) can be documented well using a color-coded graph (Figure 28). In 21/26 clusters, we observed correlation between successive ISI and a tendency of long ISIs to occur towards the end of the cluster.

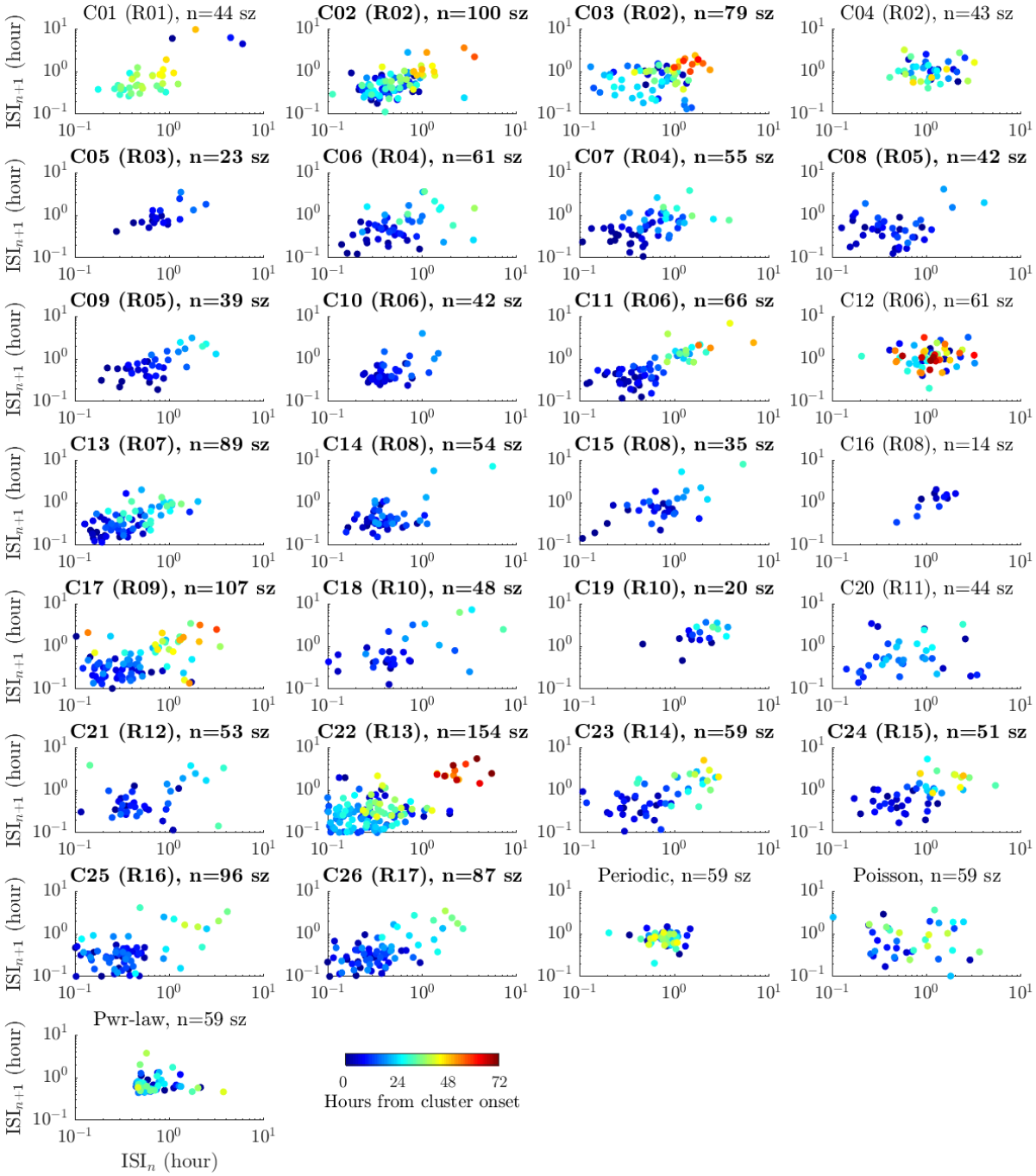

Figure 28: Successive ISI correlation with color-coded time from the beginning of the cluster. Successive ISIs tend to be similar which causes the tendency of the data points to in the vicinity of the increasing diagonal line. Moreover, shorter ISIs (lower left corner) occur at the early stages of the cluster (cold colors) whereas longer ISIs (upper right corner) occur later in the cluster (warm colors). In cluster C01, few long ISIs occurring at the beginning of the cluster can be seen as the dark blue dots at the upper right corner. This structure was observed in 21/26 clusters marked by the bold font of the title.

4.3.7.2 Correlation of seizure duration and intra-cluster time

In this analysis, we examined whether seizure duration displays intra-cluster dynamic analogous to ISIs. In 13/26 clusters the correlation was negative (in 6 cases significantly) and in 13/26 clusters it was positive (in 3 cases significantly). Thus, no general trend in seizure durations with cluster progression can be concluded. In 12/26 clusters (C02, C03, C07, C10, C11, C13, C17, C22 – C26), stabilization of the seizure duration at low values (approximately 1

minute) was observed towards the end of the cluster. In contrary, the initial parts of the cluster were characterized by high variability of seizure duration.

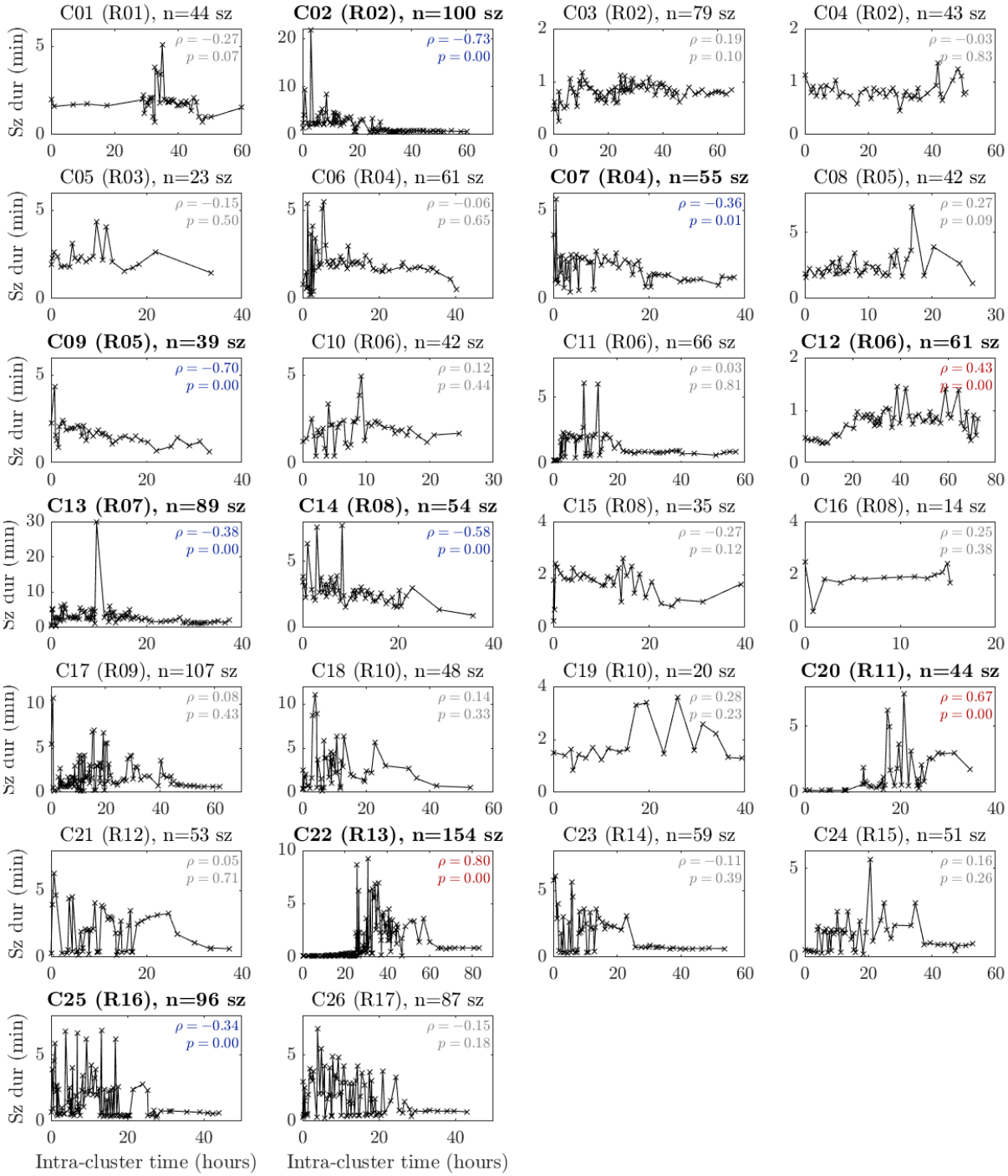

Figure 29: Dependence of seizure duration on intra-cluster time. In 13/26 clusters the correlation is negative (in 6 cases significantly) and in 13/26 clusters it is positive (in 3 cases significantly). In 12/26 clusters (C02, C03, C07, C10, C11, C13, C17, C22 – C26), stabilization of the seizure duration at low values (approximatelly 1 minute) is observed towards the end of the cluster. Spearman's ρ and its p-value are provided in each plot. Negative statistically significant ρ values are in blue and positive statistically significant ρ values are in red. Non-significant values are in grey. Statistically significant results have bold title.

In Figure 30, there is the evolution of mean seizure duration with the cluster progression. Individual clusters were again fitted by straight lines. Although the slopes of the fitted lines are positive in 8 clusters (C03 C04 C08 C12 C16 C19 C20 and C22), overall the slopes are statistically significantly negative (Wilcoxon signed rank test, p=0.0074).

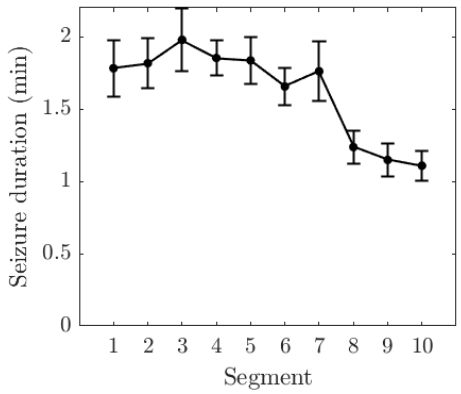

Figure 30: Population data for mean seizure duration. The mean seizure duration is slightly decreasing with the cluster progression but no consistent trend was found across clusters. Data are shown as mean±SEM.

In Figure 29, we noticed stabilization of the duration at the later part of the cluster. Therefore, we divided each cluster into 10 equal segments. In each segment, we computed the standard deviation of the durations of the seizures which was then normalized by the average seizure duration in that segment (Figure 31). The normalization was performed to show that the decrease of the standard deviation is not a simple result of the decrease of the seizure durations. Correlation of the normalized standard deviation with the cluster progression was evaluated using Spearman's ρ. In 21/26 clusters, the correlation was negative (in 14 cases statistically significantly) and in 5/26 clusters it was positive (in 1 case statistically significantly). When the data were fit by straight lines, the slopes of the lines were negative in 20/26 clusters. The Wilcoxon signed rank test revealed that the slopes were statistically significantly negative (p<0.001). The mean over the clusters reveals the tendency of the seizure duration to stabilize towards the end of the cluster (Figure 32).

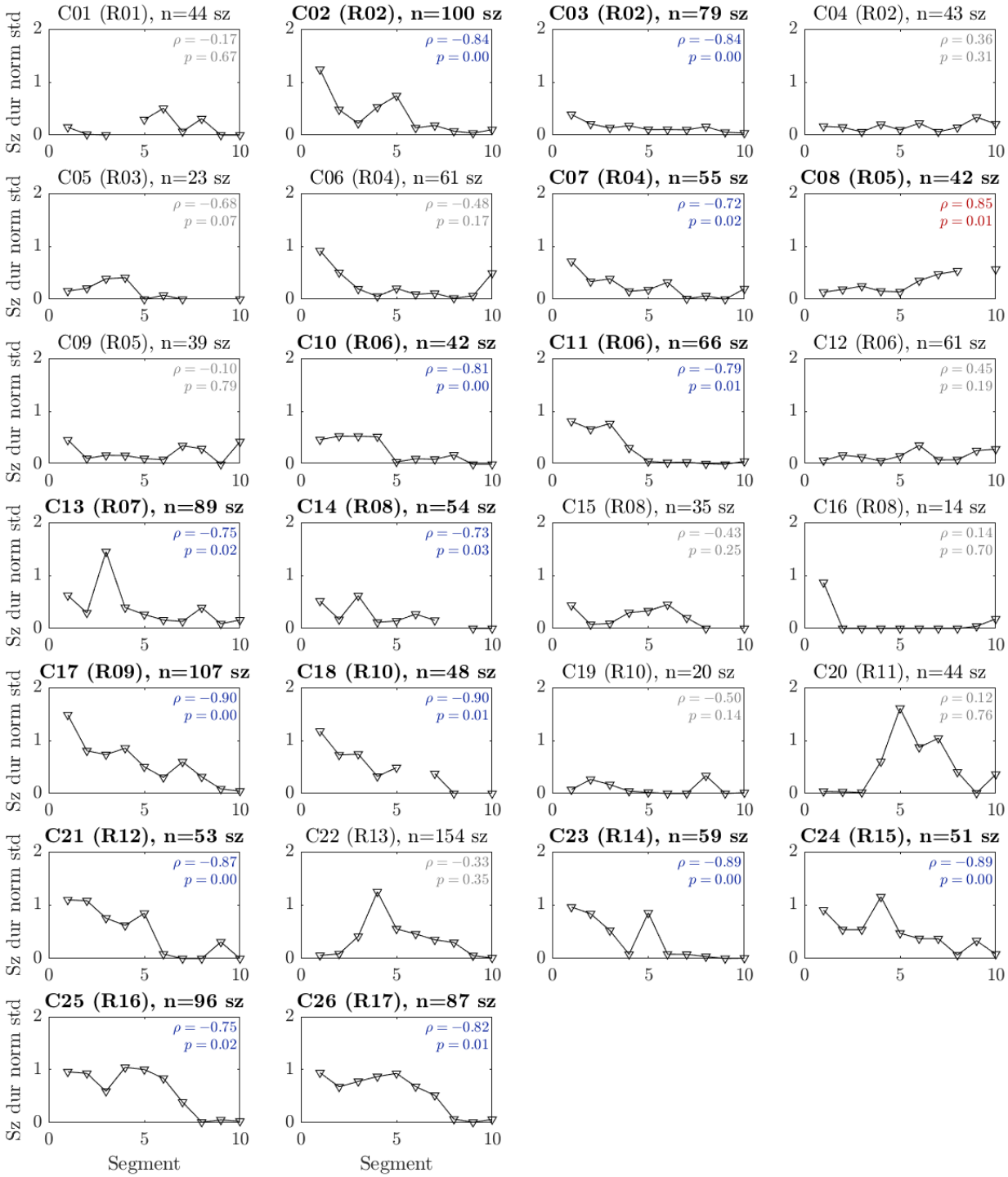

Figure 31: Normalized standard deviation of seizure durations evaluated in 10 equal bins for each cluster. Spearman's ρ and its p-value are provided in each plot. Negative statistically significant ρ values are in blue and positive statistically significant ρ values are in red. Non-significant values are in grey. Statistically significant results have bold title. Few rats had no seizure in some time bins which resulted in the break of the line.

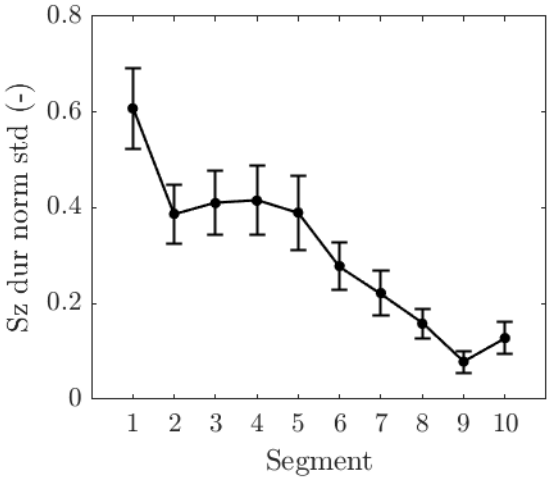

Figure 32: Mean over all 26 clusters of the normalized standard deviation of seizure durations. Stabilization of the seizure duration towards the offset of the cluster is evident. Data are shown as mean±SEM.

4.3.7.3 Correlation of seizure duration and subsequent inter-seizure interval

Based on the kindling literature and, especially the fact that more severe seizure produces more inhibitory effect on subsequent seizure, one may suspect a correlation or even causal relationship between seizure duration and subsequent ISI (Herberg & Watkins 1966, Mucha & Pinel 1977, Racine 1972). Thus we plotted ISI as a function of preceding seizure duration in Figure 34. Spearman's ρ was negative in 11/26 clusters (in 2 cases statistically significantly) and positive in 15 clusters (in 3 cases statistically significantly). No general correlation can be concluded. This is confirmed by the population data presented in Figure 33 with ρ=0.03 and its p=0.18.

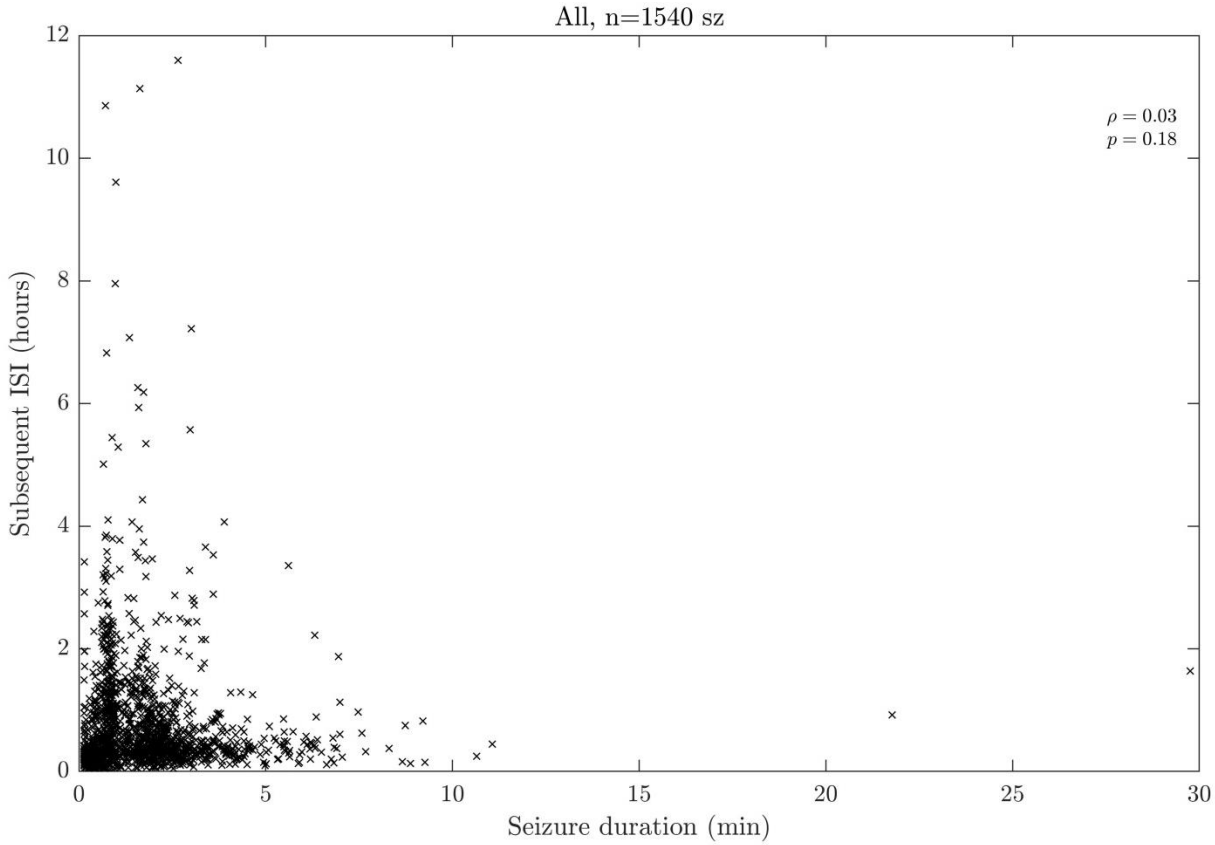

Figure 33: Aggregate of all seizure duration and all subsequent ISI shows no correlation.

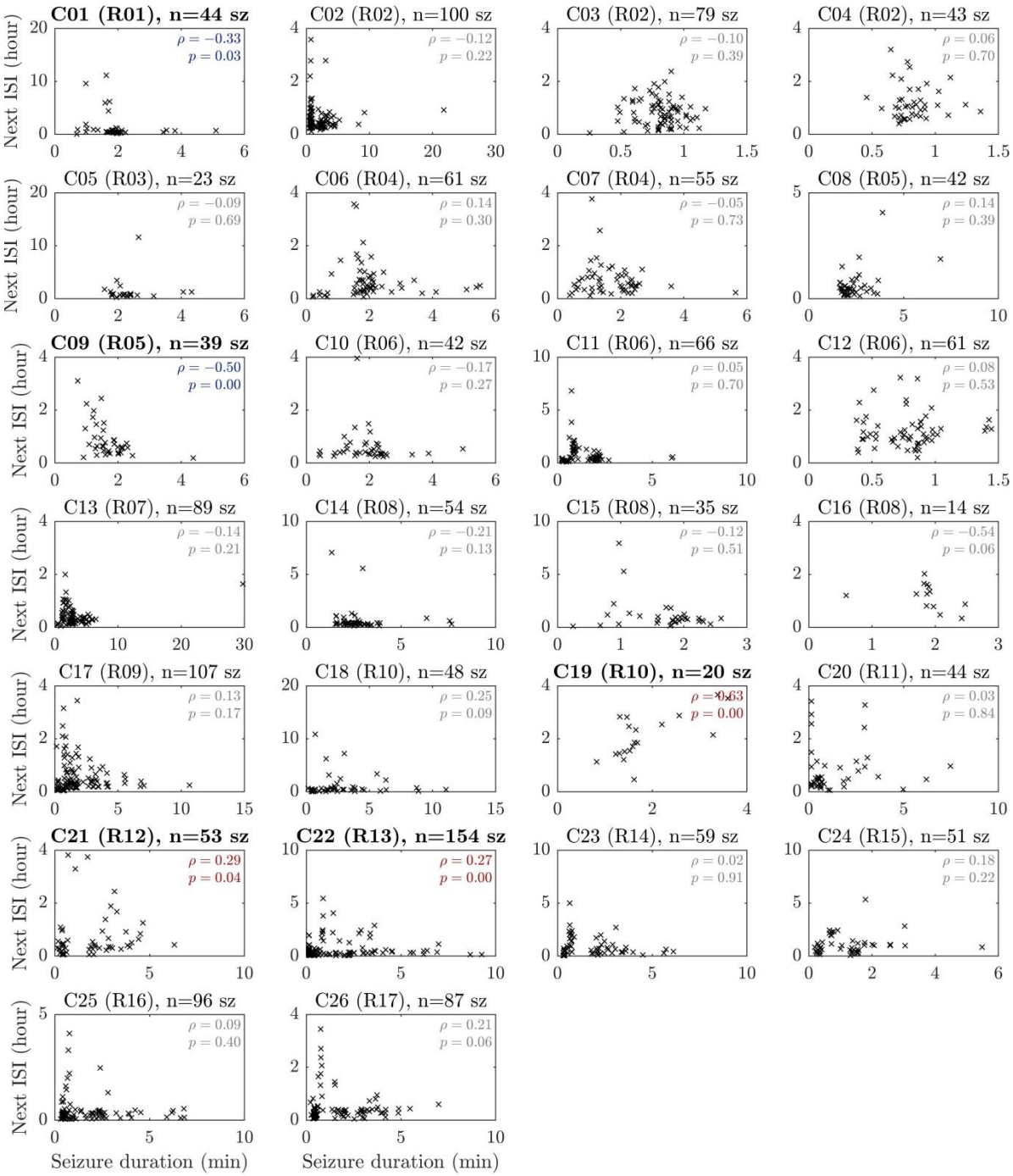

Figure 34: Dependence of ISI on preceding seizure duration. In 5/26 clusters the Spearman's ρ is statistically significantly different from zero. In C01 and C09 it was negative whereas in C19, C21 and C22 it was positive so no general correlation can be concluded.

4.3.7.4 Correlation of seizure severity with intra-cluster time

An epileptic seizure can have various behavioral manifestations depending on which brain regions are affected. Seizures in our rats begin in the hippocampus or occasionally in another component of the limbic system. Seizures can have focal nature and be restricted to the limbic system. The seizure can also progress, spread outside limbic structures and eventually become secondarily generalized. In eight clusters we were able to evaluate the following two measures of seizure generalization: 1) behavioral correlates scored according to the Racine scale (manually from the video recordings); and 2) power of EEG signal in the motor cortex (MCx)

during the final 10 seconds of the seizure. Examples of a non-motor and a motor seizure are shown in Figure 35. Moreover, in these animals we evaluated the IED rate in hippocampi and in motor cortices.

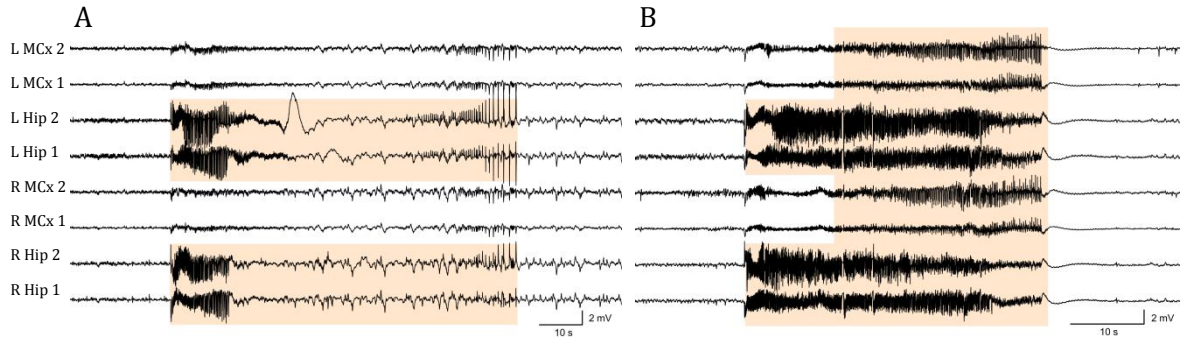

Figure 35: Examples of seizures from rat R09. A: A non-motor seizure which occured three hours after the first seizure of that rat. Note the low signal power in the motor cortices. B: Motor seizure which occurred 54 hours after the first seizure, i.e. at the end of the first cluster. Note the high signal power in the motor cortices especially towards the end of the seizure. Hip – hippocampus, MCx – motor cortex.

In 7/8 clusters, we found significant correlation between intra-cluster time and signal power in the motor cortices (Figure 36 and Figure 37B, red line; column 1 of Table 6). In 7/8 clusters, the motor seizures have significantly higher power in the motor cortices than non-motor seizures (Figure 36; column 6 of Table 6).

Along with the seizures we also plotted the rate of interictal epileptiform discharges (IEDs). IEDs are sharp EEG spikes which reflect sudden synchronized activity of a neuronal population and can be used to monitor the disease activity. In 7/8 clusters, a gradual increase in the IED rate in motor cortices (Figure 36, dashed green line and Figure 37C, red line; column 3 of Table 6) was observed during the course of the cluster. This observation may be indicative of progressively increasing excitability of the cortices. Meanwhile, the IED rate in the hippocampi tends to be higher during the first part of the cluster and starts to decrease at the onset of the motor seizures in 6/8 clusters (Figure 36, solid green line and Figure 37C, green line). The results of the statistical tests are disparate regarding the IED rate in the hippocampi (column 2 of Table 6).

In all clusters, motor seizures are followed by statistically significantly longer ISI than non-motor seizures (column 7 of Table 6). In 5/8 subjects, there is also statistically significant positive correlation between the power in the motor cortices and subsequent ISI (column 4 of Table 6). Correlation of the motor cortex power and seizure duration was found only in 2/8 subjects (column 5 of Table 6). Column 8 of Table 6 shows that there is no clear relationship between seizure duration and its behavioral accompaniment.

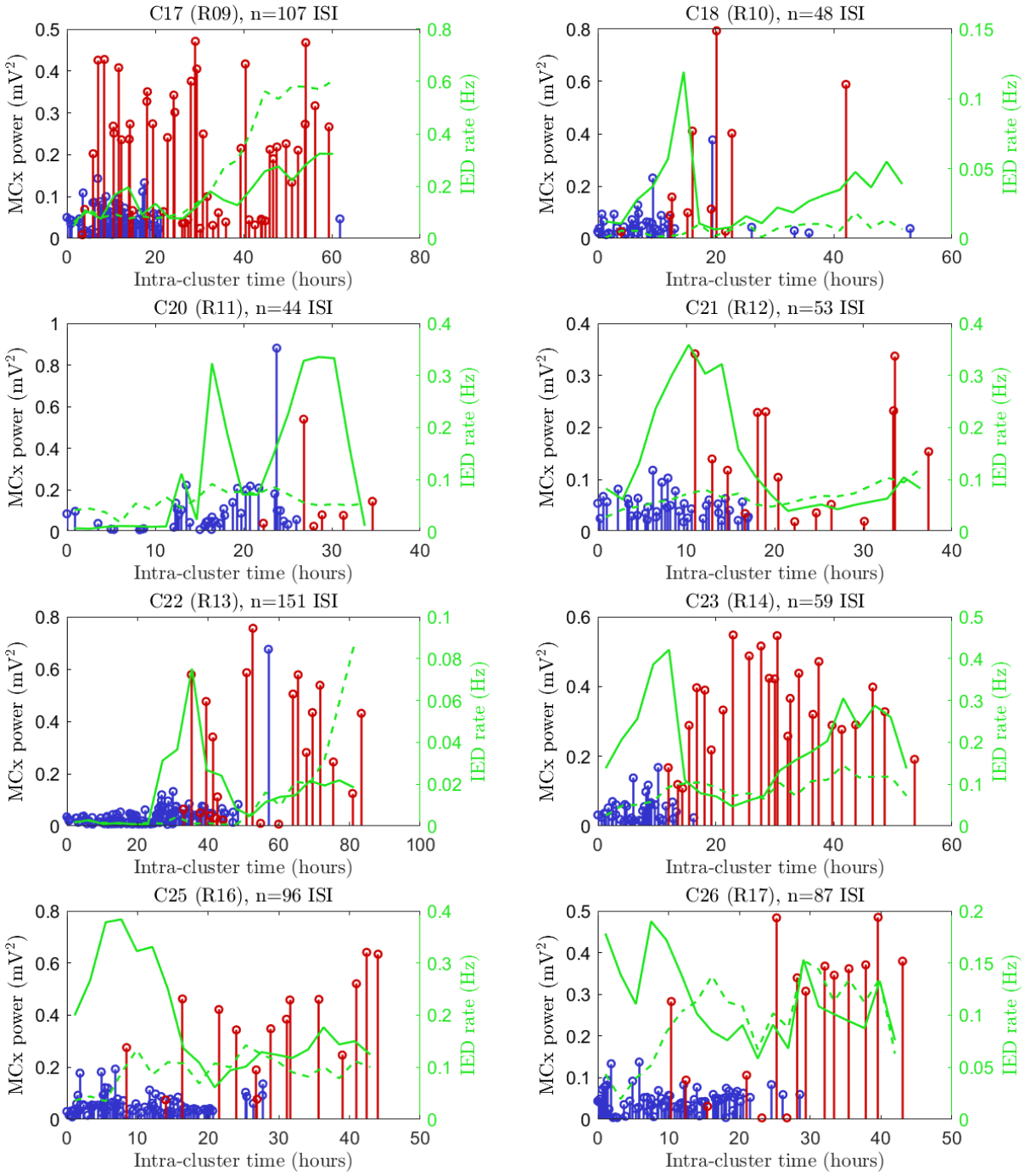

Figure 36: Seizure spread evaluation. Blue stems: non-motor seizures (Racine 1-2), red stems: motor seizures (Racine 3-5). Abscissa: time from the beginning of the seizure cluster. Height of the stems: signal power in the motor cortices during last 10 seconds of the seizure. Green solid and dashed lines represents mean IED rate in the hippocampi and motor cortices, respectively (right vertical axis). Motor seizures tend to have higher power in the motor cortices than non-motor ones. IED rate in the motor cortices gradualy increases in all clusters except for C25. In all clusters except for C17 and C20 the IED rate in the hippocampi is higher during the first half of the cluster.

Table 6: Statistical analyses of various parameters of seizures and IEDs. Correlations are expressed as Spearman's ρ with green shading indicating ρ statistically significantly different from zero at α=0.05. Last three columns are results of a two-tailed Wilcoxon rank sum test of the hypothesis that motor seizures have different MCx power (during last 10 seconds of the seizure), subsequent ISI and duration than non-motor seizures. The (+) denotes that for motor seizures the parameter is higher than for non-motor whereas (-) denotes an opposite relationship.

	Time vs. MCx power	Time vs. Hip IED rate	Time vs. MCx IED rate	MCx power vs. ISI	MCx power vs. duration	Motor vs. MCx power	Motor vs. ISI	Motor vs. Duration
	Spearman's ρ	Spearman's ρ	Spearman's ρ	Spearman's ρ	Spearman's ρ	p-value	p-value	p-value
C17 (R09)	0.31	0.81	0.92	0.22	-0.00	< 0.001 (+)	< 0.001 (+)	0.584 (-)
C18 (R10)	0.39	0.36	0.66	0.15	0.21	0.003 (+)	0.032 (+)	0.259 (+)
C20 (R11)	0.38	0.78	0.45	-0.08	0.31	0.669 (+)	0.005 (+)	0.004 (+)
C21 (R12)	0.07	-0.48	0.73	0.15	0.16	0.011 (+)	0.001 (+)	0.047 (+)
C22 (R13)	0.56	0.44	0.65	0.32	0.58	< 0.001 (+)	< 0.001 (+)	< 0.001 (+)
C23 (R14)	0.76	0.09	0.72	0.67	0.20	< 0.001 (+)	< 0.001 (+)	0.933 (-)
C25 (R16)	0.34	-0.52	0.35	0.30	0.14	< 0.001 (+)	< 0.001 (+)	0.558 (-)
C26 (R17)	0.35	-0.49	0.56	0.28	-0.19	< 0.001 (+)	< 0.001 (+)	0.462 (-)

The characteristics from Figure 36 are depicted as population data in Figure 37. Given characteristic was averaged within the time segments for each cluster separately and then the cluster curves were averaged. We can notice clear increase in the percentage of motor seizures which is paralleled by increase of two parameters in the motor cortices: 1) power of last 10 seconds of a seizure and 2) IED rate.

Individual cluster curves were fitted by a straight line. Slopes of the lines were then statistically evaluated for departure from zero. The percentage of motor seizures showed positive trend in all clusters yielding p=0.008 in Wilcoxon signed rank test. In the power in the hippocampi, the slopes were positive 2/8 clusters and negative in the 6/8 clusters (p=0.15, Wilcoxon signed rank test). In the motor cortices, the slopes were positive in all clusters (p=0.008, Wilcoxon signed rank test). IED rate in the hippocampi showed positive slope in 5/8 clusters (p=0.74, Wilcoxon signed rank test). IED rate in the motor cortices showed positive slope in all clusters (p=0.008, Wilcoxon signed rank test).

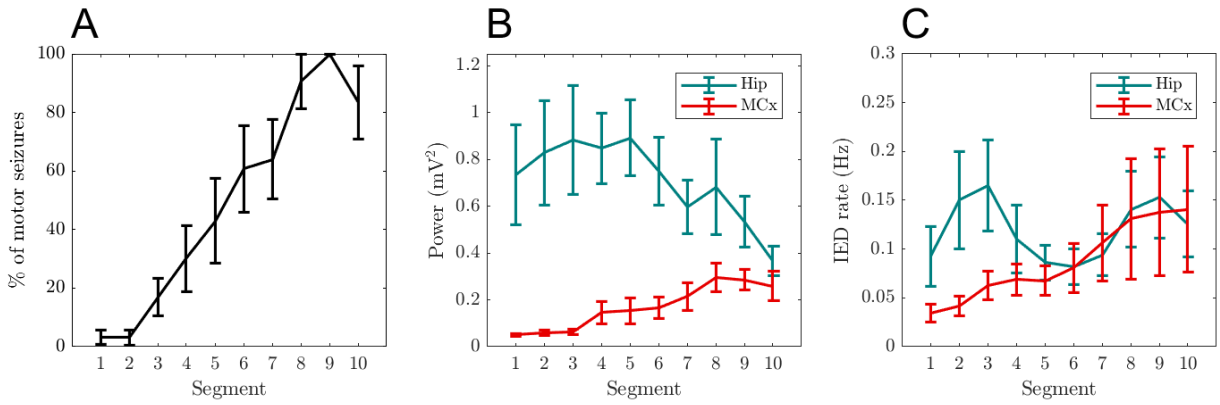

Figure 37: Population data on seizure spread from eight clusters. Each cluster was divided in to 10 equal time segments. A: Percentage of motor seizures increases with intra-cluster time. B: Mean power during last 10 seconds of each seizure was measured in hippocampi and in motor cortices. With the cluster progression, it decreases in the hippocampi whereas in the motor cortices it increases. C: IED rate in motor cortices increases with the cluster progression. In the hippocampi no uniform trend was observed. Data are shown as mean±SEM.

The data from this section indicate that with the cluster progression, the seizures are less frequent (increase in ISI) and more severe in terms of their spread outside the limbic system

(into the motor cortices) and behavioral manifestations. Moreover, we observed increase in IED rate in the motor cortices with the progression of the cluster. Motor seizures had higher power in the motor cortices and were followed by longer ISI than the non-motor ones. No correlation was found between seizure duration and subsequent ISI whereas correlation between the motor cortex power and the subsequent ISI was positive in 7/8 clusters.

4.4 Discussion

In this chapter we have shown the following findings:

1. Seizure clusters are 46±5 (median 42) hours long and contain 60±6 (median 54) seizures. Mean inter-cluster period was 61±10 (56) hours.
2. Intra-cluster seizures are not Poissonian (like the whole seizure profiles)
3. Intra-cluster seizures do not follow power law except for very limited ISI ranges (less than 1 decade) in 10/26 clusters.
4. The expected waiting time until the next seizure conditioned on the time elapsed since the last seizure (CEWT) is an increasing function
5. Successive ISI are correlated
6. Very strong and consistent trends in certain parameters with the cluster progression were found, namely:
    a. Prolongation of the ISI
    b. Decrease in the variability of seizure duration
    c. Increase in proportion of motor seizures
    d. Increase in signal power in motor cortices
    e. Increase in IED rate in motor cortices
7. Motor seizures are associated with a higher power of local field potentials in motor cortex
8. Motor seizures are followed by longer ISI than non-motor seizures

In terms of absolute durations of clusters and ISI, the seizure profiles of our rats are, as expected, the most similar to the ones observed by Hawkins & Mellanby (1987) since they also used the tetanus toxin model in rats. Similar clusters were also observed by Williams et al (2009) who used kainate model of epilepsy in rats. Also, similar seizure clustering was reported by Kadam et al (2010) who investigated epilepsy after hypoxic-ischemic injury in rat pups although she reported longer inter-cluster periods of up to 22 days.

The distributions of the intra-cluster ISI have fatter tails than exponential but thinner than power-law. This is also consistent with the increasing CEWT. There is a strong correlation of successive ISI which might, however, be a trivial consequence of the trend of ISI prolongation.

Let's now focus on the seizure severity. Motor seizures were significantly longer than non-motor ones in a small proportion of clusters which is in agreement with the findings of Hawkins & Mellanby (1987). Regarding the long-term dynamics of seizure severity, Hawkins & Mellanby (1987) reported that in tetanus toxin model seizures tended to aggravate in terms of behavioral manifestations, culminate in full blown motor seizures and finally cease for some time. Then, the process repeated (at least in some animals). This is congruent with our observations. However, in contrast to our data, they did not observe any motor seizure during the first cluster in 3/7 rats; first motor seizures appeared in the second cluster. Our rats always experienced the first motor seizure already during the first cluster. Similarly to our rats, some of their rats had only one cluster and then a long period of a constant seizure rate.

The behavioral intensification of seizures with cluster progression is readily explained by the increased propagation of the seizure activity to the motor cortices evidenced by the increased signal power during the last 10 seconds of the seizure. The easier propagation of the seizure activity might be caused by increasing excitability of the motor cortices which is

illustrated by increasing IED rate in the motor cortices. The IED rate in the hippocampi did not show a consistent trend with the cluster progression. Interestingly, Hawkins & Mellanby (1987) reported that IED rate fluctuations followed seizure rate fluctuations. Our results confirm this finding.

As to the mechanism of seizure aggravation, we speculate that the focal, non-motor seizures occurring at the beginning of the cluster may display kindling effect. Kindling is a phenomenon first described by Goddard et al (1969) who once daily electrically stimulated various subcortical areas of rats and studied the behavioral response. The stimulus was weak not to elicit any convulsion on the first day. After a variable number of days (4 – 136 days) some animals (depending on the stimulated brain structure) developed motor seizures as a response to the stimulations. Racine (1972) reported also gradual prolongation and intensification of the electrographic epileptic response to the stimulations. The rats did not experience any spontaneous seizures; all seizures were in response to the stimulation. However, the stimulation was kept on the same low intensity throughout the experiment.

Hawkins & Mellanby (1987) argued that in the tetanus toxin model the process of seizure intensification is not a true kindling because after few full blown motor seizures there is a few days gap which is not observed in kindling. However, in the kindling model, every seizure is induced artificially by electrical stimulation which is a different situation to spontaneously occurring seizures. Moreover, inhibition after the appearance of full blown motor seizures was reported in several kindling studies. As early as in 1966, Herberg & Watkins (1966) noticed that after an electrically induced motor seizure there is a refractory period during which another motor seizure is impossible to elicit by the same stimulation. This refractoriness was somewhat diminished 1 hour after the motor seizure and completely disappeared 2 hours after the motor seizure. Racine (1972) reported that in rats stimulated once each day, the duration of the seizure progressively increased from 17.4 s (range 6 – 50 s) to 104 s (range 50 – 350 s) by the time when the rats developed a full-blown motor seizure (class 5). Then the duration of the seizures started to decrease in daily stimulated rats. However, a stimulation-free rest of 48 hours or more, brought the seizure duration back up to maximum levels. Such duration of the rest is strikingly similar to the inter-cluster period in our tetanus toxin injected rats. Mucha & Pinel (1977) stimulated amygdala of their rats every day. In fully kindled animals, 100 s before the standard stimulation, they applied a conditioning stimulus of variable intensity. If and only if the stimulus induced a motor seizure (convulsions), it had an inhibitory effect on the subsequent seizure induced by the standard kindling stimulus in terms of seizure duration and behavioral severity. The most interesting results from their study are those regarding the time profile of the inhibitory effect. If the interval between the conditioning and test stimulus was 1.5 min, the test stimulation elicited almost no epileptic response. With the 20 min interval, the behavioral score was almost the same as with no antecedent stimulus but the seizures were half of the baseline duration. With the interval of 90 min, the antecedent stimulation effect was almost completely dissipated. Thus, in their experiments the post-seizure inhibition lasts roughly 1 hour which is not much different from the ISI of our rats during the second half of a cluster when predominantly motor seizures occur. Mucha and Pinel also tested the effect of a series of 19 seizures elicited with an interval of 1.5 hours. Although the responses to the 19 stimulation were not suppressed, they resulted in a prolonged inhibition which dissipated after 3 days in terms of the class of the motor seizure. This nicely corresponds to the inter-cluster period in our tetanus toxin injected rats. Not only kindled motor seizure but also spontaneously occurring ones can have inhibitory effect which is documented by Hawkins & Mellanby (1987) who noted that non-motor seizures could happen at much higher rate than motor seizures. Moreover, if a motor seizure appeared among non-motor seizures it was followed by a longer ISI.

Thus, the ISI prolongation can be viewed as a consequence of higher post-seizure inhibition after the seizures occurring towards the end of the cluster. The more inhibited neural network then requires more time to return to the initial excitability or alternatively a stronger (probably

internal or unknown external) stimulus provoking the seizure. The reason why such strong inhibition occurs only after the later seizures of the cluster is likely the fact that the later seizures are more severe in terms of behavioral manifestation and seizure propagation to extra-temporal structures, namely the motor cortices. Further, our data suggest that cumulative effect of the motor seizures may result in a prolonged period of inhibition which results in cluster termination which is in line with the experiment utilizing 19 stimulations inducing long-term inhibition (Mucha & Pinel 1977).

We conclude that the non-motor seizures at the beginning of the cluster have pro-epileptic effect in that they cause the subsequent seizures to be more severe (motor seizures), possibly via mechanisms similar to the kindling. The motor seizures have rather an anti-epileptic effect since once they begin the ISI starts to increase. The cumulative effect of the motor seizures might be the cause of seizure cessation for the period of approximately 2 to 3 days after which the inhibition dissipates and the next seizure cluster can begin.

We provide a theory on how the seizure cluster is governed and how it is terminated but an important question remains unanswered: How do the seizure clusters begin? Do they begin suddenly or is there an underlying process that drives the brain dynamics towards the next seizure cluster? The uniformity of the inter-cluster periods suggests that there could be some underlying mechanism. We will find more evidence by analysis of interictal epileptiform activity, namely epileptic bursts, in the next chapter.

5 Epileptic bursts

5.1 Introduction

Between the seizures, several epileptiform abnormities can be seen in the EEG. The most common are IEDs and during the past decade there has been a great interest in high frequency oscillations (HFOs). In certain types of epilepsy there might be also other EEG biomarkers present such as focal slowing or other forms of altered rhythmogenesis (Javidan 2012).

In the tetanus toxin rats, we observed a not very well known graphoelement called an epileptic burst or shortly a burst. It was previously reported by Hawkins & Mellanby (1987) but they did not analyze its long-term evolution. An example of a burst is in Figure 38.

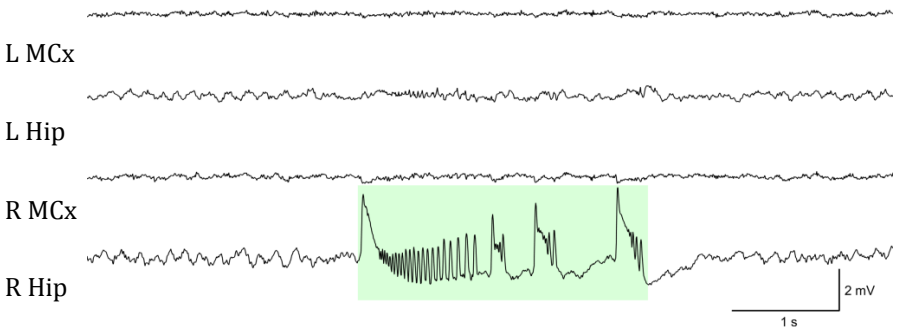

Figure 38: An example of a burst recorded in rat R14. Hip – hippocampus, MCx – motor cortex.

We define the burst as a focal high-amplitude oscillation in the alpha frequency range (occasionally overlapping also with the beta band). The frequency of discharges from which the burst is composed typically decreases during the burst. The duration of bursts is 1 – 8 s. Interestingly, they appear always in the right hippocampus (the one injected with the tetanus toxin) with occasional propagation also to the contra-lateral hippocampus and less prominently to the motor cortices. Bursts do not have any behavioral correlate. Bursts appear during seizure clusters as well as between them. This makes them suitable for the analysis of the inter-cluster periods (Chang et al 2018). Moreover, they occur also before the first seizure which gives opportunity for the investigation of the epileptogenic process. Compared to IEDs, bursts are more complex and thus, provide more parameters to be studied as a function of time.

5.2 Methods

5.2.1 Burst detection

Bursts were detected in the recordings using a detector written in Matlab. The scheme of the detector is in the Figure 39.

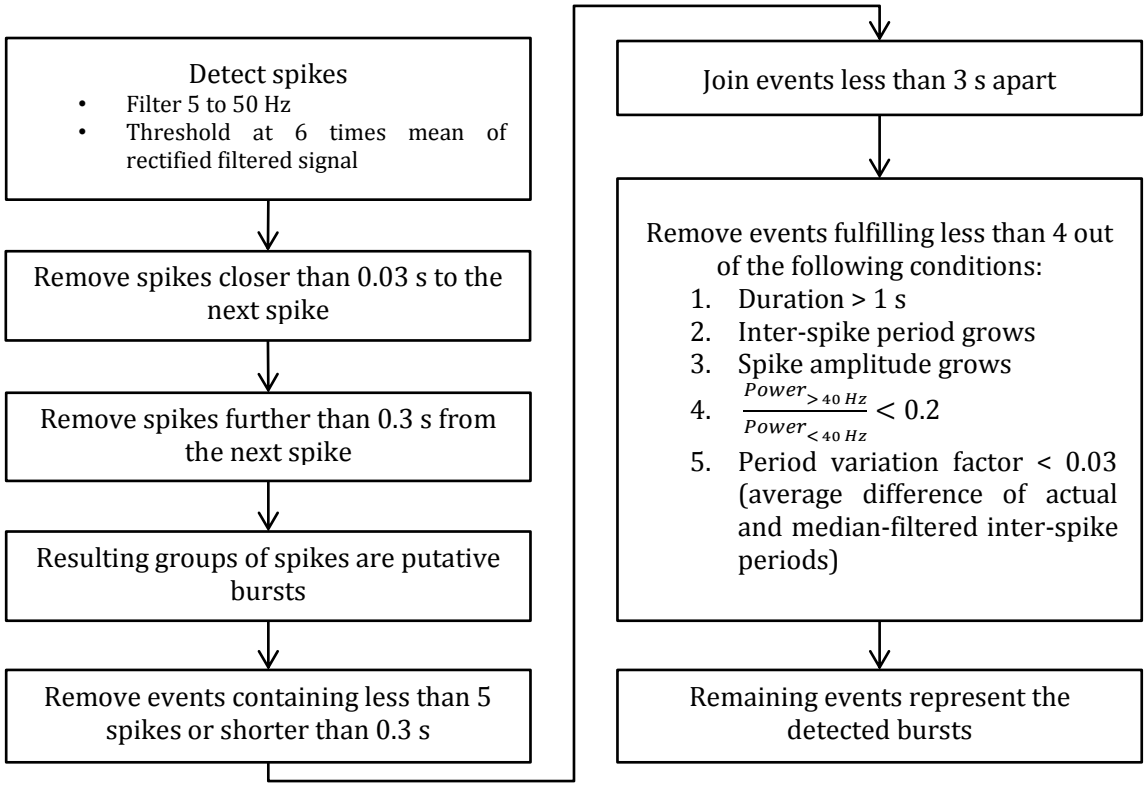

Figure 39: Scheme of the burst detector.

Detections were subsequently visually verified and manually corrected if needed.

5.2.2 Segmentation of time axis

The long-term analysis should be performed in the context of natural dynamics of the epileptic syndrome rather than in some artificial time frame such as days from the tetanus toxin injection. Thus, we decided to use the time frame determined by seizure clusters. We have divided the whole recording into 4 epochs:

1) Period before the first seizure of the same duration as is the duration of the first cluster
2) First cluster
3) Inter-cluster period
4) First 30 hours of the second high-seizure-incidence period (we will call it for simplicity the second cluster although it might have not fulfilled all the criteria of the cluster definition as stated in Paragraph 4.2)

Each of these epochs was divided into 5 equal time bins in which average properties of the burst were analyzed. Thus, in total we had 20 time bins for each rat.

5.2.3 Burst analysis

We have examined the long-term profile of the following burst parameters:

1) Frequency of occurrence
2) Duration
3) Power in each brain region (average of the two electrodes in each region)
4) Maxima of signal cross-correlation between different channels
5) Lag at which the cross-correlation maxima appear
6) Absolute value of the lag at which the cross-correlation maxima appear
7) Median period between successive peaks of the oscillation

Each of these parameters was computed for each burst and averaged over all bursts within a given time segment (see paragraph 5.2.2 for segmentation details).

The signal cross-correlation was computed using Matlab function `xcorr` with the normalization option `'coeff'` according to the following formula

$$\hat{R}_{xy}(m) = \frac{1}{\sqrt{\hat{R}_{xx}(0)\,\hat{R}_{yy}(0)}} \sum_{n=0}^{N-m-1} x_{n+m}\, y_n \qquad \textbf{(30)}$$

where *x*, *y* are the two signals, *m* is the lag between *x* and *y*, and *N* is the total length of *x*. Note that we did not detrend the signal or use any high-pass filter because a slow wave is an important characteristic of the bursts. Some bursts manifest predominantly by the slow wave with rather low-amplitude rhythmic activity superimposed. We were interested in the propagation from the right to the left hippocampus and from the right hippocampus to the both motor cortices. For each burst, we computed cross-correlation function between the pairs of channels of interest, i.e. between each of the two right hippocampal channels and each of the channels in the structures of propagation (two channels in the left hippocampus and total of four channels in the both motor cortices). This gave rise to four vectors of cross-correlation for the hippocampal propagation and eight vectors for the cortical propagation. Next, we computed maximum of the absolute value of each vector within the lag limited to ±50 ms. This limit was based on preliminary visual observation that the delay between the spikes in studied brain structures never exceeded 50 ms. We averaged the maxima from each cross-correlation vector to obtain a single value of cross-correlation magnitude between the hippocampi and one value of cross-correlation magnitude between the right hippocampus and motor cortices for each burst. From these values, we calculated median across all bursts within given time bin.

We also retained the lags at which these maxima appeared. These lags were deemed to represent the propagation delay. For this analysis we used only the cross-correlations which were significant. For the significance evaluation we used the surrogate approach. For each rat, we extracted eight at least one-hour segments of data, one day-time and one night-time segment from each of the four analysis epochs according to the paragraph 5.2.2. From these segments we extracted the set of all bursts and the set of all interictal data with no seizures and no bursts. Then, we computed mean of the absolute values of cross-correlations between the bursts and the interictal data for all combinations of channels. For each combination of channels we calculated 95th percentile of the cross-correlation value between the burst and interictal data which then served as the margin of significance at p=0.05. For the analysis of lags, only the bursts, for which the cross-correlation maximum was above the significance margin, were retained.

Then, we determined the median across the channel pairs of interest and median across bursts of the time lag. Median was preferred to mean in the cross-correlation analysis because it was more robust to outliers. We also analyzed the lags in their absolute value. The procedure was the same as in the analysis of lags apart from computing the absolute value of the lags before computing the median across the channel pairs of interest.

The period between successive spikes within the burst was analyzed as follows. First, each burst was bandpass filtered from 5 to 50 Hz using a 4th order Butterworth filter. Then, spikes were detected using Matlab function `findpeaks` with parameters `'MinPeakProminence'` set to 0.2 and `'MinPeakDistance'` set to 0.02 s. For each burst, we obtained times of its individual spikes. Then, we removed spikes appearing less than 0.03 s after the previous spike and calculated inter-spike periods by differencing the spike times. Afterwards, inter-spike

periods longer than 0.2 s were removed and median of inter-spike period for a given burst was determined. Finally, we computed the median across all bursts within a given time bin. Again, we used the median as a measure of central tendency because there were often peaks missed during the automatic detection which resulted in numerous outliers with a false inter-spike interval value.

5.2.4 Statistical evaluation of trends

The statistical evaluation of possible trends in the parameters was performed by one of the following two methods. Method 1: For each animal, we fitted a straight line to the period of interest. Then, the slopes of the fitted lines were subjected to the Wilcoxon signed rank test to determine whether they were statistically significantly positive or negative. If the trend was expected to be non-linear we used 2nd order polynomial. Method 2: In cases where we wanted to compare two periods of time, we first averaged bins in a given time period for each animal. Then, we subtracted the means of the two time periods for each animal separately. The differences were then evaluated using Wilcoxon signed rank test for being significantly positive or negative.

5.3 Results

Bursts were analyzed in six animals. We have analyzed 1690±317 (1681) bursts from each animal. Bursts could have various shapes, durations, amplitudes and spatial properties even within one subject (Figure 40). We analyzed the long-term evolution of the burst properties.

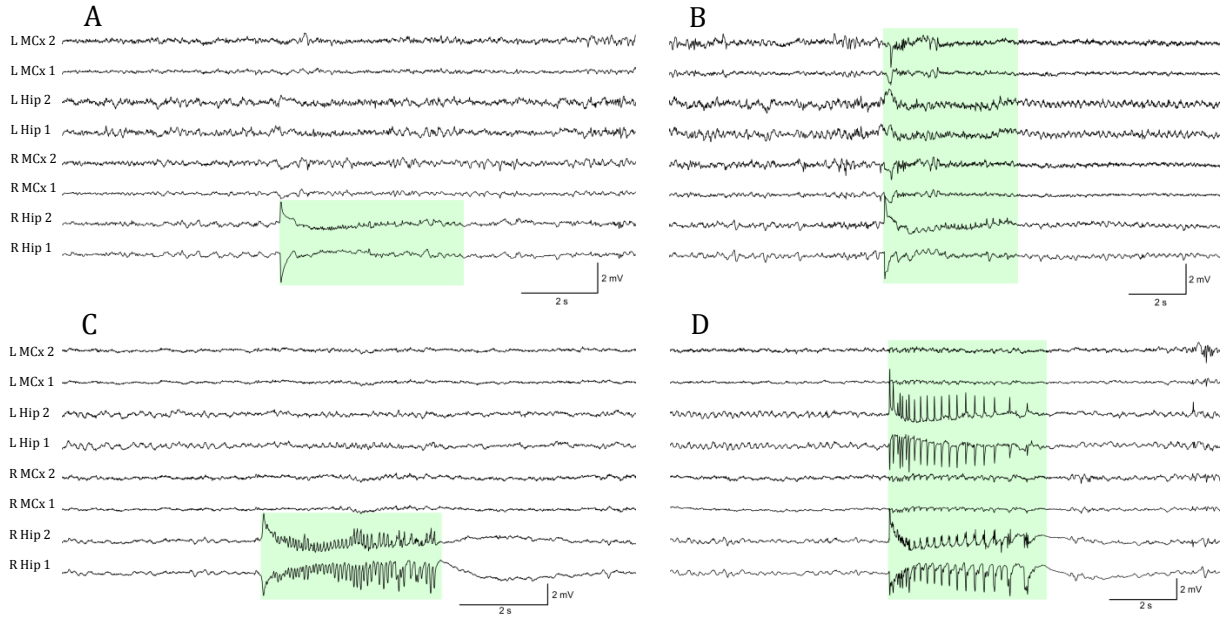

Figure 40: Different bursts recorded in R09. A: Unilateral weak burst which appeared 21 hours before the first seizure. B: Weak burst occurring 16 hours before the first seizure. Weak propagation the contralateral hippocampus and to the motor cortices can be seen. C: Unilateral hippocampal burst 23 hours after the first seizure. D: Bilateral hippocampal burst with weak propagation to motor cortices five hours after the first seizure. Hip – hippocampus, MCx – motor cortex.

5.3.1 Burst frequency of occurrence and duration

Frequency of burst occurrence (burst rate) is depicted in Figure 41 along with mean burst duration. In 6/6 rats, bursts started to emerge gradually before the first seizure. In 5/6 animals in which more than one segment before the first seizure contained bursts, we can see also gradual increase in the duration (p=0.0625, Method 1). After the first seizure, the burst rate

increase not always continued but there was a marked decrease in the duration. Median difference was 3.5 s (bin 5 – bin 6, p=0.0625, Method 2).

In the middle of the inter-cluster period there was a dramatic increase in burst rate (bins 12 through 14) in all rats (p=0.0313, Method 1) which was followed by a mild decrease (bins 14 to 15) in 5/6 rats (p=0.0625, Method 1). Inter-cluster period was also accompanied by a U-shape profile of the burst duration. When the bins 11 through 15 were fitted by a 2nd order polynomial the coefficient of the quadratic term was positive for 6/6 subjects (p=0.0313, Method 1).

After the onset of the second cluster, the burst rate decreased profoundly in 6/6 rats (p=0.0313, bins 15 vs. 16, Method 1). We computed mean rate during the second cluster (bins 16 through 20) and compared it to the mean of the rest of the recording (bins 1 through 15). In all subjects the difference was negative with median of -3.23 events/hour (p=0.0313, Method 2).

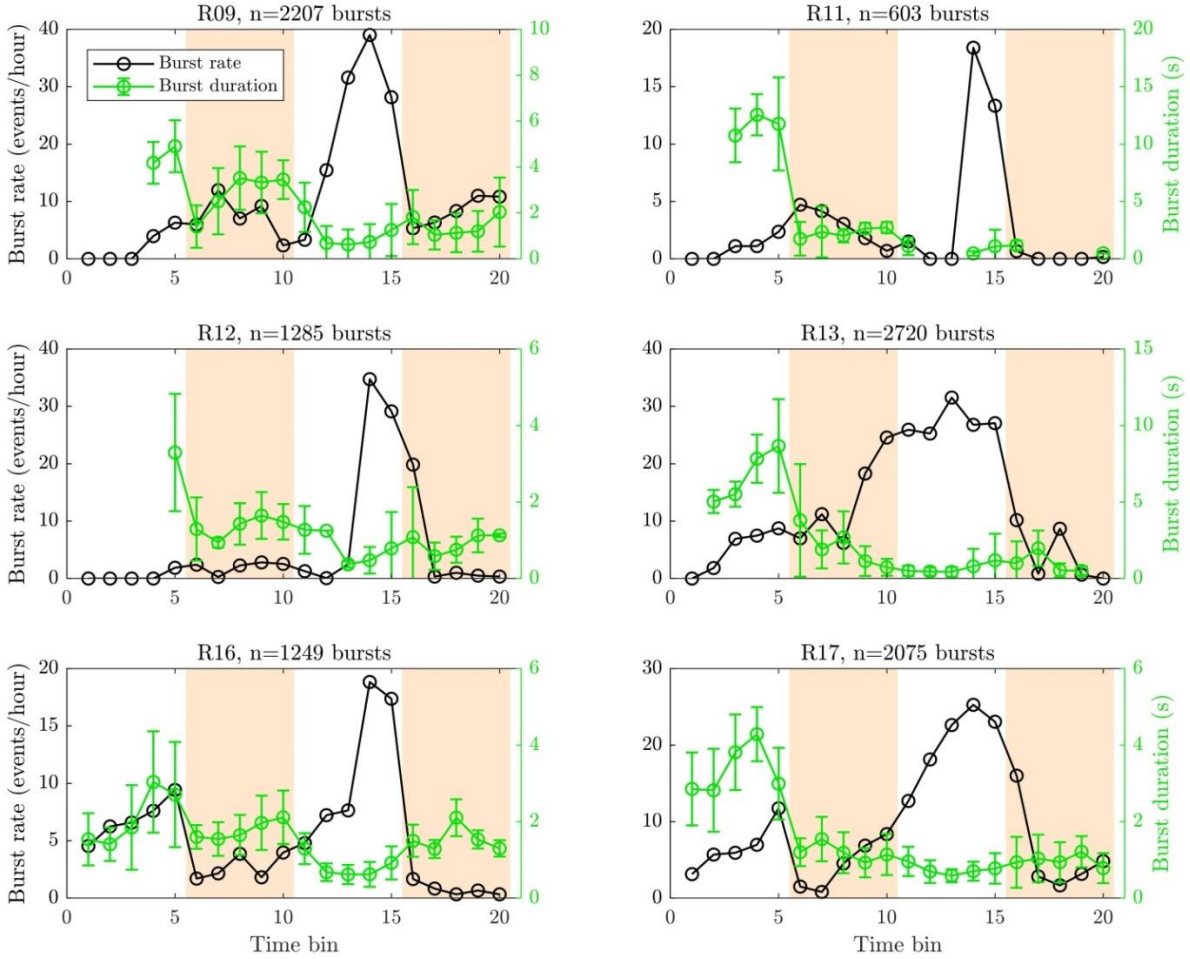

Figure 41: Burst rate (black, left ordinate) and duration (green, right ordinate). Red shading indicates seizure clusters. Error bars – standard deviation.

5.3.2 Burst signal power

Long-term profiles of burst power in the hippocampi and in the motor cortices are in Figure 42 and in Figure 43, respectively. Bursts were generated always in the tetanus toxin injected right hippocampus with variable propagation to the left hippocampus or to the motor cortices. The signal power is a measure of the burst strength or severity (i.e. cellular recruitments and synchronization of neuronal activity) but in the left hippocampus and in the motor cortices, the power can also be interpreted as a measure of the burst propagation. One can clearly see that

the highest power is always in the right hippocampus except for R12 and R17 where the power in the left hippocampus occasionally gets comparable to power in the right hippocampus.

Before the first seizure, 6/6 animals had lower power of bursts than during the first seizure cluster in all recorded brain regions (p=0.0313 for all regions, Method 2). The median differences were –0.36 mV^2 for the right hippocampus, –0.10 mV^2 for the left hippocampus, –0.02 mV^2 for the right motor cortex, and –0.02 mV^2 for the left motor cortex.

In all regions of 5/6 rats, there was a period of increased power at the beginning of the first seizure cluster. In the right hippocampus, the mean difference between the first part (bins 6 through 8) and the second part (bins 9 and 10) of the first cluster was 0.31 mV^2 (p=0.0625, Method 2). In the left hippocampus, it was 0.16 mV^2 (p=0.0313, Method 2). In the motor cortices the difference was not significant.

All 6/6 rats presented an increase of burst power in both hippocampi during the second half of the inter-cluster period (bins 13 through 15, p=0.0313 for both hippocampi, Method 1). Power in the motor cortices did not show any consistent trend across animals.

During the second cluster (bins 16 through 20), bursts were less frequent (Figure 41) but had higher power than during the rest of the recording (bins 1 through 15). In the right hippocampus the median difference was 0.46 mV^2 (p=0.0313, Method 2), In the left hippocampus it was 0.22 mV^2 (p=0.0313, Method 2), in the right motor cortex it was 0.04 mV^2 (p=0.0625, Method 2) and in the left motor cortex it was 0.05 mV^2 (p=0.0625, Method 2).

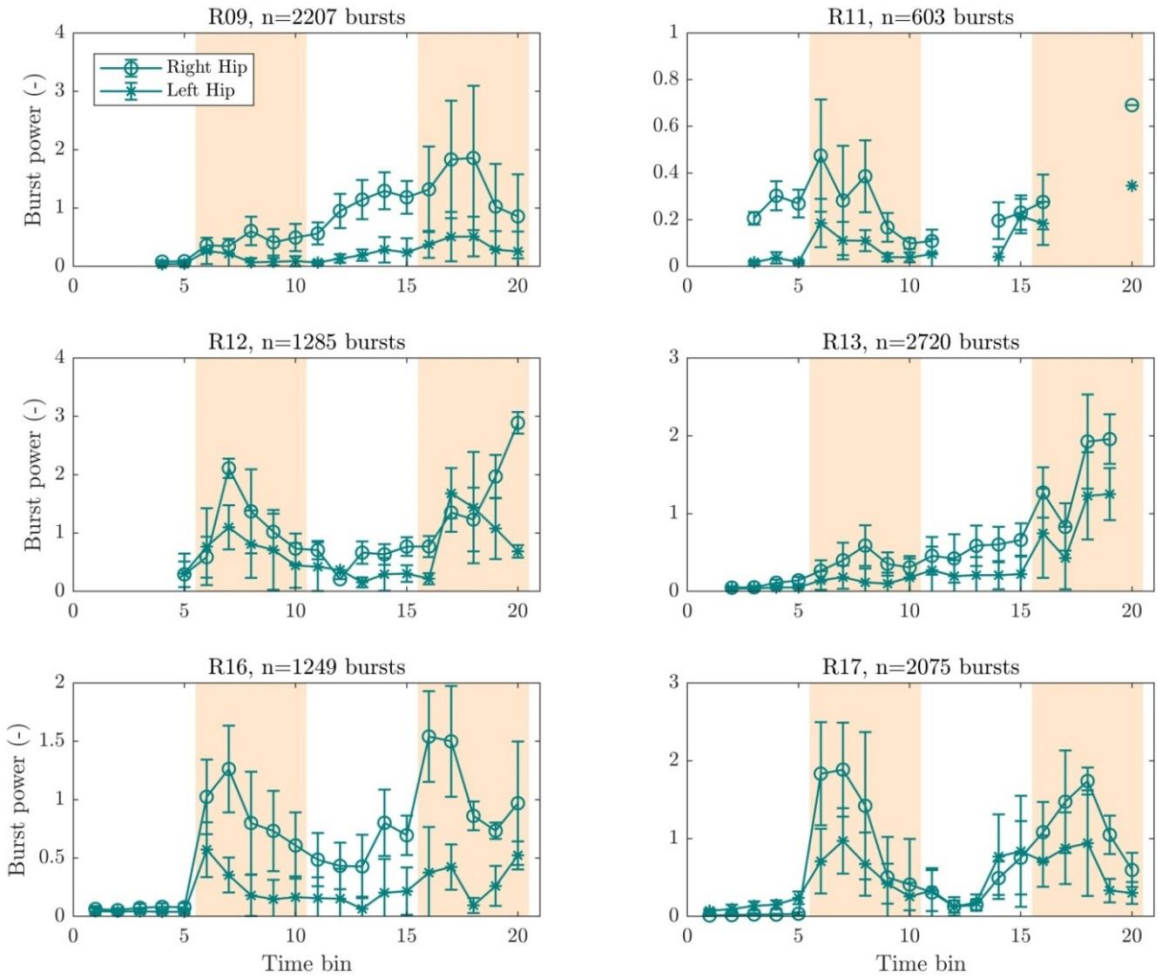

Figure 42: Signal power in the hippocampi. Red shading indicates seizure clusters. Error bars – standard deviation.

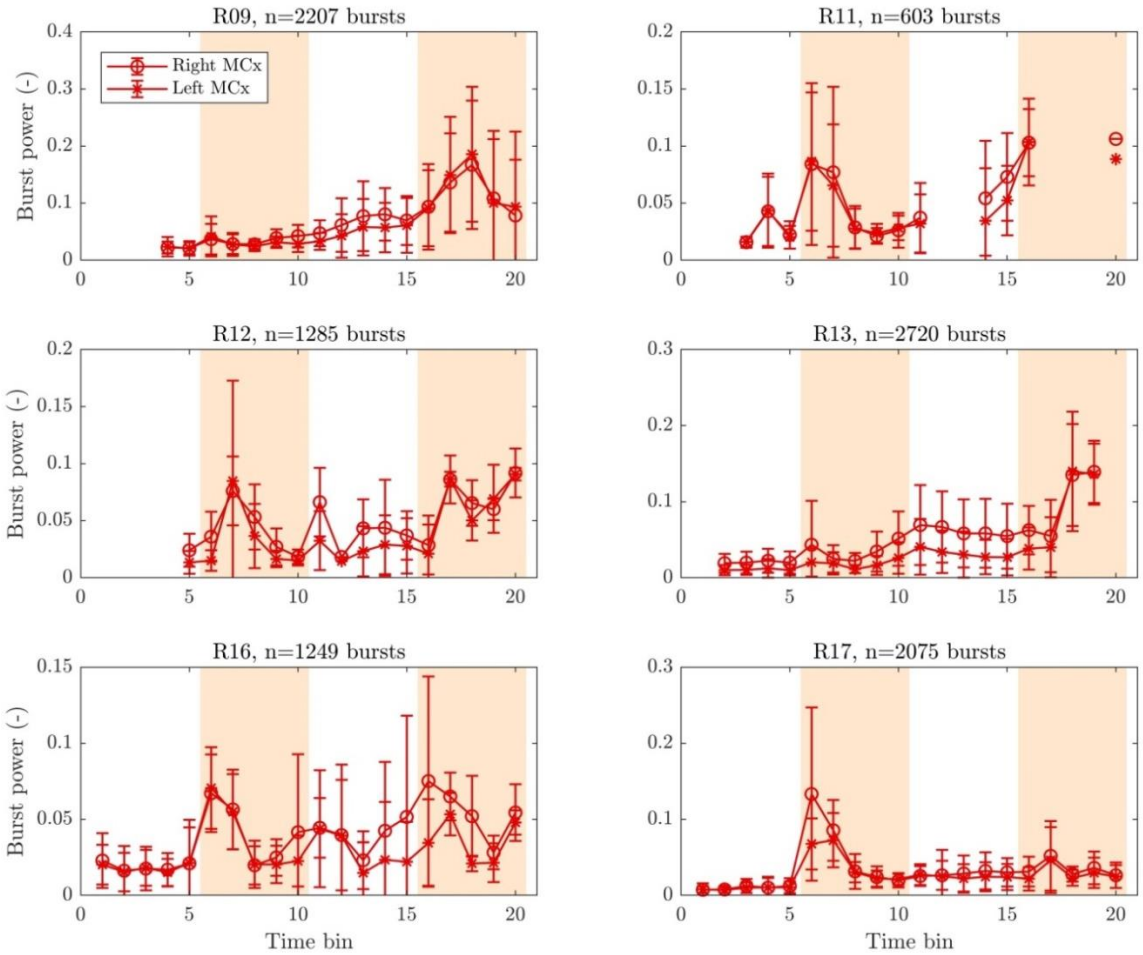

Figure 43: Signal power in motor cortices. Red shading indicates seizure clusters. Error bars – standard deviation.

5.3.3 Burst signal cross-correlation

Cross-correlation function is a measure of signal similarity and as such can be used as another method of burst propagation assessment. The method of computation is described in paragraph 5.2.3. Figure 44 shows the maximum of absolute value of the normalized cross-correlation function.

Before the first seizure, the pattern of cross-correlation maximum fluctuations is rather inconsistent. During the first cluster, the maximum of cross-correlation between the right hippocampus and the motor cortices (red line) decreased in 5/6 rats (p=0.094, Method 1). The decrease in the correlation is consistent with the decrease in the power in motor cortices (Figure 43, paragraph 5.3.2) and probably reflects decreasing propagation of bursts to the motor cortices.

In all rats, there is a clear increase in cross-correlation between the hippocampi as well as between the right hippocampus and the motor cortices during the inter-cluster period (p=0.0313 for both curves, bins 11 through 15, Method 1).

During the second cluster, the cross-correlation function between the right hippocampus and motor cortices gets comparable or even exceeds the correlation between the hippocampi in 5/6 rats which further supports the notion of wide spread of the bursts during this period (see also signal power in Figure 42, Figure 43 and paragraph 5.3.2).

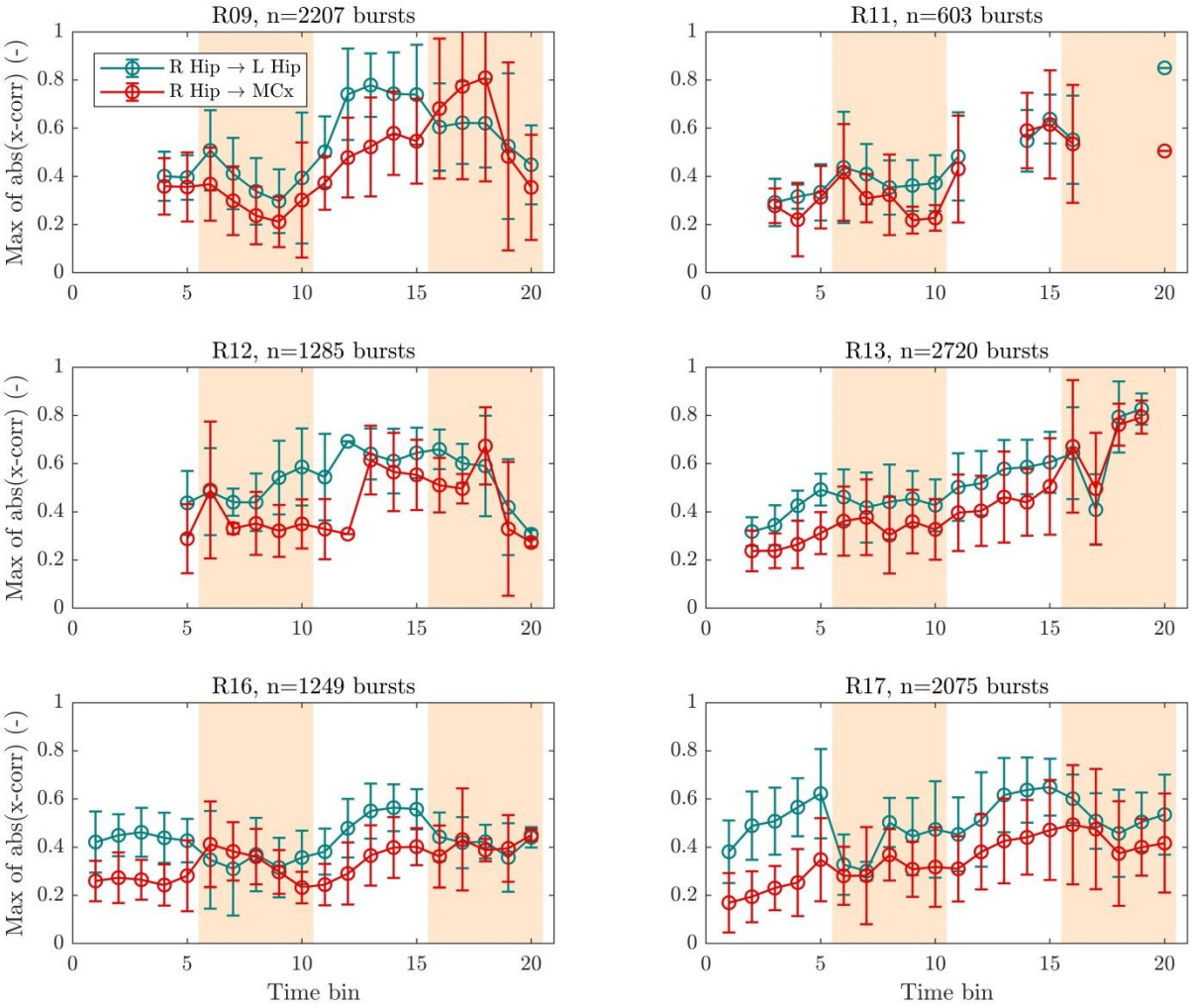

Figure 44: Normalized cross-correlation function during burst – maximum of absolute value. Hip – hippocampus, MCx – motor cortex. Red shading indicates seizure clusters. Error bars – inter-quartile range.

Figure 45 displays the time delay of propagation of burst activity between the hippocampi and between the right hippocampus and the motor cortices. The time delay is represented by the lag at which the absolute value of the cross-correlation function reaches the maximum (these maxima are plotted in Figure 44). Apart from a tendency to lower delays and lower interquartile ranges during the inter-cluster period, there are no consistent trends across animals.

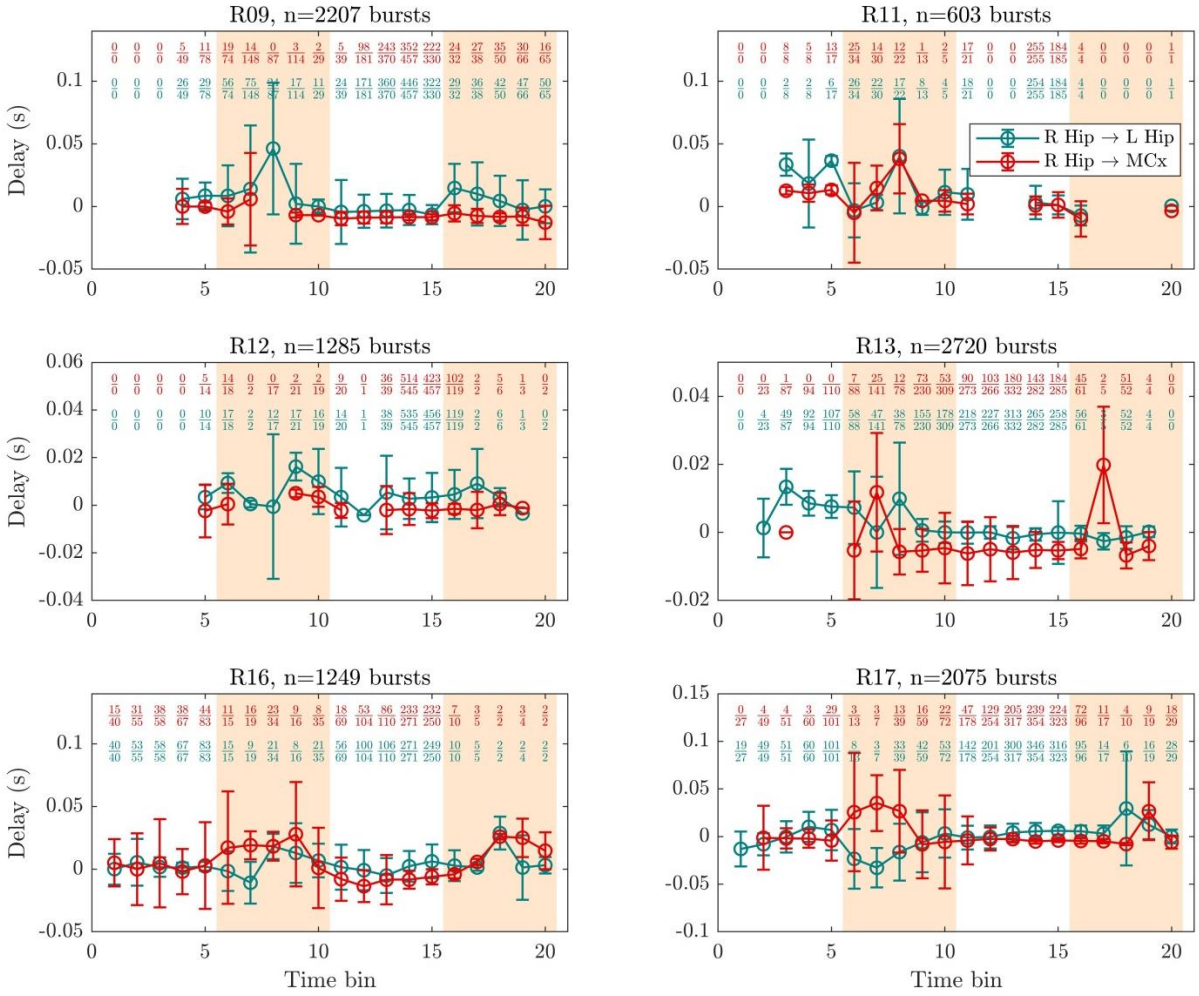

Figure 45: Normalized cross-correlation function during burst – lag of the maximum absolute value. Fractions above the data points indicate the numbers of bursts used for the analysis divided by the total number of burst within the time segment. Only the bursts in which at least one cross-correlation of interest was significant were used. Red shading indicates seizure clusters. Error bars – inter-quartile range.

We also computed absolute values of the delays before averaging, the result of which can be seen in (Figure 46). There was a weak and not absolutely consistent decrease of the delay between the hippocampi (p=0.094, Method 1). This decrease in the delay may be interpreted as an increased synchrony which further supports the idea of increasing ease of propagation of bursts during the inter-cluster period.

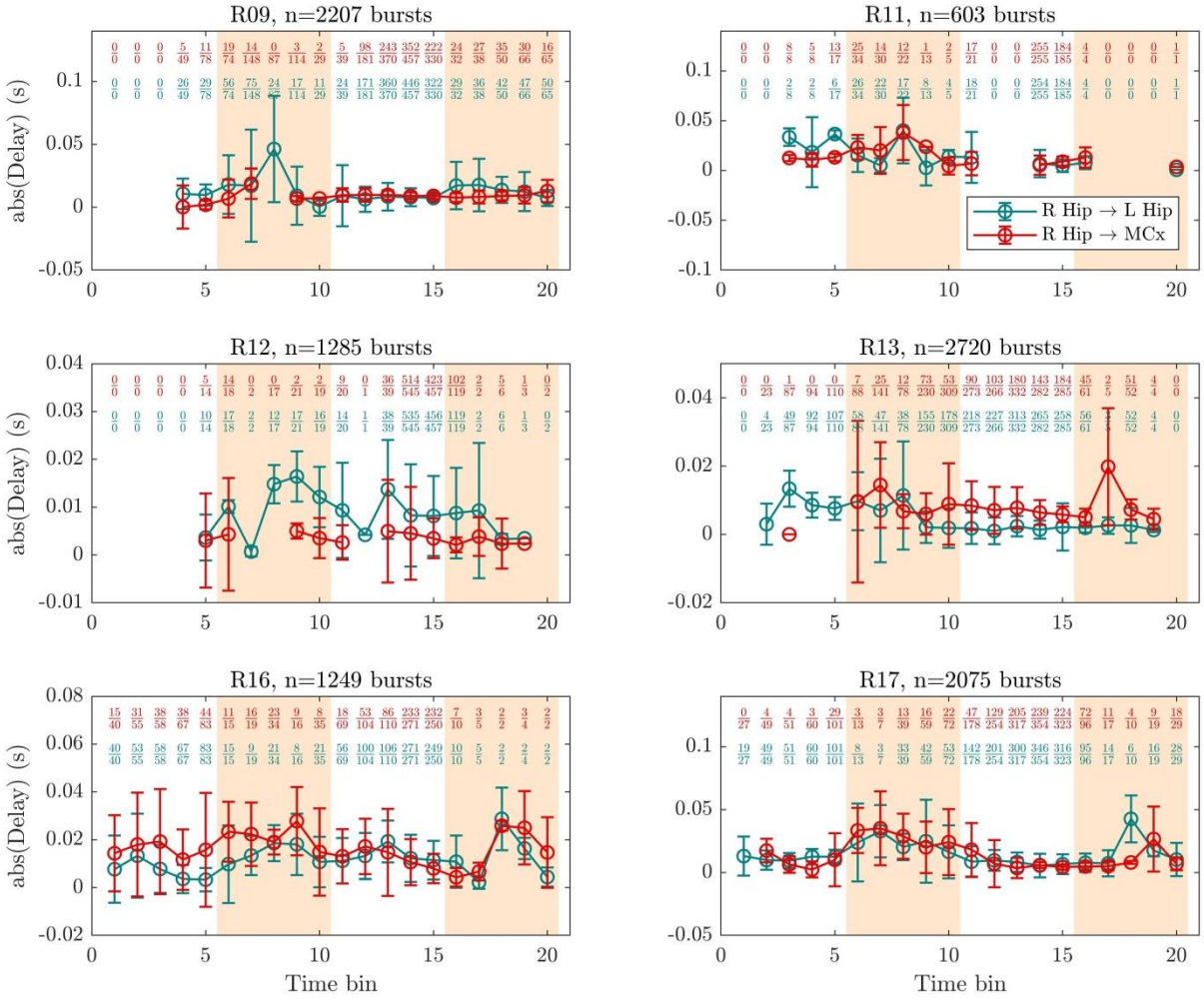

Figure 46: Normalized cross-correlation function during burst – absolute value of the lag of the maximum absolute value. Fractions above the data points indicate the numbers of bursts used for the analysis divided by the total number of burst within the time segment. Only the bursts in which at least one cross-correlation of interest was significant were used. Red shading indicates seizure clusters. Error bars – inter-quartile range.

5.3.4 Burst spikes' frequency

Bursts consist of spikes at the fundamental frequency usually in the alpha EEG frequency band. An important parameter is the exact frequency of the spikes. We analyzed its inverse, the inter-spike period (Figure 47).

Before the first seizure, the inter-spike interval was decreasing in 3/4 animals in which more than two time segments contained bursts (p=0.375, Method 1). During the first cluster the inter-spike interval stabilized at subject-specific frequencies which is illustrated by a gradual decrease of the IQRs in 5/6 rats (p=0.219, Method 1 on IQRs). During the inter-cluster period, there was a decrease of the inter-spike period in 5/6 animals (bins 11 through 15, p=0.0625, Method 1).

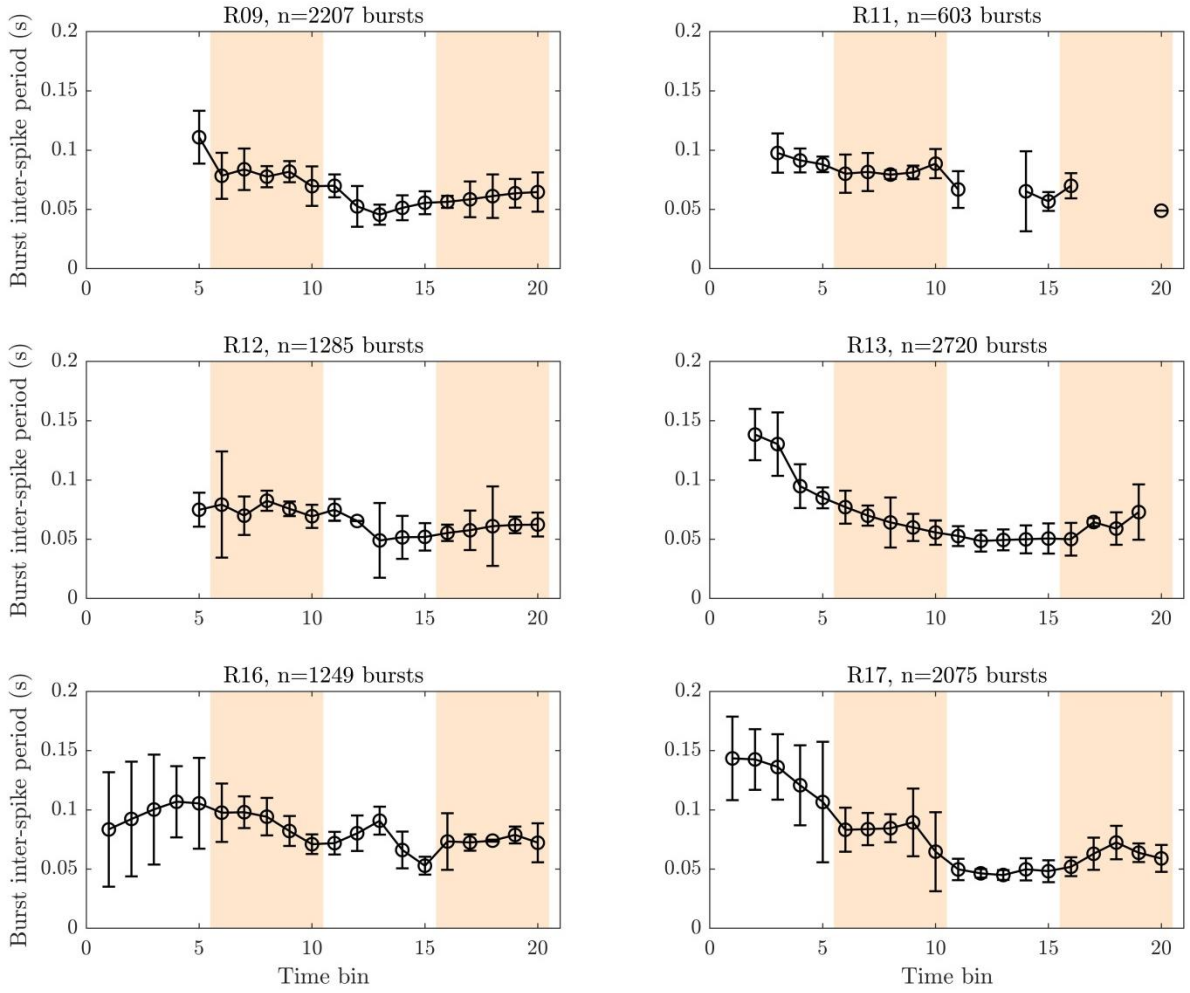

Figure 47: Median inter-spike period of bursts. Red shading indicates seizure clusters. Error bars – inter-quartile range.

5.3.5 Bursts – population data

In Figure 48, the population data from all the measured characteristics of bursts are depicted.

Before the first seizure we observed gradual increase in burst rate (Figure 48A; p=0.0625, Method 1). The duration (Figure 48B) was also increasing (p=0.125, Method 1) and higher than during the rest of the recording (p=0.0625, Method 2). The power of the bursts (Figure 48C,D) during this period was lower than during the first cluster in all the recorded regions (p=0.0625 for all regions, Method 2). No consistent trends were seen in the cross-correlation function (Figure 48E,F,G) The inter-spike period (Figure 48H) of the bursts was non-significantly decreasing (p=0.375, Method 1).

During the first seizure cluster, the burst rate (Figure 48A) and the duration (Figure 48B) did not display any consistent pattern. The average power is higher during the first part of the cluster (Figure 48C,D). Moreover, the burst power in all regions was higher during the seizure clusters than outside the clusters (p=0.0313 for all regions, Method 2). The maximum of cross-correlation between the right hippocampus and the motor cortices (Figure 48E, red line) showed a decrease (p=0.094, Method 1). The decrease in the correlation is consistent with the decrease in the power in motor cortices and probably reflects decreasing propagation of bursts to the motor cortices. The lag of the cross-correlation maximum and inter-spike period did not show any consistent trend (Figure 48F,G,H).

In the middle of the inter-cluster period there was a dramatic increase in burst rate (bins 12 through 14) in all rats (p=0.0313, Method 1). Inter-cluster period was also accompanied by a U-shape profile of the burst duration (p=0.0313, Method 1 on the quadratic term of a 2nd order polynomial). Power increased in both hippocampi during the second half of the inter-cluster period (bins 13 through 15, p=0.0313 for both hippocampi, Method 1). Power in the motor cortices did not show any consistent trend. In all rats, there is a clear increase in cross-correlation between the hippocampi as well as between the right hippocampus and the motor cortices (p=0.0313 for both curves, Method 1). The lag of the cross-correlation maximum did not show any consistent trend (Figure 48F) but when the absolute values of the lags were considered a consistent decreasing trend was found in the cross-correlation between the right hippocampus and motor cortices (p=0.0313, Method 1). In the cross-correlation between the hippocampi, the absolute value of the lag was less consistent (p=0.094, Method 1). There was a decrease of the inter-spike period (p=0.0313, Method 1; Figure 48H).

After the onset of the second cluster, the burst rate dramatically decreased (p=0.0313, bins 15 vs. 16, Method 2; Figure 48A). The duration (Figure 48B) did not show any consistent trend during the second cluster. The power in all regions (Figure 48C,D) was higher than during the rest of the recording. The maximum of the cross-correlation between the right hippocampus and motor cortices gets comparable to the correlation between the hippocampi (Figure 48E). The lag of the cross-correlation maximum (Figure 48F,G) and the inter-spike period (Figure 48H) did not show any consistent trends in the second cluster.

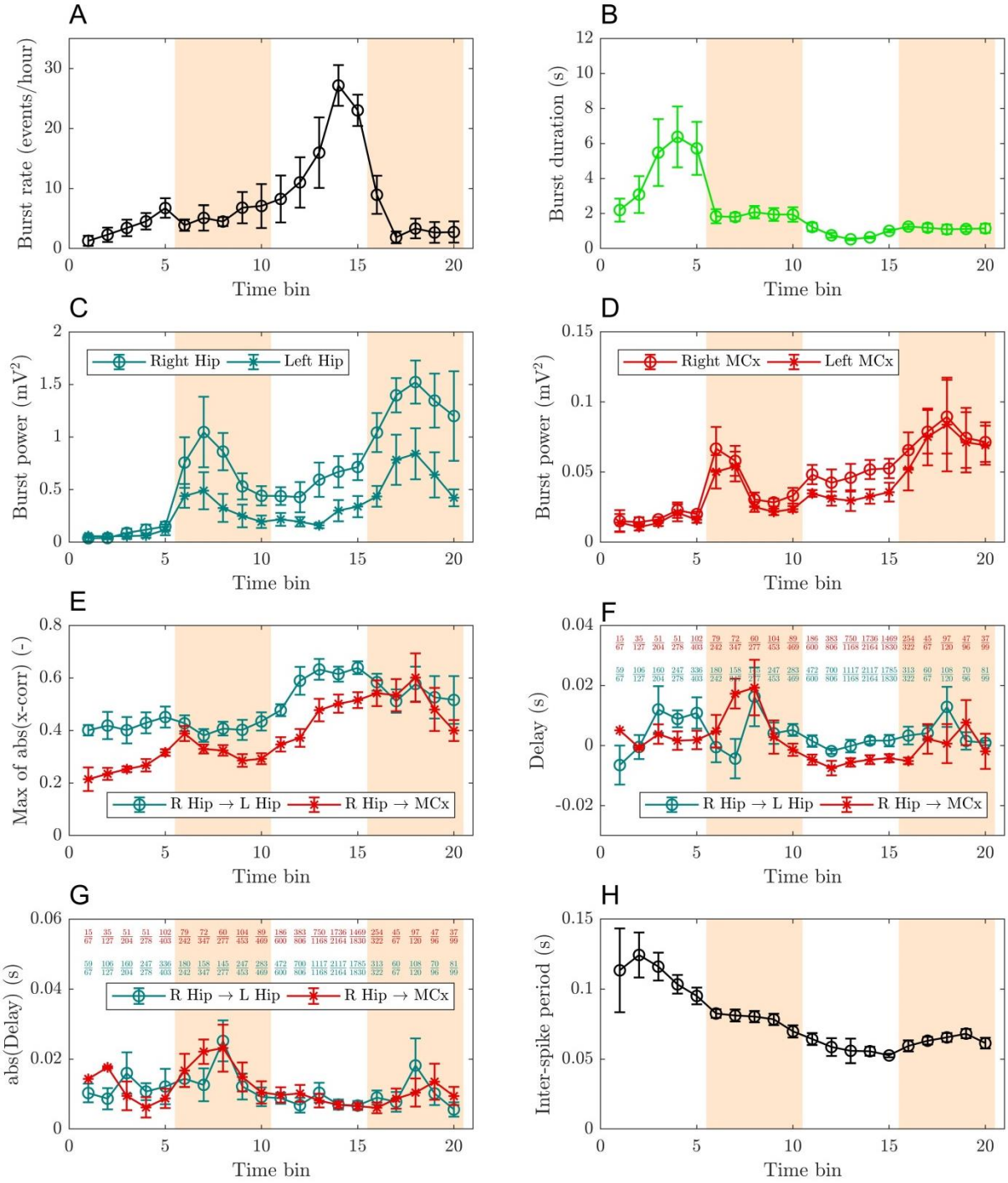

Figure 48: Population data from analysis of bursts in 6 rats. Errorbars denote standard error of the mean (SEM). A: Rate. B: Duration. C: Power in the hippocampi. D: Power in the motor cortices. E: Maximum of the cross-correlation function's absolute value. F: Lag of the cross-correlation maximum interpreted as delay of propagation of the burst activity from the right hippocampus to the left hippocampus or to the motor cortices. G: Absolute values of the delays from F. H: Median intervals between spikes within the burst.

6 Discussion

In this chapter, we focused on a not very well known epileptic graphoelement called burst. Hawkins & Mellanby (1987) speculated that bursts are damped seizures since they morphologically resemble beginnings of seizures. We did not find such a striking similarity. The most salient difference between bursts and seizures is that while majority of bursts are spatially limited events localized to the right hippocampus seizures practically always start simultaneously in both hippocampi. Apart from that, there are inter-individual differences in the long-term profiles of hippocampal burst power (Figure 42). These individual profiles in the first cluster approximately correspond to the individual long-term profiles of hippocampal IED rate (Figure 36) which suggests that the mechanism of the burst generation may be similar to the mechanism of IED generation rather than seizure generation.

Regardless of their mechanistic origin, bursts are suitable for studying the long-term evolution of the syndrome even in the periods when there are no seizures. We have shown that the bursts were subject to changes in several of their parameters during our observation period. The main findings are as follows:

1. All bursts appear in the tetanus toxin injected (right) hippocampus with occasional propagation to the contralateral hippocampus or to the motor cortices
2. Before the first seizure, bursts start appearing with gradually increasing
    a. Rate of occurrence
    b. Duration
    c. Frequency of spikes (inverse of the inter-spike period)
3. During the first cluster
    a. The power is higher in the first half of the cluster than in the second half
    b. Cross-correlation between the right hippocampus and the motor cortices decreases
    c. The frequency of spikes stabilizes
4. During the inter-cluster period
    a. In its middle portion, the burst rate sharply increases
    b. Duration produces a U shape with values very similar across subjects
    c. Power in the hippocampi increases
    d. Maximum of the cross-correlation function between the hippocampi as well as between the right hippocampus and the motor cortices increases
    e. Absolute value of delay between the hippocampi as well as between the right hippocampus and the motor cortices decreases
    f. Spike frequency increases
5. After the beginning of the second cluster
    a. Rate of occurrence greatly decreases
    b. Power in all structures increases
    c. Maximum of the cross-correlation function between the right hippocampus and the motor cortices gets comparable to the maximum of the cross-correlation function between the hippocampi

Similarly to Hawkins & Mellanby (1987), we observed bursts before the first seizure (during the latent period). We also observed them during the inter-cluster periods. Our data from the latent period support the notion of epileptogenesis as a gradual process rather than a step function of time as was earlier proposed by Hellier & Dudek (1999) and Williams et al (2009) based on observations in kainate treated rats. Hellier & Dudek (1999) postulated that epileptogenesis continues beyond the first seizure because once the seizures began their frequency of occurrence was not constant but gradually increased until it reached a plateau after several months. Williams et al (2007) took this consideration a step further by backward extrapolating the seizure frequency and speculated that the seizure probability slowly increases

since the initial insult irrespective of the actual time of first seizure occurrence. They supported this theory also by the fact that the times from the initial insult (status epilepticus) to the first seizure are extremely variable from 2 days to months. Here, we bring more direct evidence in a different model of epilepsy that the epileptogenesis is a slow and gradual process before the first seizure in the form of gradually increasing epileptiform EEG activity (bursts) before the first seizure. Similar results were reported by White et al (2010) who observed IEDs before the first seizure in the kainate model of epilepsy. However, in contrast to the kainate studies we did not observe an increase in seizure frequency after the first seizure. But we cannot say that there is no more progression of the syndrome after the latent period because complex changes in seizure properties take place (see chapter 4).

We can also speculate that the epileptogenesis in the tetanus toxin model is driven by the bursts. The tetanus toxin was injected only into the right hippocampus but in most rats the first seizure began in both hippocampi simultaneously. It could be that the functional connectivity between the hippocampi is so strong that any pathological activity immediately propagates to the contralateral hippocampus. However, most bursts are unilateral or at least their propagation is so weak that they are barely discernible from the background activity in the left hippocampus. This is evidence that unilateral epileptic activity is possible in the rat hippocampus. Moreover, we often see unilateral IEDs and occasionally unilateral non-motor seizures. Thus, we propose the following scenario. Tetanus toxin increases the excitability of the injected hippocampus which results in bursts. Repeated bursts then may cause synaptic changes similar to those observed in kindling. Indeed, during kindling, the first elicited seizures (after-discharges) are focal seizures but they facilitate the spreading of the subsequent seizures. Similarly, the bursts can facilitate the pathways for ictal activity propagation between the hippocampi. An alternative scenario could be that the excitability of the contralateral hippocampus proper could be increased through a mechanism similar to long-term potentiation (LTP) which is a commonly used model of learning and memory. This would then also enable bilateral seizures.

During the first cluster the bursts got more similar across the animals and their rate continued to rise whereas duration kept constant at approximately 2 s. The energy in the hippocampi as well as in the motor cortices was relatively high during the first part of the cluster and then decreased which was consistent with the IED rate in the hippocampus in most animals. Interestingly, there were slight inter-individual differences in the hippocampal IED rate intra-cluster evolution which were mirrored by the energy of bursts in the hippocampus. This observation may suggest some shared mechanisms of generation between the IEDs and burst and support the view that the bursts are mechanistically more similar to the IEDs than seizures.

Very interesting trends in burst parameters were observed during the inter-cluster period. During this period, since seizures are absent, the bursts are a good way of exploring the dynamics of the brain. IEDs could be also used to monitor the syndrome but bursts offer more parameters to be studied. During the inter-cluster period we found increase in the rate of bursts, increase in their power, increase in the propagation from the right hippocampus to other structures, decrease of the delay of this propagation and decrease in the inter-spike period (the bursts are “faster”). We interpret these changes as increase in excitability and increase in the ease of propagation of epileptiform activity. We find these observations as an evidence of an underlying process which leads the brain dynamics towards the next seizure cluster. Whether the bursts are the cause or the result of this process is impossible to tell from our data. Litt et al (2001) analyzed few-days long recordings from invasive monitoring of 5 epilepsy surgery candidates with the goal of finding preseizure changes in the EEG. In one patient, they reported increasing rate of Focal Subclinical Seizures (FSCSs) which were few second long bursts spikes. At the beginning of the FSCS, the spikes had frequency 20 – 25 Hz. With the progression of the FSCS, the frequency decreased to 6 – 10 Hz. The FSCSs appeared in the seizure focus of this patient. These two facts lead us to speculate that the FSCSs in this patient may represent a phenomenon similar to the bursts. However, we did not observe any increase in the burst rate

with in advance of a single seizure (data not shown). Instead, we observed the increase of the burst rate on a larger time scale, i.e. with impending cluster of seizures.

During the beginning of the second cluster, bursts get more generalized with high power. They often resembled fast series of IEDs and, indeed, were sometimes difficult to distinguish. This qualitative as well as quantitative change could be the result of the processes occurring during the inter-cluster period which might, again, have a kindling-like nature.

7 General discussion and conclusion

In this work, we examined long-term seizure dynamics in the tetanus toxin model of mesial temporal lobe epilepsy in rats. In Chapter 3, we examined the whole seizure profiles. We found out that the seizures are not Poissonian which is congruent with most human studies (Balish et al 1991, Bauer & Burr 2001, Binnie et al 1984, Cook et al 2014, Karoly et al 2016, Milton et al 1987, Tauboll et al 1991). We also tested the statistical distribution of inter-seizure intervals (ISIs) and in contrast to Osorio et al (2009) and Cook et al (2014) we did not find them power-law distributed although their distribution had a fat tail. The fat tail was also confirmed by the analysis of the expected time until the next seizure conditioned on the time elapsed since the last (Sornette & Knopoff 1997) which revealed a positive trend similarly to Osorio et al (2010). Unlike most human (Frederick L. Patry 1931, Goldenholz et al 2018, Griffiths & Fox 1938, Karoly et al 2016, Mirzoev et al 2012) and animal studies (Arida et al 1999, Bertram & Cornett 1994, Cavalheiro et al 1991, Fenoglio-Simeone et al 2009, Hellier & Dudek 1999, Pitsch et al 2017, Raedt et al 2009, Sedigh-Sarvestani et al 2014, Stewart et al 2001, Stewart et al 2008), we did not find any consistent pattern of circadian seizure distribution and thus, our results are similar rather to those of Bajorat et al (2011), although when data from all rats were aggregated, the seizures appeared more prevalent during the light period (inactive period of rats) which is in agreement with the study of Sedigh-Sarvestani et al (2014) who used the same model of epilepsy as we did. In all rats we identified seizure clustering. In each rat we identified one to three clusters. The clusters were placed under scrutiny in Chapter 4.

Chapter 4 describes the thorough analysis or seizure clusters. We have revealed that similarly to the whole profiles, the intra-cluster profiles are not Poissonian and intra-cluster ISIs are not power-law distributed. However, compared to the whole profiles, the tail of the distribution was somewhat thinner, presumably due to the absence of the inter-cluster ISIs. The main novelty of this work consists in the analysis of seizure properties along the cluster progression. We have found significant gradual increase of the following parameters with the intra-cluster time: inter-seizure interval, power in the motor cortices (seizure spread), percentage of motor seizures (behavioral severity – a correlate of the seizure spread) and interictal epileptiform discharge (IED) rate in the motor cortices. These observations can be viewed as gradual intensification of the seizures and simultaneous decrease of their frequency of occurrence. Interestingly, gradual intensification of seizures is commonly observed also in human patients (Karoly et al 2016). It would be interesting to analyze the seizure clusters also in other animal models of epilepsy which hasn't been done so far.

The mechanisms of seizure propensity fluctuations are not fully understood but certain theories exist. In the case of the circadian fluctuation, one possible factor could be the level of melatonin. Melatonin is a hormone synthesized and secreted by the pineal gland during night. Its main function is to distribute the information about light or darkness to the whole body (Claustrat & Leston 2015). Agomelatine, an agonist of MT1 and MT2 melatonin receptors, was shown to have an anti-seizure effect (Aguiar et al 2012, Dastgheib & Moezi 2014). In humans, the melatonin level is highest at night. Interestingly, at night, there is low probability of seizures in the mesial temporal lobe epilepsy patients (Leite Goes Gitai et al 2019, Mirzoev et al 2012). Expression of several genes showing circadian pattern (e.g. mTOR, mechanistic target of rapamycin) was shown to influence the seizure propensity (Leite Goes Gitai et al 2019). In catamenial epilepsy, several patterns are observed, one of which is perimenstrual seizure exacerbation. This may be caused by the withdrawal of progesterone during premenstrual period which results in decrease of allopregnanolone, a positive allosteric modulator of $GABA_A$ receptors. Thus, women suffering from perimenstrual seizures may benefit from progesterone supplement taken during the perimenstrual period (Herzog 2015). However, there are plenty of cases where the fluctuation of seizure susceptibility is not related to the obvious biological cycles or environmental changes. This was also the case for our tetanus toxin injected rats which

were all males and were kept in a constant environment except for the 12/12 light/dark cycle which, however, did not result in any circadian pattern of seizures consistent across the animals.

We believe that the cause of the seizure propensity fluctuation in the tetanus toxin model of epilepsy can be the seizures per se. We speculate that the focal seizures occurring at the first part of the cluster facilitate generalization of later seizures, which is essentially a kindling effect (Racine 1972). This phenomenon is in line with the old saying of epileptology "seizures beget seizures" which was first coined by Sir William Gowers (Gowers 1881). However, only focal seizures and not generalized seizures have such potentiating effect (Loscher & Kohling 2010). Once the generalized seizures appear, they have rather anticonvulsive effect in that the seizures become less and less frequent. We speculate that the cumulative effect of the generalized seizures finally leads to the termination of the seizure cluster. The inhibitory effect of a generalized seizure was documented in kindling (Mucha & Pinel 1977) as well as in experiments with maximal electroshock (Handforth 1982). In these two studies a series of preconditioning generalized seizures produced a marked increase of threshold for seizure induction. This inhibition then slowly dissipated over several days. In clinics, several generalized seizures are induced in few-days interval as the electroconvulsive therapy, a standard procedure in the treatment of pharmacoresistant major depression. The seizure threshold is known to gradually increase during the course of the treatment (Fink 1978, Green 1960, Reisner 2003, Shapira et al 1996) which further supports our view of the generalized seizures as a factor lowering the seizure propensity. This result is rather in the contradiction with the Gowers' aphorism "seizures beget seizures". Indeed, results of studies are at least disparate as to whether the aphorism is valid and under which circumstances (Blume 2006, Hauser & Lee 2002).

The mechanism of the seizure-induced inhibition is likely the same as one that terminates the seizure (Loscher & Kohling 2010). One can think of several factors influencing the excitability that may change during the seizure and be responsible for its termination and for post-ictal depression. Energy failure due to oxygen or glucose depletion seems rather unlikely. Although glucose and glycogen levels may decrease during the seizures, ATP and high-energy phosphate levels are almost unchanged even during long-lasting seizures (Folbergrova et al 2000, Kovacs et al 2018). Metabolic disturbances during seizures may even rather promote than inhibit the synchronous activity (Otahal et al 2014). Depletion of glutamate, increase in GABA concentration or changes in gap junction function are also rather discussible theories (Loscher & Kohling 2010). Ca^{2+} influx occurs during the excessive neuronal activity may activate potassium outflux and thus repolarize the depolarized neurons. However, this theory remains to be corroborated (Loscher & Kohling 2010). Changes in the ionic environment may be also responsible. In particular, the extracellular K^+ increase may lead to depolarization block of neuronal activity but it is doubtful whether the extracellular K^+ rises to sufficient levels during seizures in chronic epilepsy (Loscher & Kohling 2010). Another factor is pH. In the low Mg+ in vitro model of seizures, artificial acidification increased the interval between seizure-like events or even completely suppressed them, probably via blockade of NMDA receptors (Velisek et al 1994). In an in vivo study, during most seizures acidification took place and even a cumulative effect of such acidification was seen during a series of seizures. Artificial acidification induced by apnea and resulting increase in pCO_2, prevented seizures. Nevertheless, the authors concluded that the acidification is not the primary mechanism of seizure arrest since in some seizures rather alkalinization was observed which had, however, no influence on the seizure duration (Caspers & Speckmann 1972). Another study has shown that inhalation of 5% CO2 had a potent anticonvulsant effect in rats, macaques and human patients (Tolner et al 2011). The main mechanisms speculated to be responsible for the effect were decrease in pH which may influence ion channel conductances and facilitate adenosine signaling (Dulla et al 2009). Ictal production of lactate which then takes up to 24 hours to be cleared (Folbergrova et al 2000) is another source of acidification (Kovacs et al 2018). Thus, the change in the pH might be one of the mechanisms of seizure termination and post-ictal depression (Kovacs et al 2018, Loscher & Kohling 2010).

The most probable mechanisms of post-ictal depression and possibly termination of the seizure cluster are neuromodulators. Neuromodulators are substances which alter synaptic transmission (Loscher & Kohling 2010). It was shown that endogenous opioids are released in the epileptic foci of patients with reading-induced seizures (Koepp et al 1998). Endogenous cannabinoids may also have anti-seizure effect although their release during the seizures was not confirmed so far (Loscher & Kohling 2010).

An important inhibitory neuromodulator is adenosine (Boison 2005). Adenosine analog 2-chloroadenosine was shown to decrease severity and duration of kindled seizures (Dragunow et al 1985) and block pilocarpine induced seizures (Cavalheiro et al 1987). On the other hand, adenosine is released during seizures (Berman et al 2000). It was also shown that in human patients during focal seizures, adenosine concentration in the focus increases from 2 μM to as much as 65 μM (During & Spencer 1992) which was more than the concentration of 40–50 μM which was shown to potently inhibit epileptic activity in the human epileptogenic cortex in vitro (Kostopoulos et al 1989). In the patients, the adenosine concentration remained elevated for at least 18 minutes post seizure (During & Spencer 1992). Conversely, blockage of A_1 adenosine receptors by theophylline leads to status epilepticus (Fukuda et al 2010). Thus, adenosine is likely an important factor contributing to seizure termination and postictal depression. We speculate that adenosine released during the seizures could be responsible for the decrease of seizure rate with the cluster progression and its accumulation could be responsible the termination of the seizure clusters in the tetanus toxin model of epilepsy.

Another extensively studied neuromodulator is neuropeptide Y (NPY). NPY targets 5 classes of receptors (Y1–Y5). In the hippocampus, the most abundant one is Y2 which reduces excitation (Lado & Moshe 2008). NPY was shown to inhibit electrically elicited seizures in rats (Woldbye et al 1996). NPY expression is enhanced by recurrent seizures in various brain areas. Following kainate-induced status epilepticus, the NPY overexpression is maximal after 6–12 hours, depending on the brain region. NPY system is believed to represent another seizure-limiting factor (Lado & Moshe 2008, Loscher & Kohling 2010, Vezzani & Sperk 2004) and possibly it could also contribute to the prolongation of inter-seizure intervals with the seizure cluster progression and finally the cluster arrest.

In Chapter 5, we dealt with epileptic bursts – short burst of seizure-like activity. We have shown that bursts appear not only during seizure clusters but also between them and even before the first seizure. During the whole observation period, they undergo profound changes in several properties. Interestingly, all bursts appeared in the tetanus toxin injected hippocampus with occasional contra-lateral propagation which potentially gives them also a spatially localizing value (which was not possessed by seizures or IEDs). Experiments utilizing different site of the tetanus toxin injection, such as the ventral hippocampus, would be useful to confirm this idea. We have shown that before the first seizure the burst rate increases and other parameters are highly individual. We speculated that the development of chronic epilepsy might be driven by the bursts. This could be seen in line with the saying “seizures beget seizures” if we generalize it to “epileptic activity begets seizures”. It would be interesting to perform an experiment in which the bursts would be blocked (e.g. pharmacologically, optogenetically or chemogenetically) and see whether the animals would develop seizures. Such experiment could prove or disprove our speculation. During the inter-cluster period we observed marked increase of burst rate, energy in all regions, cross-correlation between regions and frequency of burst constituting spikes. Absolute value of delay between the regions decreased. We interpret these changes as an evidence of increasing excitability and facilitated propagation of epileptic activity throughout the brain. This gradual increase is an evidence of the underlying mechanism which leads the brain dynamics toward the second seizure cluster, i.e. the second seizure cluster does not initiate suddenly and randomly.

An obvious clinical application of the knowledge of the long-term seizure probability fluctuation would be chronotherapy. Chronotherapy refers to "the administration of medication or treatment in coordination with the body's circadian rhythms to maximize effectiveness and minimize side effects" (Merriam-Webster 2019). In a broader meaning it does not necessarily have to be only circadian rhythms but also other biological rhythms (Ramgopal et al 2013). Since the dysregulation of clock genes and clock-controlled genes expression was identified in the hippocampus in mTLE it has been suggested that restoring the circadian rhythms may alleviate the seizures as well as comorbidities such as memory impairment, mood disorder or sleep. Possible ways of restoring the circadian rhythms include pharmacotherapy, diet, light exposure and physical exercise (Leite Goes Gitai et al 2019). For example melatonin or its agonist tasimelteon has been already used for the resetting of the circadian rhythms in totally blind people (Emens & Eastman 2017, Lockley et al 2015). Another chronotherapeutic approach is so-called differential dosing, i.e. administration of a higher dose of an anti-seizure drug when higher seizure susceptibility is expected. Several studies have shown advantages of this approach in the situation of the circadian seizure susceptibility fluctuation (Baud & Rao 2018, Guilhoto et al 2011, Yegnanarayan et al 2006). On the other hand, the troughs in the blood concentration of the drug (so-called drug holiday) can decrease drug tolerance and increase the drug efficacy at the period of the disease exacerbation (M Kenny et al 1986). Similar approach can be used in the case of catamenial seizures in women (Crawford 2005, Voinescu & Pennell 2017). A physician can for example increase the drug dose during the period of high seizure propensity (Navis & Harden 2016). Another option is an add-on therapy during the higher risk periods. Intermittent clobazam was reported to significantly improve seizure control (Feely & Gibson 1984). The intermittency is crucial in this drug since long-term treatment leads to development of tolerance within few weeks (Gastaut & Low 1979).

Similar approaches may be useful also in case of other types of seizure probability fluctuation, typically on longer time-scales. The patterns of these fluctuations are usually less obvious but with the use of chronically implanted intracranial EEG recording devices, they can be unraveled. Baud et al (2018) observed circadian as well as multidien cycles of IED rate and reported that seizures preferred the rising edge of both cycles. Although this was a retrospective study, prospective studies on estimation of seizure risk (i.e. seizure forecasting) by similar methods can be expected in the near future (Baud & Rao 2018).

Successful implementation of chronopharmacology would result in higher efficacy, less side effects and lower cost of the treatment. Moreover, it would enable the use of drugs to which tolerance is developed when used chronically. Alternatively, a closed-loop electronic system such as neurostimulator controlled by the seizure risk could be used. Again, delivering a continuous stimulation only during the high risk period would minimize side effects (Baud & Rao 2018, Loddenkemper 2012). With the closed-loop systems it is also feasible to use a short-term stimulation protocol to prevent impending seizure in case of successful seizure prediction or at least early detection algorithm is available (Morrell 2011). In case of seizures refractory to any treatment, it would be helpful to at least warn the patients about the periods of heightened seizure risk so that they could better plan their activities. All these efforts would benefit from better understanding of the long-term seizure dynamics (Baud & Rao 2018). In this work we suggested that the interplay between focal and generalized seizures may govern the processes responsible for changes in seizure propensity. Moreover, we found that during long seizure-free periods, interictal EEG activity (bursts) might be indicative of the processes that gradually lead to the next seizure cluster. In the future, it will be needed to confirm whether our findings apply to some epileptic syndromes found in patients.

Practical implementation of these techniques is dependent on the possibility of long-term ambulatory recording of the required data. Two clinical trials using two different devices (NeuroVista and NeuroPace) have demonstrated feasibility of long-term ambulatory intracranial EEG monitoring (Baud et al 2018, Cook et al 2014). Moreover, the EEG data can be combined

with other physiological signals such as heart rate, skin conductance and accelerometry which can be easily measured using wearable sensors such as a wristband (Onorati et al 2017). The non-EEG data can provide information about the behavioral severity of the seizures which may even improve the seizure forecasting performance. We believe that the new techniques will greatly improve the care for people with epilepsy which will result in their better quality of life.

8 References

Aguiar CCT, Almeida AB, Araújo PVP, Vasconcelos GS, Chaves EMC, et al. 2012. Anticonvulsant effects of agomelatine in mice. *Epilepsy & Behavior* 24: 324-28

Arida RM, Scorza FA, Peres CA, Cavalheiro EA. 1999. The course of untreated seizures in the pilocarpine model of epilepsy. *Epilepsy Res* 34: 99-107

Backstrom T. 1976. Epileptic seizures in women related to plasma estrogen and progesterone during the menstrual cycle. *Acta neurologica Scandinavica* 54: 321-47

Bajorat R, Wilde M, Sellmann T, Kirschstein T, Kohling R. 2011. Seizure frequency in pilocarpine-treated rats is independent of circadian rhythm. *Epilepsia* 52: e118-22

Bak P. 1996. *How Nature Works: The Science of Self-Organized Criticality*. Copernicus.

Balish M, Albert PS, Theodore WH. 1991. Seizure frequency in intractable partial epilepsy: a statistical analysis. *Epilepsia* 32: 642-9

Bandler B, Dykens JW, Kaufman IC, Schleifer M, Shapiro LN. 1957. Seizures and the menstrual cycle. *Am J Psychiatry* 113: 704-8

Baud MO, Kleen JK, Mirro EA, Andrechak JC, King-Stephens D, et al. 2018. Multi-day rhythms modulate seizure risk in epilepsy. *Nature Communications* 9: 88

Baud MO, Rao VR. 2018. Gauging seizure risk. *Neurology* 91: 967-73

Bauer J, Burr W. 2001. Course of chronic focal epilepsy resistant to anticonvulsant treatment. *Seizure* 10: 239-46

Beggs JM, Plenz D. 2003. Neuronal Avalanches in Neocortical Circuits. *The Journal of Neuroscience* 23: 11167-77

Berman RF, Fredholm BB, Aden U, O'Connor WT. 2000. Evidence for increased dorsal hippocampal adenosine release and metabolism during pharmacologically induced seizures in rats. *Brain Res* 872: 44-53

Bertram EH. 2009. Temporal lobe epilepsy: where do the seizures really begin? *Epilepsy Behav* 14 Suppl 1: 32-7

Bertram EH, Cornett JF. 1994. The evolution of a rat model of chronic spontaneous limbic seizures. *Brain Res* 661: 157-62

Binnie CD, Aarts JH, Houtkooper MA, Laxminarayan R, Martins da Silva A, et al. 1984. Temporal characteristics of seizures and epileptiform discharges. *Electroencephalogr Clin Neurophysiol* 58: 498-505

Blauwblomme T, Jiruska P, Huberfeld G. 2014. Mechanisms of ictogenesis. *Int Rev Neurobiol* 114: 155-85

Blume WT. 2006. The progression of epilepsy. *Epilepsia* 47 Suppl 1: 71-8

Boison D. 2005. Adenosine and epilepsy: from therapeutic rationale to new therapeutic strategies. *Neuroscientist* 11: 25-36

Caspers H, Speckmann EJ. 1972. Cerebral pO 2 , pCO 2 and pH: changes during convulsive activity and their significance for spontaneous arrest of seizures. *Epilepsia* 13: 699-725

Cavalheiro EA, Calderazzo Filho LS, Bortolotto ZA, Mello L, Turski L. 1987. Anticonvulsant role of adenosine. *Pol J Pharmacol Pharm* 39: 537-43

Cavalheiro EA, Leite JP, Bortolotto ZA, Turski WA, Ikonomidou C, Turski L. 1991. Long-term effects of pilocarpine in rats: structural damage of the brain triggers kindling and spontaneous recurrent seizures. *Epilepsia* 32: 778-82

Chang WC, Kudlacek J, Hlinka J, Chvojka J, Hadrava M, et al. 2018. Loss of neuronal network resilience precedes seizures and determines the ictogenic nature of interictal synaptic perturbations. *Nat Neurosci* 21: 1742-52

Claustrat B, Leston J. 2015. Melatonin: Physiological effects in humans. *Neurochirurgie* 61: 77-84

Cook MJ, O'Brien TJ, Berkovic SF, Murphy M, Morokoff A, et al. 2013. Prediction of seizure likelihood with a long-term, implanted seizure advisory system in patients with drug-resistant epilepsy: a first-in-man study. *The Lancet Neurology* 12: 563-71

Cook MJ, Varsavsky A, Himes D, Leyde K, Berkovic SF, et al. 2014. The dynamics of the epileptic brain reveal long-memory processes. *Front Neurol* 5: 217
Cox DR, Lewis PAW. 1966. *The statistical analysis of series of events*. London,: Methuen. viii, 285 p. pp.
Crawford P. 2005. Best practice guidelines for the management of women with epilepsy. *Epilepsia* 46 Suppl 9: 117-24
Dastgheib M, Moezi L. 2014. Acute and chronic effects of agomelatine on intravenous penthylenetetrazol-induced seizure in mice and the probable role of nitric oxide. *European Journal of Pharmacology* 736: 10-15
Davis PM, Jackson DD, Kagan YY. 1989. The Longer It Has Been since the Last Earthquake, the Longer the Expected Time Till the Next. *B Seismol Soc Am* 79: 1439-56
de Curtis M, Jefferys JGR, Avoli M. 2012. Interictal Epileptiform Discharges in Partial Epilepsy: Complex Neurobiological Mechanisms Based on Experimental and Clinical Evidence In *Jasper's Basic Mechanisms of the Epilepsies*, ed. th, JL Noebels, M Avoli, MA Rogawski, RW Olsen, AV Delgado-Escueta. Bethesda MD: Michael A Rogawski, Antonio V Delgado-Escueta, Jeffrey L Noebels, Massimo Avoli and Richard W Olsen.
Dragunow M, Goddard GV, Laverty R. 1985. Is adenosine an endogenous anticonvulsant? *Epilepsia* 26: 480-7
Dudek FE, Staley KJ. 2011a. Seizure probability in animal models of acquired epilepsy: a perspective on the concept of the preictal state. *Epilepsy Res* 97: 324-31
Dudek FE, Staley KJ. 2011b. The time course of acquired epilepsy: implications for therapeutic intervention to suppress epileptogenesis. *Neurosci Lett* 497: 240-6
Dulla CG, Frenguelli BG, Staley KJ, Masino SA. 2009. Intracellular acidification causes adenosine release during states of hyperexcitability in the hippocampus. *Journal of neurophysiology* 102: 1984-93
During MJ, Spencer DD. 1992. Adenosine: a potential mediator of seizure arrest and postictal refractoriness. *Ann Neurol* 32: 618-24
Emens JS, Eastman CI. 2017. Diagnosis and Treatment of Non-24-h Sleep-Wake Disorder in the Blind. *Drugs* 77: 637-50
Feely M, Gibson J. 1984. Intermittent clobazam for catamenial epilepsy: tolerance avoided. *Journal of Neurology, Neurosurgery & Psychiatry* 47: 1279
Fenoglio-Simeone KA, Wilke JC, Milligan HL, Allen CN, Rho JM, Maganti RK. 2009. Ketogenic diet treatment abolishes seizure periodicity and improves diurnal rhythmicity in epileptic Kcna1-null mice. *Epilepsia* 50: 2027-34
Ferecsko AS, Jiruska P, Foss L, Powell AD, Chang WC, et al. 2014. Structural and functional substrates of tetanus toxin in an animal model of temporal lobe epilepsy. *Brain structure & function*
Fink M. 1978. Efficacy and safety of induced seizures (EST) in man. *Compr Psychiatry* 19: 1-18
Fisher RS, Bartfeld E, Cramer JA. 2015. Use of an online epilepsy diary to characterize repetitive seizures. *Epilepsy Behav* 47: 66-71
Fisher RS, Cross JH, French JA, Higurashi N, Hirsch E, et al. 2017. Operational classification of seizure types by the International League Against Epilepsy: Position Paper of the ILAE Commission for Classification and Terminology. *Epilepsia* 58: 522-30
Fisher RS, van Emde Boas W, Blume W, Elger C, Genton P, et al. 2005. Epileptic seizures and epilepsy: definitions proposed by the International League Against Epilepsy (ILAE) and the International Bureau for Epilepsy (IBE). *Epilepsia* 46: 470-2
Fisher RS, Vickrey BG, Gibson P, Hermann B, Penovich P, et al. 2000. The impact of epilepsy from the patient's perspective I. Descriptions and subjective perceptions. *Epilepsy Res* 41: 39-51
Folbergrova J, Haugvicova R, Mares P. 2000. Behavioral and metabolic changes in immature rats during seizures induced by homocysteic acid: the protective effect of NMDA and non-NMDA receptor antagonists. *Exp Neurol* 161: 336-45
Frederick L. Patry. 1931. THE RELATION OF TIME OF DAY, SLEEP, AND OTHER FACTORS TO THE INCIDENCE OF EPILEPTIC SEIZURES. *American Journal of Psychiatry* 87: 789-813

Fukuda M, Suzuki Y, Hino H, Kuzume K, Morimoto T, Ishii E. 2010. Adenosine A1 receptor blockage mediates theophylline-associated seizures. *Epilepsia* 51: 483-87
Gastaut H, Low MD. 1979. Antiepileptic properties of clobazam, a 1-5 benzodiazepine, in man. *Epilepsia* 20: 437-46
Goddard GV, McIntyre DC, Leech CK. 1969. A permanent change in brain function resulting from daily electrical stimulation. *Exp Neurol* 25: 295-330
Goffin K, Nissinen J, Van Laere K, Pitkanen A. 2007. Cyclicity of spontaneous recurrent seizures in pilocarpine model of temporal lobe epilepsy in rat. *Exp Neurol* 205: 501-5
Goldenholz DM, Rakesh K, Kapur K, Gaínza-Lein M, Hodgeman R, et al. 2018. Different as night and day: Patterns of isolated seizures, clusters, and status epilepticus. *Epilepsia* 0
Gowers WR. 1881. *Epilepsy and other chronic convulsive diseases : their causes, symptoms, & treatment*. London: Churchil.
Grabenstatter HL, Ferraro DJ, Williams PA, Chapman PL, Dudek FE. 2005. Use of chronic epilepsy models in antiepileptic drug discovery: the effect of topiramate on spontaneous motor seizures in rats with kainate-induced epilepsy. *Epilepsia* 46: 8-14
Green MA. 1960. Relation between threshold and duration of seizures and electrographic change during convulsive therapy. *J Nerv Ment Dis* 131: 117-20
Griffiths G, Fox JT. 1938. RHYTHM IN EPILEPSY. *The Lancet* 232: 409-16
Guilhoto LM, Loddenkemper T, Vendrame M, Bergin A, Bourgeois BF, Kothare SV. 2011. Higher evening antiepileptic drug dose for nocturnal and early-morning seizures. *Epilepsy Behav* 20: 334-7
Handforth A. 1982. Postseizure inhibition of kindled seizures by electroconvulsive shock. *Exp Neurol* 78: 483-91
Hauser WA, Lee JR. 2002. Do seizures beget seizures? *Prog Brain Res* 135: 215-9
Haut SR, Lipton RB, LeValley AJ, Hall CB, Shinnar S. 2005a. Identifying seizure clusters in patients with epilepsy. *Neurology* 65: 1313-15
Haut SR, Shinnar S, Moshe SL. 2005b. Seizure clustering: risks and outcomes. *Epilepsia* 46: 146-9
Hawkins CA, Mellanby JH. 1987. Limbic epilepsy induced by tetanus toxin: a longitudinal electroencephalographic study. *Epilepsia* 28: 431-44
Hellier JL, Dudek FE. 1999. Spontaneous motor seizures of rats with kainate-induced epilepsy: effect of time of day and activity state. *Epilepsy Res* 35: 47-57
Herberg LJ, Watkins PJ. 1966. Epileptiform Seizures induced by Hypothalamic Stimulation in the Rat : Resistance to Fits following Fits. *Nature* 209: 515
Herzog AG. 2015. Catamenial epilepsy: Update on prevalence, pathophysiology and treatment from the findings of the NIH Progesterone Treatment Trial. *Seizure - European Journal of Epilepsy* 28: 18-25
Herzog AG, Harden CL, Liporace J, Pennell P, Schomer DL, et al. 2004. Frequency of catamenial seizure exacerbation in women with localization-related epilepsy. *Ann Neurol* 56: 431-4
Herzog AG, Klein P, Ransil BJ. 1997. Three patterns of catamenial epilepsy. *Epilepsia* 38: 1082-8
Hofstra WA, Spetgens WP, Leijten FS, van Rijen PC, Gosselaar P, et al. 2009. Diurnal rhythms in seizures detected by intracranial electrocorticographic monitoring: an observational study. *Epilepsy Behav* 14: 617-21
Hopkins A, Davies P, Dobson C. 1985. Mathematical models of patterns of seizures. Their use in the evaluation of drugs. *Archives of neurology* 42: 463-7
Howbert JJ, Patterson EE, Stead SM, Brinkmann B, Vasoli V, et al. 2014. Forecasting seizures in dogs with naturally occurring epilepsy. *PLoS One* 9: e81920
Janca R, Jezdik P, Cmejla R, Tomasek M, Worrell GA, et al. 2015. Detection of interictal epileptiform discharges using signal envelope distribution modelling: application to epileptic and non-epileptic intracranial recordings. *Brain topography* 28: 172-83
Janca R, Krsek P, Jezdik P, Cmejla R, Tomasek M, et al. 2018. The Sub-Regional Functional Organization of Neocortical Irritative Epileptic Networks in Pediatric Epilepsy. *Front Neurol* 9: 184
Javidan M. 2012. Electroencephalography in mesial temporal lobe epilepsy: a review. *Epilepsy Res Treat* 2012: 637430

Jefferys J, Steinhauser C, Bedner P. 2015. Chemically-induced TLE models: Topical application. *J Neurosci Methods*

Jefferys JG, Evans BJ, Hughes SA, Williams SF. 1992. Neuropathology of the chronic epileptic syndrome induced by intrahippocampal tetanus toxin in rat: preservation of pyramidal cells and incidence of dark cells. *Neuropathol.Appl.Neurobiol.* 18: 53-70

Jiruska P, Bragin A. 2011. High-frequency activity in experimental and clinical epileptic foci. *Epilepsy Res* 97: 300-7

Jiruska P, Shtaya AB, Bodansky DM, Chang WC, Gray WP, Jefferys JG. 2013. Dentate gyrus progenitor cell proliferation after the onset of spontaneous seizures in the tetanus toxin model of temporal lobe epilepsy. *Neurobiol Dis* 54: 492-8

Kadam SD, White AM, Staley KJ, Dudek FE. 2010. Continuous Electroencephalographic Monitoring with Radio-Telemetry in a Rat Model of Perinatal Hypoxia–Ischemia Reveals Progressive Post-Stroke Epilepsy. *The Journal of Neuroscience* 30: 404-15

Karoly PJ, Freestone DR, Boston R, Grayden DB, Himes D, et al. 2016. Interictal spikes and epileptic seizures: their relationship and underlying rhythmicity. *Brain* 139: 1066-78

Klaus A, Yu S, Plenz D. 2011. Statistical analyses support power law distributions found in neuronal avalanches. *PLoS One* 6: e19779

Koepp MJ, Richardson MP, Brooks DJ, Duncan JS. 1998. Focal cortical release of endogenous opioids during reading-induced seizures. *Lancet* 352: 952-5

Kostopoulos G, Drapeau C, Avoli M, Olivier A, Villemeure JG. 1989. Endogenous adenosine can reduce epileptiform activity in the human epileptogenic cortex maintained in vitro. *Neurosci Lett* 106: 119-24

Kovacs R, Gerevich Z, Friedman A, Otahal J, Prager O, et al. 2018. Bioenergetic Mechanisms of Seizure Control. *Front Cell Neurosci* 12: 335

Kudlacek J, Chvojka J, Posusta A, Kovacova L, Hong SB, et al. 2017. Lacosamide and Levetiracetam Have No Effect on Sharp-Wave Ripple Rate. *Frontiers in Neurology* 8

Lado FA, Moshe SL. 2008. How do seizures stop? *Epilepsia* 49: 1651-64

Leite Goes Gitai D, de Andrade TG, Dos Santos YDR, Attaluri S, Shetty AK. 2019. Chronobiology of limbic seizures: Potential mechanisms and prospects of chronotherapy for mesial temporal lobe epilepsy. *Neurosci Biobehav Rev* 98: 122-34

Litt B, Esteller R, Echauz J, D'Alessandro M, Shor R, et al. 2001. Epileptic Seizures May Begin Hours in Advance of Clinical Onset: A Report of Five Patients. *Neuron* 30: 51-64

Lockley SW, Dressman MA, Licamele L, Xiao C, Fisher DM, et al. 2015. Tasimelteon for non-24-hour sleep-wake disorder in totally blind people (SET and RESET): two multicentre, randomised, double-masked, placebo-controlled phase 3 trials. *Lancet* 386: 1754-64

Loddenkemper T. 2012. Chrono-epileptology: time to reconsider seizure timing. *Seizure* 21: 411

Loscher W, Kohling R. 2010. Functional, metabolic, and synaptic changes after seizures as potential targets for antiepileptic therapy. *Epilepsy Behav* 19: 105-13

M Kenny A, B Schneider M, R Baden D, Pfeiffer R, Murrin LC. 1986. *Bromocriptine holiday: Effects on dopamine receptors and turning behavior in rats*. 400-4 pp.

Mazzuferi M, Kumar G, Rospo C, Kaminski RM. 2012. Rapid epileptogenesis in the mouse pilocarpine model: video-EEG, pharmacokinetic and histopathological characterization. *Exp Neurol* 238: 156-67

Mellanby J, George G, Robinson A, Thompson P. 1977. Epileptiform syndrome in rats produced by injecting tetanus toxin into the hippocampus. *Journal of neurology, neurosurgery, and psychiatry* 40: 404-14

Merriam-Webster. 2019. Chronotherapy. In *Merriam Webster*: Merriam-Webster, Inc.

Milton JG, Gotman J, Remillard GM, Andermann F. 1987. Timing of seizure recurrence in adult epileptic patients: a statistical analysis. *Epilepsia* 28: 471-8

Mirzoev A, Bercovici E, Stewart LS, Cortez MA, Snead OC, 3rd, Desrocher M. 2012. Circadian profiles of focal epileptic seizures: a need for reappraisal. *Seizure* 21: 412-6

Morrell MJ. 2011. Responsive cortical stimulation for the treatment of medically intractable partial epilepsy. *Neurology* 77: 1295-304

Mucha RF, Pinel PJ. 1977. Postseizure inhibition of kindled seizures. *Exp Neurol* 54: 266-82

Mula M, Cock HR. 2015. More than seizures: improving the lives of people with refractory epilepsy. *Eur J Neurol* 22: 24-30

Navis A, Harden C. 2016. A Treatment Approach to Catamenial Epilepsy. *Curr Treat Options Neurol* 18: 30

Newman MEJ. 2005. Power laws, Pareto distributions and Zipf's law. *Contemporary Physics* 46: 323-51

Onorati F, Regalia G, Caborni C, Migliorini M, Bender D, et al. 2017. Multicenter clinical assessment of improved wearable multimodal convulsive seizure detectors. *Epilepsia* 58: 1870-79

Osorio I, Frei MG, Sornette D, Milton J. 2009. Pharmaco-resistant seizures: self-triggering capacity, scale-free properties and predictability? *The European journal of neuroscience* 30: 1554-8

Osorio I, Frei MG, Sornette D, Milton J, Lai YC. 2010. Epileptic seizures: Quakes of the brain? *Phys Rev E* 82

Otahal J, Folbergrova J, Kovacs R, Kunz WS, Maggio N. 2014. Epileptic focus and alteration of metabolism. *Int Rev Neurobiol* 114: 209-43

Parish LM, Worrell GA, Cranstoun SD, Stead SM, Pennell P, Litt B. 2004. Long-range temporal correlations in epileptogenic and non-epileptogenic human hippocampus. *Neuroscience* 125: 1069-76

Paxinos G, Watson C. 1998. The Rat Brain. In *The Rat Brain In Stereotaxic Coordinates*, pp. 474. San Diego, California 92101-4495, USA: Academic Press, Inc.

Petermann T, Thiagarajan TC, Lebedev MA, Nicolelis MA, Chialvo DR, Plenz D. 2009. Spontaneous cortical activity in awake monkeys composed of neuronal avalanches. *Proc Natl Acad Sci U S A* 106: 15921-6

Pitsch J, Becker AJ, Schoch S, Muller JA, de Curtis M, Gnatkovsky V. 2017. Circadian clustering of spontaneous epileptic seizures emerges after pilocarpine-induced status epilepticus. *Epilepsia* 58: 1159-71

Quigg M, Clayburn H, Straume M, Menaker M, Bertram EH, 3rd. 2000. Effects of circadian regulation and rest-activity state on spontaneous seizures in a rat model of limbic epilepsy. *Epilepsia* 41: 502-9

Racine RJ. 1972. Modification of seizure activity by electrical stimulation. II. Motor seizure. *Electroencephalogr Clin Neurophysiol* 32: 281-94

Raedt R, Van Dycke A, Van Melkebeke D, De Smedt T, Claeys P, et al. 2009. Seizures in the intrahippocampal kainic acid epilepsy model: characterization using long-term video-EEG monitoring in the rat. *Acta neurologica Scandinavica* 119: 293-303

Ramgopal S, Thome-Souza S, Loddenkemper T. 2013. Chronopharmacology of anti-convulsive therapy. *Curr Neurol Neurosci Rep* 13: 339

Reisner AD. 2003. The electroconvulsive therapy controversy: evidence and ethics. *Neuropsychol Rev* 13: 199-219

Scharfman HE. 2007. The Neurobiology of Epilepsy. *Current neurology and neuroscience reports* 7: 348-54

Schiff SJ, Colella D, Jacyna GM, Hughes E, Creekmore JW, et al. 2000. Brain chirps: spectrographic signatures of epileptic seizures. *Clinical neurophysiology : official journal of the International Federation of Clinical Neurophysiology* 111: 953-8

Sedigh-Sarvestani M, Thuku GI, Sunderam S, Parkar A, Weinstein SL, et al. 2014. Rapid eye movement sleep and hippocampal theta oscillations precede seizure onset in the tetanus toxin model of temporal lobe epilepsy. *J Neurosci* 34: 1105-14

Shapira B, Lidsky D, Gorfine M, Lerer B. 1996. Electroconvulsive therapy and resistant depression: clinical implications of seizure threshold. *J Clin Psychiatry* 57: 32-8

Sillanpaa M, Schmidt D. 2008. Seizure clustering during drug treatment affects seizure outcome and mortality of childhood-onset epilepsy. *Brain* 131: 938-44

Sloviter RS. 2005. The neurobiology of temporal lobe epilepsy: too much information, not enough knowledge. *Comptes Rendus Biologies* 328: 143-53

Sornette D, Knopoff L. 1997. The paradox of the expected time until the next earthquake. *B Seismol Soc Am* 87: 789-98
Stewart LS, Leung LS, Persinger MA. 2001. Diurnal variation in pilocarpine-induced generalized tonic-clonic seizure activity. *Epilepsy Res* 44: 207-12
Stewart LS, Nylen KJ, Persinger MA, Cortez MA, Gibson KM, Snead OC, 3rd. 2008. Circadian distribution of generalized tonic-clonic seizures associated with murine succinic semialdehyde dehydrogenase deficiency, a disorder of GABA metabolism. *Epilepsy Behav* 13: 290-4
Sunderam S, Osorio I, Frei MG. 2007. Epileptic seizures are temporally interdependent under certain conditions. *Epilepsy Res* 76: 77-84
Tauboll E, Lundervold A, Gjerstad L. 1991. Temporal distribution of seizures in epilepsy. *Epilepsy Res* 8: 153-65
Thom M, Mathern GW, Cross JH, Bertram EH. 2010. Mesial temporal lobe epilepsy: How do we improve surgical outcome? *Ann Neurol* 68: 424-34
Tolner EA, Hochman DW, Hassinen P, Otahal J, Gaily E, et al. 2011. Five percent CO(2) is a potent, fast-acting inhalation anticonvulsant. *Epilepsia* 52: 104-14
Toyoda I, Bower MR, Leyva F, Buckmaster PS. 2013. Early activation of ventral hippocampus and subiculum during spontaneous seizures in a rat model of temporal lobe epilepsy. *J Neurosci* 33: 11100-15
Varsavsky A, Mareels I, Cook M. 2011. *Epileptic seizures and the EEG : measurement, models, detection and prediction*. Boca Raton: Taylor & Francis. xxi, 346 p. pp.
Velisek L, Dreier JP, Stanton PK, Heinemann U, Moshe SL. 1994. Lowering of extracellular pH suppresses low-Mg(2+)-induces seizures in combined entorhinal cortex-hippocampal slices. *Exp Brain Res* 101: 44-52
Vezzani A, Sperk G. 2004. Overexpression of NPY and Y2 receptors in epileptic brain tissue: an endogenous neuroprotective mechanism in temporal lobe epilepsy? *Neuropeptides* 38: 245-52
Voinescu PE, Pennell PB. 2017. Delivery of a Personalized Treatment Approach to Women with Epilepsy. *Semin Neurol* 37: 611-23
White A, Williams PA, Hellier JL, Clark S, Dudek FE, Staley KJ. 2010. EEG spike activity precedes epilepsy after kainate-induced status epilepticus. *Epilepsia* 51: 371-83
Williams PA, Hellier JL, White AM, Staley KJ, Dudek FE. 2007. Development of spontaneous seizures after experimental status epilepticus: implications for understanding epileptogenesis. *Epilepsia* 48 Suppl 5: 157-63
Williams PA, White AM, Clark S, Ferraro DJ, Swiercz W, et al. 2009. Development of spontaneous recurrent seizures after kainate-induced status epilepticus. *J Neurosci* 29: 2103-12
Woldbye DP, Madsen TM, Larsen PJ, Mikkelsen JD, Bolwig TG. 1996. Neuropeptide Y inhibits hippocampal seizures and wet dog shakes. *Brain Res* 737: 162-8
Yegnanarayan R, Mahesh SD, Sangle S. 2006. Chronotherapeutic dose schedule of phenytoin and carbamazepine in epileptic patients. *Chronobiol Int* 23: 1035-46

9 List of authors publications

In all the publications, the author contributions were equal.

9.1 Publications related to the topic of the doctoral thesis

9.1.1 WoS Expanded Q1

Chang, W.Ch.; **Kudláček, J.**; Hlinka, J.; Chvojka, J.; Hadrava, M.; Kumpošt, V.; Powell, A.D.; Janča, R. et al.: Loss of neuronal network resilience precedes seizures and determines the ictogenic nature of interictal synaptic perturbations. *Nature Neuroscience. 2018, 21 1742-1752. ISSN 1097-6256.* (16 authors, 6.25% author contribution)

9.1.2 WoS Expanded Q2

Kudláček, J.; Chvojka, J.; Pošusta, A.; Kováčová, L.; Hong, S.B.; Weiss, S.; Volná, K.; Marusič, P. et al.: Lacosamide and Levetiracetam Have No Effect on Sharp-Wave Ripple Rate. *Frontiers in Neurology. 2017, 8 ISSN 1664-2295. doi: 10.3389/fneur.2017.00687.* (10 authors, 10% author contribution)

9.1.3 WoS Others

Kudláček, J.; Chvojka, J.; Pošusta, A.; Kováčová, L.; Hong, S.B.; Weiss, S.; Volná, K.; Marusič, P. et al.: Lacosamide And Levetiracetam Have No Effect On Sharp-Wave Ripple Rate. *In: 13th European Congress on Epileptology Vienna, Austria 26th - 30th August 2018. The International League Against Epilepsy, 2018. p. S258-S259. vol. 59. ISSN 1528-1167.* (poster, abstract)

Chvojka, J.; **Kudláček, J.**; Otáhal, J.; Jiruška, P.: State-Dependent Effect of Interictal Epileptiform Discharges. *In: 13th European Congress on Epileptology Vienna, Austria 26th – 30th August 2018. The International League Against Epilepsy, 2018. p. S23. vol. 59. ISSN 1528-1167.* (lecture, abstract)

Kudláček, J.; Vlk, P.; Chvojka, J.; Heřmanovská, B.; Kováčová, Ľ.; Janča, R.; Kumpošt, V.; Pošusta, A. et al.: Changes in microseizure properties anticipate seizure clusters in tetanus toxin model of temporal lobe epilepsy. *In: 32nd International Congress on Epilepsy - Barcelona. The International League Against Epilepsy, 2017.* (poster, abstract)

Kudlacek J, Vlk P, Demeterova L, Hermanovska B, Kumpost V, Posusta A, Otahal J, Jiruska P. Micro-seizures reliably localize primary epileptogenic areas in tetanus toxin model of temporal lobe epilepsy. *12th European Congress on Epileptology, Prague, Czech Republic, 12th – 15th September, 2016. doi: 10.1111/epi.13609.* (poster, abstract)

Havel T, **Kudlacek J**, Jiruska P, Jezdik P, Cmejla R. High-frequency oscillation ability to localize epileptogenic tissue in animal epilepsy model. *12th European Congress on Epileptology, Prague, Czech Republic, 12th – 15th September, 2016. doi: 10.1111/epi.13609.* (poster, abstract)

Jiruska P, Demeterova L, **Kudlacek J**, Vlk P, Posusta A, Otahal J: Morphological Alterations in the Model of Non-lesional Temporal Lobe Epilepsy. *In: 31st International Epilepsy Congress, Istanbul, 05th - 09th September 2015. Epilepsia, 56 (Suppl. 1): p. 120, 2015. doi: 10.1111/epi.13241.* (abstract)

Kudlacek J, Vlk P, Demeterova L, Posusta A, Otahal J, Jiruska P: Spatio-temporal Profile of Seizer Initiation in Temporal Lobe Epilepsy of Hippocampal Origin. *In: 31st International Epilepsy Congress, Istanbul, 05th - 09th September 2015.Epilepsia, 56 (Suppl. 1): 3–262, 2015. doi: 10.1111/epi.13241*. (poster, abstract)

Jiruska P, Otahal J, Cmejla R, **Kudlacek J**, Vlk P, Palus M, Hlinka J, Marusic P, Jefferys JGR. Long-term profile and seizure clustering in the tetanus toxin model of temporal lobe epilepsy. *In: 11th European Congress on Epileptolog. Stockholm, Sweden, 29th June - 3rd July, 2014. Epilepsia, 55(Suppl. 2), 2014, p. 121–122. doi: 10.1111/epi.12675* (poster, abstract)

9.1.4 Others

Kudláček, J.; Chvojka, J.; Pošusta, A.; Otáhal, J.; Jiruška, P.: Transition to seizure via critical slowing in a chronic model of temporal lobe epilepsy. *In: 11th FENS Forum of Neuroscience. Kenes Group, 2018. p. 1900.* (poster, abstract)

Chvojka, J.; Chang, W.; Hlinka, J.; **Kudláček, J.**; Otáhal, J.; Paluš, M.; Kumpošt, V.; Janča, R. et al.: Dual role of interictal discharges in hippocampal ictogenesis. *In: The Eleventh Conference of the Czech Neuroscience Society. Praha: Czech Neuroscience Society, 2017.* (lecture, abstract)

Chvojka, J.; Chang, W.-Ch.; Hlinka, J.; **Kudláček, J.**; Otáhal, J.; Paluš, M.; Kumpošt, V.; Janča, R. et al.: Úloha interiktálních výbojů v patogenezi vzniku záchvatů. *In: 31. český a slovenský neurologický sjezd, 29. česko-slovenský epileptologický sjezd. Praha: Česká lékařská společnost J. E. Purkyně, 2017. ISSN 1802-4041.* (lecture, abstract)

Kudláček, J.; Chvojka, J.; Vlk, P.; Pošusta, A.; Kováčová, Ľ.; Heřmanovská, B.; Otáhal, J.; Jiruška, P. et al.: Long-term fluctuations in seizure probability in tetanus toxin model of epilepsy. *In: The Eleventh Conference of the Czech Neuroscience Society. Praha: Czech Neuroscience Society, 2017.* (lecture, abstract)

Kudláček, J.; Chvojka, J.; Vlk, P.; Kováčová, Ľ.; Janča, R.; Heřmanovská, B.; Kumpošt, V.; Pošusta, A. et al.: Před vznikem shluků záchvatů dochází ke změnám parametrů mikrozáchvatů v tetanotoxinovém modelu epilepsie temporálního laloku. *In: 31. český a slovenský neurologický sjezd, 29. česko-slovenský epileptologický sjezd. Praha: Česká lékařská společnost J. E. Purkyně, 2017. ISSN 1802-4041.* (lecture, abstract)

Kudlacek J, Palus M, Vlk P, Posusta A, Kumpost V, Demeterova L, Hermanovska B, Otahal J, Jiruska P. Long-term seizure dynamics is determined by the nature of seizures. *70th AES Annual Meeting, Houston, Texas, USA, 2nd to 6th December, 2016.* (poster, abstract)

Jiruska P, Cmejla R, **Kudlacek J**, Vlk P, Hlinka J, Palus M, Jefferys JGR. Epileptic seizures are characterized by progressive decrease in stability of epileptic networks. *In: XXXIV Dynamics Days Europe. Bayreuth, Germany, 8th - 12th September 2014.* (abstract)

Jiruska P, Cmejla R, Vlk P, **Kudlacek J**, Hlinka J, Palus M. Unstable neuronal network dynamics precedes transition to seizure and seizure termination. *In: Causality, Information Transfer and Dynamical Networks Workshop. Dresden, Germany, 1st - 5th June 2014.* (abstract)

9.2 Publications not related to the topic of the doctoral thesis

9.2.1 Others

Kudlacek J, Husnik L, Jiruska P. Acoustic Navigation System for the Visually Impaired. *In: PhD meeting in Trest 2013: Institute of physiology. Trest, 22nd - 24th October 2013. ISBN 978-80-7080-863-4.* (poster, abstract)